Dissertation zur Erlangung des Doktorgrades
der Fakultät für Chemie und Pharmazie
der Ludwig-Maximillians-Universität München

# Pharmacokinetic Profiling of Therapeutic Proteins and Variants by Mass Spectrometry

Fabian Benjamin Higel

aus

Villingen-Schwenningen, Deutschland

2014

Erklärung

Diese Dissertation wurde im Sinne von § 7 der Promotionsordnung vom 28. November 2011 von Herrn Prof. Dr. Fritz Sörgel betreut
und von Herrn Prof. Dr. Wolfgang Frieß
von der Fakultät für Chemie und Pharmazie vertreten.

Eidesstattliche Versicherung

Diese Dissertation wurde eigenständig und ohne unerlaubte Hilfe erarbeitet.

München,

Fabian Benjamin Higel

Dissertation eingereicht am 27.06.2014

1. Gutachter: Prof. Dr. Wolfgang Frieß

2. Gutachter: Prof. Dr. Fritz Sörgel

Mündliche Prüfung am 11.09.2014

# Table of contents



## Chapter 1:

## *N-glycosylation heterogeneity and the influence on structure, function and pharmacokinetics of monoclonal antibodies and Fc fusion proteins*

## Chapter 2:

## *Reversed-phase liquid-chromatographic mass spectrometric N-glycan analysis of biopharmaceuticals*

## Chapter 3:

## *Small scale affinity purification and high sensitivity reversed phase nanoLC-MS N-glycan characterization of mAbs and fusion proteins*

## Chapter 4:

## *Development and qualification of a high-throughput affinity purification and N-glycan analysis methodology for glycan PK profiling of monoclonal antibodies*

## Chapter 5:

## *Influence of glyco-variants on the pharmacokinetics of an IgG1 biopharmaceutical*

## Chapter 6:

## *The influence of glyco-variants on the pharmacokinetics of a multiply glycosylated therapeutic Fc fusion protein*



## Chapter 7


SIGILL: UNIVERSI TAT: LUDOVIC: MAXIM:

# Acknowledgement

This PhD-Thesis was performed at the laboratories of HEXAL AG/ Sandoz Biopharmaceuticals in Oberhaching in collaboration with the Institute for Biomedical and Pharmaceutical Research (IBMP) in Nürnberg-Heroldsberg and the Department of Pharmacy, Pharmaceutical Technology and Biopharmaceutics, at the Ludwig-Maximilians Universität München (LMU). The thesis was supervised by Dr. Andreas Seidl and Dr. Uwe Demelbauer from HEXAL AG/ Sandoz Biopharmaceuticals, by Prof. Dr. Fritz Sörgel from the IBMP and Prof. Dr. Wolfgang Frieß from the LMU.

First, I want to thank HEXAL AG/ Sandoz Biopharmaceuticals for the funding of this work.

Furthermore, I want to thank my academic supervisors, Prof. Frieß and Prof. Sörgel, for their willingness to supervise this work and their scientific guidance and fruitful discussions during our regular meetings that helped to move on with the project and for the input during the writing of the publications and the dissertation.

I want to express my gratitude to Dr. Andreas Seidl and Dr. Uwe Demelbauer from HEXAL AG for their excellent support throughout the thesis, the critical questions, the scientific input and their ideas. Moreover I want to thank Dr. Andreas Seidl for the detailed proofreading of the publications, the thesis and the critical comments. I also want to thank Dr. Uwe Demelbauer for sharing his extensive knowledge about mass spectrometry and his helpfulness with problems in the lab.

I want to thank the groups of Prof. Frieß and Prof. Winter from LMU for the friendly and open atmosphere during the rare time together.

I want to thank my colleagues in Oberhaching and the coworkers at Sandoz Kundl, Schaftenau and Menges who were somehow involved for their support, helpfulness and suggestions in the scientific meetings.

Last but not least I want to express my deepest gratitude to my family and friends who always supported me during the years of my studies and graduation.

# *Objectives of the thesis*

The active pharmaceutical ingredients of biopharmaceuticals, therapeutic proteins, are heterogeneous mixtures containing many protein variants. The variants encompass protein modifications (e.g. oxidation or deamidation) and post-translational modifications (e.g. glycosylation or phosphorylation). These variants can have an influence on the structure and function of the therapeutic protein. The introduction (**Chapter 1)** reviews modifications of therapeutic proteins and gives an overview of published methods, studies and analytical technologies. Main focus is on N-glycosylation, a complex post-translational modification with potential influence on the pharmacokinetics. As described in the introduction the impact of N-glycosylation on the pharmacokinetics of biopharmaceuticals is not yet fully understood. Studies investigating the criticality of N-glycans performed with different analytical approaches for different types of biopharmaceuticals resulted in part in contradictory conclusions. Consequently, a case by case evaluation has to be done for each type of biopharmaceutical. The aim of this thesis was to contribute to a better understanding of the structure-function relationship of N-glycosylation and pharmacokinetics of monoclonal antibodies and fusion proteins. The model proteins studied in this work were an Fc N-glycosated but not Fab–glycosylated IgG1 and an Fc fusion protein with multiple N-glycosylation sites. Central goal was to establish new highly sensitive, selective and robust analytical methods encompassing an affinity purification and LC-MS. The developed methodologies were to be implemented in the existing preclinical and clinical development. The major objectives were:

- Development of an on-line LC-MS method based on RP chromatography for N-glycan analytics. (**Chapter 2**)
- Development of high sensitivity N-glycosylation analysis of biopharmaceuticals by nanoLC-MS with high-throughput sample preparation. (**Chapter 3**)
- Development and qualification of a high sensitivity affinity purification methodology for the isolation of monoclonal antibodies from complex matrices (serum). (**Chapter 4**)

Use of the developed methods to investigate the

- Influence of glyco-variants on the pharmacokinetics of an IgG1 biopharmaceutical. (**Chapter 5**)

and the

- Influence of glyco-variants on the pharmacokinetics of a therapeutic Fc fusion protein. (**Chapter 6**)

# Chapter 1

## *Introduction: N-glycosylation heterogeneity and the influence on structure, function and pharmacokinetics of monoclonal antibodies and Fc fusion proteins*

This chapter is intended for publication.


### Abstract

Monoclonal antibody drugs are complex and heterogenic protein mixtures with many different variants and modifications. These alterations can greatly influence the structure and function of biopharmaceuticals. N-glycosylation as one of the most complex post-translational modification influences the structural characteristics of the antibodies Fc part thereby modulating the effector functions which potentially affects the pharmacokinetics. Several investigations on the relationship of N-glycosylation and pharmacokinetics have been published; however, this structure-function relationship is not yet fully understood. In this review potential alterations with focus on N-glycosylation of mAbs and Fc fusion proteins and the possible effects on the protein structure and function and finally on the pharmacokinetics are reviewed. The current understandings of the underlying mechanisms are described as well.

## 1.1. Introduction

The fusion of murine myeloma cells with B-cells was a groundbreaking experiment of Köhler and Milstein and made production of antibodies in cell culture possible (*1*). It was the beginning of immunoassays and therapeutic antibodies. In 2012, more than 35 years later, 34 recombinant monoclonal antibodies (mAbs) are marketed in the EU and US, mostly produced in CHO and SP2/0 cells (*2*). The vast majority of marketed mAbs belong to the IgG class or more precisely to the subclasses IgG1 and some IgG2 and IgG4. Two thirds of the marketed mAbs are either human or humanized and a small percentage is chimeric or murine (*2*).

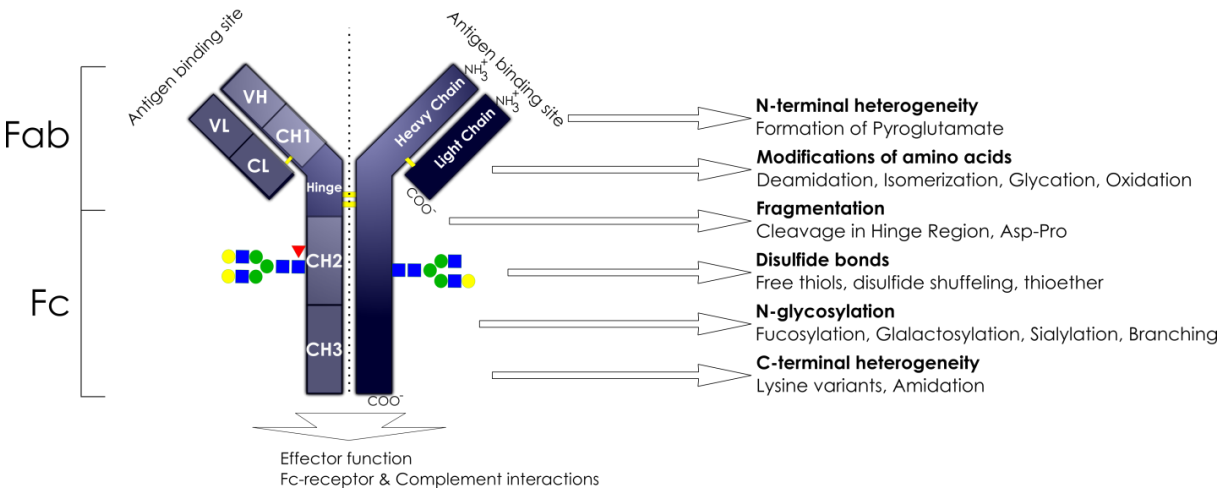


**Figure 1: Schematic structure of an IgG molecule. An IgG consists of two heavy and two light chains that contain several domains. The variable domains VL (variable light) and VH (variable heavy) that form the antigen binding site and the constant domains CL (constant light) and CH1-3 (constant heavy) building the framework. The IgG can be furthermore divided into the Fab (fragment antigen binding) and Fc (fragment crystallizable) which induce the effector functions. On the right possible modifications and alterations of the IgG are listed.**

With more than 1300 amino acids resulting in a mass of approximately 150 kDa mAbs are large molecules built from two heavy chains with 50 kDa each and two light chains with 25 kDa each (Figure 1). The different heavy chains (γ1, γ2, γ3 and γ4) divide the IgGs into their subclasses 1-4. The light chains are the κ-type and λ-type. Heavy and light chains are connected by disulfide bridges giving the antibody its Y-shaped structure (Figure 1). Intra-chain disulfide bridges further stabilize the folding, 16 disulfide bridges per IgG1 and 7 per chain. The heavy and light chains consist of different domains. The variable domains VL (variable light) and VH (variable heavy) contain hypervariable regions that are responsible for antigen binding. The remaining domains are conserved sequences named the constant domains CL (constant light) and CH1-3 (constant heavy). The CH2 domain of each heavy chain contains one N-glycosylation site at approximately Asn297 and about one fifth of human IgGs carry a N-glycosylation motif in the variable region (*3*). The size and structure of

IgGs give rise to a large number of possible alterations and modifications turning IgG drugs and in conclusion recombinant mAb drugs to heterogenic protein mixtures.

The N-terminal amino acid residue, Glu or Gln, can undergo cyclization to pyroglutamate which results in mass reduction of 17 or 18 Da respectively and the loss of the positively charged N-terminal amine (*4*–*7*). Like the N-terminus, the C-terminus may be heterogenous because of different numbers of lysine residues at the heavy chain C-terminus, which in turn introduce additional positive charges (*6*). Deamidation of asparagine to aspartic acid or isoaspartic acid is another possible modification which increases the mass by 1 Da and introduces one additional negative charge to the protein (*4*, *6*, *8*). Deamidation of glutamine is possible too (*9*). Isomerization of aspartic acid to iso-aspartic acid or formation of iso-aspartic acid as a result from deamidation introduces an additional $CH_2$ group to the protein backbone, which can have tremendous effects on the mAb structure depending on the location of the modification (*4*, *6*, *10*, *11*). Glycation, the non-enzymatic addition of a sugar to a primary amine (e.g. to a lysine side chain) of antibodies decreases the positive charge (*6*, *12*). Oxidation of methionine, tyrosine, tryptophan, histidine or cysteine increases the size by 16 Da per oxidation reaction and increases the polarity of the respective residue (*4*, *6*). Disulfide bond exchange and fragmentation of the IgG backbone, e.g. in the hinge region resulting in the loss of an entire antigen binding arm are also possible alterations of IgGs. All these alteration can have tremendous influence on the structure and function of monoclonal antibodies. The most complex post-translational modification of antibodies, N-glycosylation, is discussed in detail in the following.

## 1.2. N-glycosylation and its influence on mAb structure and mAb effector function

Like most extracellular glycoproteins, therapeutic proteins and specifically also mAbs undergo glycosylation in the ER and Golgi network of cells. The glycan structures of mAbs are important for the efficacy and safety of the drug (*13*). Consequently, glyco-engineering, controlled biosynthesis of only distinct glycan structures is of high interest and some sophisticated approaches have been described (*14*, *15*).

Monoclonal antibodies have one conserved N-linked glycosylation at the Fc part at position N297. Approximately 20% contain a second N-linked glycosylation site in their variable region. Both sites are located on the heavy chain (*3*, *13*). Glycosylation of biopharmaceuticals shows a high grade of heterogeneity and N-glycans belong to the most complex and diverse structures in nature due to the high number of different sugar moieties and the multitude of possible linkages. Figure 2 shows the three different N-glycan types high mannose, complex

and hybrid that are found on IgGs with their respective linkage. Complex and hybrid type exist with core fucosylation, addition of a fucose residue to the innermost N-acetylglucosamine, and without core fucosylation.

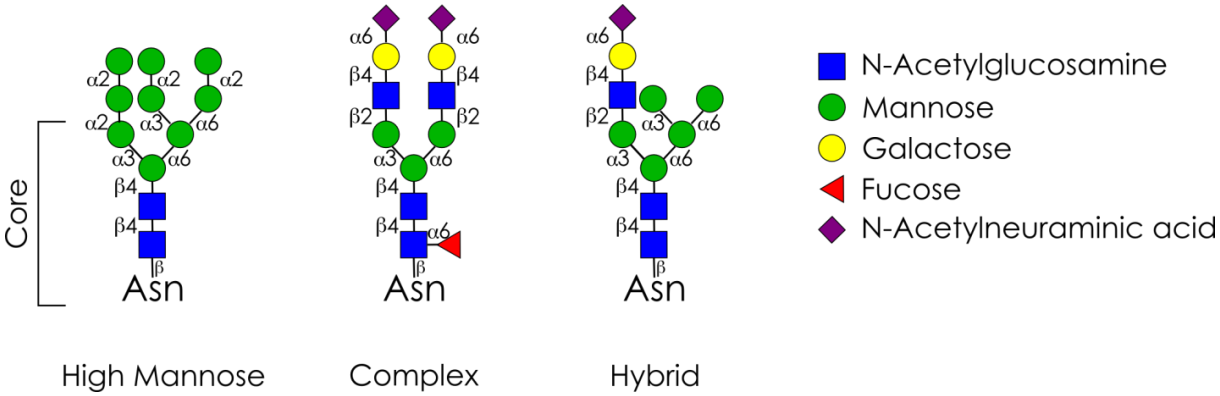


**Figure 2: Types of N-glycans. The three different types (High Mannose, Complex and Hybrid) share a common core structure including the first two N-acetylglucosamine residues and the first three mannose residues.**

mAbs represent a special group of glycoproteins as their N-glycans are of limited size. This circumstance can be explained by the buried glycosylation site in the CH2 domain at Asn297, mAbs are usually free of N-glycans with more than two antennae and furthermore the sialic acid content is low compared with other glycoproteins (*16*). Typically, antibodies contain a high percentage of complex bi-antennary glycans with core-fucosylation (*16*–*18*).

N-glycans have important structural functions. They stabilize the CH2 domain of IgGs and deglycosylation makes mAbs thermally less stable and more susceptible to chaotrope induced unfolding. In addition deglycosylated mAbs are more prone for aggregation (*19*). Beside the thermal and the colloidal stability, also the functionality of the IgG is influenced by the attached N-glycans and their size (*20*). In addition to the stabilization of the CH2 domain the attached N-glycans greatly influence the folding of the Fc part. *Krapp et al.* investigated crystalized Fc parts of IgG molecules with different homogenous glycosylations and could demonstrate that the conformation of the CH2 domain depends on the attached N-glycans (*21*). Larger N-glycans, e.g. bi-antennary complex type with terminal galactosylation, open up the Fc part in the CH2 region to a horseshoe like structure whereas smaller attached N-glycans like the core structure favors a more “closed” Fc conformation. This open and closed formation can greatly influence the effector functions induced by interactions of the Fc part with Fc receptor molecules. The fact that crystallization of deglycosylated IgG was not possible due to the high flexibility of the CH2 domain shows the importance of N-glycan protein interactions (*21*). Hydrogen/Deuterium exchange MS experiments resulted in similar findings. *Houde et al*. showed that terminal galactosylation has major impact on the

conformation of the Fc part and that fucosylation alone does not impact the conformation (*22*). NMR analysis of G2F glycosylated mAbs revealed that the terminal galactose residues are exposed and accessible for protein binding and that there are differences between the 1,3 and the 1,6 arm concerning flexibility and accessibility (*23*). These findings led to the assumption that Fc N-glycosylation influences the effector function of proteins interacting with the CH2 domain. Upon antigen binding mAbs are able to induce effector functions mediated by their Fc-part. By binding to Fc-receptors or complement proteins mAbs induce ADCC (antibody dependent cell-mediated cytotoxicity) or CDC (complement dependent cytotoxicity), respectively. ADCC is induced after binding of Fc-γ receptors (FcγR) to the Fc part (*24*). The affinity of FcγRs to the Fc part is influenced by N-glycosylation in the CH2 domain (*22*, *25*–*28*). As a consequence ADCC is enhanced for IgGs with lower fucosylation (*25*, *29*). Binding affinity of the complement protein C1q to the IgG Fc which is involved in CDC is also influenced by N-glycosylation. and an increasing content of terminal galactose enhances CDC (*29*). By influencing CDC and ADCC, two important effector functions of therapeutic mAbs, N-glycosylation was thought to also have an impact on the pharmacokinetics of the glycosylated biopharmaceuticals.

## 1.3. Pharmacokinetics of mAbs

Monoclonal antibodies are large and complex structures with a different behavior in terms of their pharmacology and pharmacokinetics (PK) compared to low molecular weight drugs. Monoclonal antibodies show dose-dependent maximal concentrations typically in the range of µg/ml (nM range). mAbs typically exhibit a body half-life between 10 and 25 days, since they are not eliminated through kidney filtration due to their size and additionally escape fast degradation in the lysosomes through the neonatal Fc receptor (FcRn) recycling mechanism (*30*, *31*). mAbs are usually administered by subcutaneous (sc), intramuscular (im) or intravenous (iv) injection. Whereas iv bioavailability is 100% per definition, for sc and im administration bioavailability values of 50 to 100% are reported (*30*).

## 1.4. N-glycosylation and Pharmacokinetics

Already in the 1970s, first evidence for the influence of sialic acids on the pharmakokinetics of glycoproteins was reported. *Morell et al*. observed that desialylated plasma proteins were cleared faster from circulation after injection into rats (*32*). There are two known major pathways for selective glycoprotein clearance. Glycoproteins in circulation with accessible terminal galactosylation are bound and cleared by the asialoglycoprotein receptor expressed

in the liver (*33*, *34*). The second way of selective clearance of glycoproteins is through the mannose receptor (MR) which is most markedly expressed on immune cells (*35*–*37*). The mannose receptor binds selectively to mannose and N-Acetylglucosamine residues of N-glycans (*35*, *36*). Beside these pathways distinct mAb glycoforms may be faster cleared from circulation due to enhanced affinity to specific proteins rendering effector function (e.g. ADCC or CDC). The enzymatic conversion of glycans *in vivo* is the third option explaining the selective removal of distinct glycoforms. These possible pathways are pictured in Figure 1.

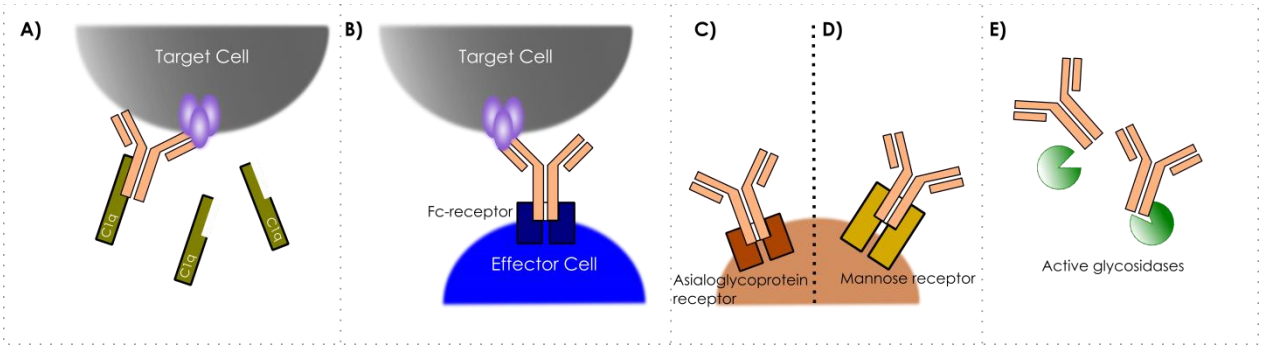


**Figure 3: N-glycosylation specific IgG interactions with a potential effect on the pharmacokinetics. (A) CDC activation through binding of C1q to the Fc part removes mAb from circulation. (B) ADCC is activated by binding of FcγR to the Fc part which is influenced by glycosylation. (C) Asialoglycoprotein receptor and (D) Mannose receptor mediated clearance routes of glycoproteins from circulation. (E) Enzymatic conversion of the mAb N-glycans during circulation by glycosidases.**

There are two basic options to investigate the effect of different glyco-variants on protein pharmacokinetics. Either distinct glyco-variants are enriched and compared in several study groups or the relative composition of different glyco-variants is directly followed in one study group. *Millward et al*. studied a mAb enriched to a high mannose portion at the Fc part of approximately 50% and a second mAb enriched for glycosylation in the Fab region. The PK profiles of the different mAb preparations were compared in mice by ELISA and the glycan pattern was analyzed at several time points by HPLC. No significant differences in PK properties were found (*38*). A second investigation in mice which compared PK parameters of degalactosylated IgGs with non-modified IgG came to the conclusion that degalactosylated IgG with terminal GlcNAc has a significantly longer half-life (*39*). Production and characterization of three differently glycosylated mAb qualities (Hybrid (+/- F), Complex (+/- F) and high mannose) against CD20 with bioassays (CDC, ADCC) and an in vivo study in mice demonstrated that the complex glycosylated mAb has a longer half-life, which is independent from fucosylation. Hybrid glycosylated mAb has a slightly shorter half-life and high mannose glycosylated mAb showed a strong decrease in half-life (*40*). Summarizing, the results from mice glycan PK profiling render an unclear picture with two studies reaching contradictory conclusions concerning the influence of high mannose structures on mAb PK in mice (*38*, *40*).

Analysis of affinity purified mAb (IgG2) from clinical samples of two healthy human test subjects showed that the relative contribution of high mannose species M6-M9 to the total mAb plasma concentration decreased over time whereas M5 levels increased about the same percentage. It was hypothesized that the reduction of the IgG2 high mannose glycan blood levels is due to glycosidase activity in serum converting M6-M9 into M5 and not due to faster clearance. This hypothesis was supported with results from an *in vitro* assay. Incubation of the IgG2 in serum led to the same high mannose conversion as observed in the case study (*41*). The same group later published a second glycan PK profiling by mass spectrometry approach based on glycopeptide analysis by MS (*42*). Analysis of samples from four human subjects after administration of either one IgG1 or one of three IgG2 molecules resulted in the finding that high mannose N-glycan M5 is selectively cleared from serum (Figure 4) (*42*). The authors furthermore showed that the IgG1 M5:M5 glycoform, the pairing of two M5 glycosylated heavy chains during protein biosynthesis is favored. A similar investigation of an IgG1 biopharmaceutical in humans confirmed the previously published (*41*) conversion of high mannose glycans *in vitro*. The results of the clinical study including 15 healthy volunteers published in combination with the *in vitro* study showed that M5 had an increased serum clearance whereas M6 and M7 decreased in the first 6 h after administration followed by decreasing M5 levels and constant M6 and M7 (*43*).

The production of mAbs with one distinct N-glycan and administration to mice demonstrated that a mAb with only M5 or M8/9 has an increased clearance and a shorter half-life. Furthermore, it was highlighted that the glycan pattern of the mAb with M8/9 changed over time to a high percentage of M6. This observation could be reproduced *in vitro* by incubation of the mAb in mice serum (*44*). The conversion of high mannose glycans to M6 instead of M5 reported for mice implies a different underlying mechanism. A mouse study comparing yeast N-glycosylation (yeast specific high mannose type) and human glycosylation (complex type) revealed that antibodies carrying yeast glycosylation have shorter serum half-life than antibodies with human glycosylation (*45*). The influence of the glycosylation of the variable domain on antibody clearance was investigated by different groups (*38*, *46*). As already mentioned *Millward et al.* did not find any influence of the variable domain N-glycosylation on the PK. In contrast *Huang et al.* came to the conclusion that molecules with bi-antennary glycans lacking galactosylation (terminal GlcNAc) attached in the variable domain are cleared slightly faster from circulation (*46*).

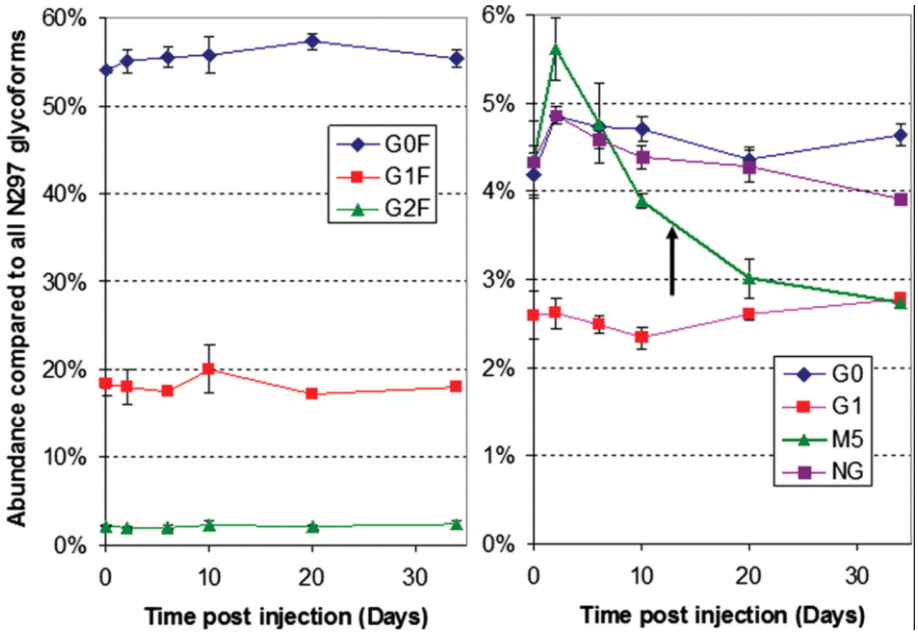


**Figure 4: Reprinted from Goetze et *al.* with permission (*42*). The average percentages of IgG1 N297 glycans from two subjects dosed with 1000 mg IgG1 intravenously are represented. Values represent the relative levels based on MS peak areas of all identified N297 glycopeptides. Error bars represent the range. Full-scale view shows several of the most abundant peptides (left); zoomed view showing representative lower abundance glycopeptides (right).**

Fc part containing fusion proteins are closely related to mAbs, because of the effector function induced by the Fc part of both biopharmaceuticals. Fc fusion proteins often carry several N-glycosylation sites in the non-IgG fusion protein part (*47–49*). There are a few reports on an influence of the terminal glycan residues of Fc fusion proteins on PK. Keck et al. compared Fc fusion protein batches with different N-glycosylation pattern, specifically terminal GlcNAc, galactosylation and sialylation (*49*). However, no site specific N-glycan analysis was performed which would enable to link effects to the Fc or the fusion protein part. The authors found that terminal GlcNAc is cleared faster. It was hypothesized that the mannose receptor might be responsible for the clearance as the 3D structure of the receptors demonstrated that the receptor can bind terminal GlcNAc containing glycans (*49*). In accordance with these findings *Jones et al.* represented that N-glycans with terminal GlcNAc residues have a higher clearance rate. Their protein of interest was the fusion protein lenercept containing a Fc part and two extracellular domains of a TNF-alpha receptor. Sialic acids and terminal galactosylation revealed only minor to no impact on the PK (*48*). *Kogelberg et al.* postulated a clearance mechanism for highly mannosylated proteins after studying an antibody Fc-enzyme fusion protein produced in the yeast *P. Pastoris*. They provided evidence for clearance of the glycoprotein by the mannose receptor, a glycan specific receptor which is expressed in sinusoidal endothelial cells in the liver (*50*). Reports from *Liu et al.* comparing differently glycosylated fusion proteins and mAbs produced in either glyco-engineered *P. Pastoris* or CHO cells highlighted that the sialic acid content of

fusion proteins modulates the pharmacokinetics (*45*, *51*). Lower levels of sialic acids correlated with decreased serum half-life.

## 1.5. Analysis of N-glycosylation in pharmacokinetic studies

Immunoassays became the reference technique for PK-studies of therapeutic proteins, especially ELISA where the protein is captured by a specific antibody or in the case of therapeutic antibodies also by an anti-idiotypic antibody, an anti-species antibody or the appropriate antigen and finally detected by an enzyme-linked secondary antibody (*52*). However structural changes like deamidation, oxidation and especially the heterogeneity of glycoforms of the therapeutic protein, as discussed in previous sections, could alter the pharmacokinetic properties (*53*, *54*) and immunoassay techniques are not able to detect such types of differences (*52*, *55*). ELISA purely quantifies proteins and cannot distinguish between glyco-variants. Hence different analytical techniques are necessary. For the investigation of individual N-glycans LC and MS based approaches were mostly used in the previously described literature (*38*, *40–43*, *46–48*). Beside the analysis of intact glycoproteins which provides information about the most abundant glycoforms, the analysis of glycopeptides and released N-glycans is frequently used. Enzymatic release of N-glycans following labeling with a fluorophore like 2-AB or 2-AA and analysis by LC or LC-MS is perhaps the most widespread approach used in industry and academia (*17*, *18*, *56–61*). More sensitive approaches like nanoLC-MS, CE and CE-MS with LIF detection are also common and suitable for glycan related PK investigations (*62–69*). The advantage of these technologies for the glycan PK profiling is the possibility to analyze each N-glycan individually from a complex mixture which in turn leads to more accurate results compared to e.g. studies employing immunoassays after enrichment of specific glycoforms.

## 1.6. Conclusion

Monoclonal antibody drugs are complex and heterogeneous protein mixtures. The N-glycosylation on the antibody structure influences the function. Several investigations were published during the last decade trying to shed light on the relationship between N-glycosylation and pharmacokinetics. In some studies distinct glycosylation fractions were enriched. However, with this approach a new artificial glycosylation pattern is generated that does not reflect the normal N-glycosylation of the biologic of interest and may render different outcome. The benefit of this approach is that simple standard analytics e.g. utilizing immunoassays can be performed to characterize the PK. Individual N-glycans analysis by MS based approaches can be used to analyze the heterogeneous biopharmaceutical directly. The major advantage of this MS approach is that the N-glycan levels can be analyzed in a relative manner. Individual N-glycans with influence on the PK can be identified rather simply. However, the MS approach requires high sensitivity.

The studies investigating the relationship between N-glycosylation and pharmacokinetics led to in part contradictory findings. Overall, it is conclusive that high mannose glycans influence the PK of IgGs by increasing the clearance rate. For other N-glycans and glycoforms the results are less clear. Two studies investigating IgG variable domain glycosylation rendered inconsistent results and another study comparing differently glycosylated enriched fractions reported no difference. These inconsistent findings may be due to differences in study set-up (e.g. enrichment of distinct glycoforms), species (mouse, human), IgG subclass and IgG source (human, humanized, etc.).

Results for the more complex glycosylated Fc fusion proteins with additional glycosylation sites in the fusion protein part also show an unclear picture for the effect of N-glycosylation on the pharmacokinetics. The N-glycans of the fusion proteins were mostly analyzed without site specificity. The N-glycans at the Fc part are buried between the heavy chains whereas the receptor part N-glycans could be more accessible for the interaction with specific enzymes or receptors. This phenomenon could result in different impact on the pharmacokinetics.

Thus, over the last decade several investigations on the relationship between N-glycosylation of therapeutic proteins and pharmacokinetics were performed. With the use of sensitive technologies like LC-MS it became possible to change the analysis from comparing fractions of biopharmaceuticals enriched for specific N-glycans to the direct analysis of the complex glycosylated biopharmaceutical of interest. This results in more reproducible findings. With the rising number of biopharmaceuticals and biosimilars in development the need for N-

glycan PK profiling and comparative studies will rise as well as the need for glyco-engineering and optimization.

## 1.7. References:

1. G. Köhler, C. Milstein, Continuous cultures of fused cells secreting antibody of predefined specificity, *Nature* **256**, 495–497 (1975).

2. J. M. Reichert, Marketed therapeutic antibodies compendium., *MAbs* **4**, 413–5 (2012).

3. C. a. Abel, H. L. Spiegelberg, H. M. Grey, Carbohydrate content of fragments and polypeptide chains of human .gamma.G-myeloma proteins of different heavy-chain subclasses, *Biochemistry* **7**, 1271–1278 (1968).

4. W. E. I. Wang *et al.*, Antibody Structure , Instability , and Formulation, **96**, 1–26 (2007).

5. Y. D. Liu, A. M. Goetze, R. B. Bass, G. C. Flynn, N-terminal glutamate to pyroglutamate conversion in vivo for human IgG2 antibodies., *J. Biol. Chem.* **286**, 11211–7 (2011).

6. H. Liu, G. Gaza-Bulseco, D. Faldu, C. Chumsae, J. Sun, Heterogeneity of monoclonal antibodies., *J. Pharm. Sci.* **97**, 2426–47 (2008).

7. F. Matsuda *et al.*, The complete nucleotide sequence of the human immunoglobulin heavy chain variable region locus., *J. Exp. Med.* **188**, 2151–62 (1998).

8. D. Chelius, D. S. Rehder, P. V Bondarenko, Identification and characterization of deamidation sites in the conserved regions of human immunoglobulin gamma antibodies., *Anal. Chem.* **77**, 6004–11 (2005).

9. H. Liu, G. Gaza-bulseco, C. Chumsae, Glutamine deamidation of a recombinant monoclonal antibody, , 4081–4088 (2008).

10. L. W. Dick, D. Qiu, R. B. Wong, K.-C. Cheng, Isomerization in the CDR2 of a monoclonal antibody: Binding analysis and factors that influence the isomerization rate., *Biotechnol. Bioeng.* **105**, 515–23 (2010).

11. R. J. Harris *et al.*, Identification of multiple sources of charge heterogeneity in a recombinant antibody., *J. Chromatogr. B. Biomed. Sci. Appl.* **752**, 233–45 (2001).

12. A. M. Goetze, Y. D. Liu, T. Arroll, L. Chu, G. C. Flynn, Rates and Impact of Human Antibody Glycation In Vivo., *Glycobiology* **22**, 221–234 (2011).

13. R. Jefferis, Glycosylation as a strategy to improve antibody-based therapeutics., *Nat. Rev. Drug Discov.* **8**, 226–34 (2009).

14. K. M. Cox *et al.*, Glycan optimization of a human monoclonal antibody in the aquatic plant Lemna minor., *Nat. Biotechnol.* **24**, 1591–7 (2006).

15. A. Beck *et al.*, Trends in glycosylation, glycoanalysis and glycoengineering of therapeutic antibodies and Fc-fusion proteins., *Curr. Pharm. Biotechnol.* **9**, 482–501 (2008).

16. G. C. Flynn, X. Chen, Y. D. Liu, B. Shah, Z. Zhang, Naturally occurring glycan forms of human immunoglobulins G1 and G2., *Mol. Immunol.* **47**, 2074–82 (2010).

17. F. Higel, U. Demelbauer, A. Seidl, W. Friess, F. Sörgel, Reversed-phase liquid-chromatographic mass spectrometric N-glycan analysis of biopharmaceuticals., *Anal. Bioanal. Chem.* **405**, 2481–93 (2013).

18. X. Chen, G. C. Flynn, Analysis of N-glycans from recombinant immunoglobulin G by on-line reversed-phase high-performance liquid chromatography/mass spectrometry., *Anal. Biochem.* **370**, 147–61 (2007).

19. K. Zheng, C. Bantog, R. Bayer, The impact of glycosylation on monoclonal antibody conformation and stability., *MAbs* **3**, 568–76 (2011).

20. Y. Mimura *et al.*, The influence of glycosylation on the thermal stability and effector function expression of human IgG1-Fc: properties of a series of truncated glycoforms., *Mol. Immunol.* **37**, 697–706 (2001).

21. S. Krapp, Y. Mimura, R. Jefferis, R. Huber, P. Sondermann, Structural Analysis of Human IgG-Fc Glycoforms Reveals a Correlation Between Glycosylation and Structural Integrity, *J. Mol. Biol.* **325**, 979–989 (2003).

22. D. Houde, Y. Peng, S. a Berkowitz, J. R. Engen, Post-translational modifications differentially affect IgG1 conformation and receptor binding., *Mol. Cell. Proteomics* **9**, 1716–28 (2010).

23. A. W. Barb, J. H. Prestegard, NMR analysis demonstrates immunoglobulin G N-glycans are accessible and dynamic., *Nat. Chem. Biol.* **7**, 147–53 (2011).

24. S. Radaev, P. Sun, Recognition of immunoglobulins by Fcgamma receptors., *Mol. Immunol.* **38**, 1073–83 (2002).

25. R. Abès, J.-L. Teillaud, Impact of Glycosylation on Effector Functions of Therapeutic IgG, *Pharmaceuticals* **3**, 146–158 (2010).

26. G. Zou *et al.*, Chemoenzymatic Synthesis and Fcγ Receptor Binding of Homogeneous Glycoforms of Antibody Fc Domain . Presence of a Bisecting Sugar Moiety Enhances the Affinity of Fc to FcγIIIa Receptor, *J. Am. Chem. Soc.* **133**, 18975–18991 (2011).

27. Y. Mimura *et al.*, Role of oligosaccharide residues of IgG1-Fc in Fc gamma RIIb binding., *J. Biol. Chem.* **276**, 45539–47 (2001).

28. M. Satoh, S. Iida, K. Shitara, Non-fucosylated therapeutic antibodies as next-generation therapeutic antibodies., *Expert Opin. Biol. Ther.* **6**, 1161–73 (2006).

29. T. S. Raju, Terminal sugars of Fc glycans influence antibody effector functions of IgGs., *Curr. Opin. Immunol.* **20**, 471–8 (2008).

30. E. D. Lobo, R. J. Hansen, J. P. Balthasar, Antibody pharmacokinetics and pharmacodynamics., *J. Pharm. Sci.* **93**, 2645–68 (2004).

31. D. C. Roopenian, S. Akilesh, FcRn: the neonatal Fc receptor comes of age., *Nat. Rev. Immunol.* **7**, 715–25 (2007).

32. A. G. Morell, G. Gregoriadis, I. H. Scheinberg, J. Hickman, G. Ashwell, The role of sialic acid in determining the survival of glycoproteins in the circulation., *J. Biol. Chem.* **246**, 1461–7 (1971).

33. R. J. Stockert, The asialoglycoprotein receptor: relationships between structure, function, and expression., *Physiol. Rev.* **75**, 591–609 (1995).

34. G. Ashwell, J. Harford, Carbohydrate-specific receptors of the liver., *Annu. Rev. Biochem.* **51**, 531–54 (1982).

35. P. Allavena, M. Chieppa, P. Monti, L. Piemonti, From Pattern Recognition Receptor to Regulator of Homeostasis: The Double-Faced Macrophage Mannose Receptor, *Crit. Rev. Immunol.* **24**, 179–192 (2004).

36. S. J. Lee *et al.*, Mannose receptor-mediated regulation of serum glycoprotein homeostasis., *Science* **295**, 1898–901 (2002).

37. P. R. Taylor, S. Gordon, L. Martinez-Pomares, The mannose receptor: linking homeostasis and immunity through sugar recognition., *Trends Immunol.* **26**, 104–10 (2005).

38. T. a Millward *et al.*, Effect of constant and variable domain glycosylation on pharmacokinetics of therapeutic antibodies in mice., *Biologicals* **36**, 41–7 (2008).

39. M. M. Newkirk, J. Novick, M. M. Stevenson, M. J. Fournier, P. Apostolakos, Differential clearance of glycoforms of IgG in normal and autoimmune-prone mice., *Clin. Exp. Immunol.* **106**, 259–64 (1996).

40. Y. Kanda *et al.*, Comparison of biological activity among nonfucosylated therapeutic IgG1 antibodies with three different N-linked Fc oligosaccharides: the high-mannose, hybrid, and complex types., *Glycobiology* **17**, 104–18 (2007).

41. X. Chen, Y. D. Liu, G. C. Flynn, The effect of Fc glycan forms on human IgG2 antibody clearance in humans., *Glycobiology* **19**, 240–9 (2009).

42. A. M. Goetze *et al.*, High-mannose glycans on the Fc region of therapeutic IgG antibodies increase serum clearance in humans., *Glycobiology* **21**, 949–59 (2011).

43. L. Alessandri, D. Ouellette, A. Acquah, Increased serum clearance of oligomannose species present on a human IgG1 molecule, *MAbs* , 1–12 (2012).

44. M. Yu, D. Brown, C. Reed, S. Chung, J. Lutman, Production, characterization, and pharmacokinetic properties of antibodies with N-linked Mannose-5 glycans, *MAbs* , 1–13 (2012).

45. L. Liu *et al.*, Pharmacokinetics of IgG1 monoclonal antibodies produced in humanized Pichia pastoris with specific glycoforms: a comparative study with CHO produced materials., *Biologicals* **39**, 205–10 (2011).

46. L. Huang, S. Biolsi, K. R. Bales, U. Kuchibhotla, Impact of variable domain glycosylation on antibody clearance: an LC/MS characterization., *Anal. Biochem.* **349**, 197–207 (2006).

47. J. Bongers *et al.*, Characterization of glycosylation sites for a recombinant IgG1 monoclonal antibody and a CTLA4-Ig fusion protein by liquid chromatography-mass spectrometry peptide mapping., *J. Chromatogr. A* **1218**, 8140–9 (2011).

48. A. J. S. Jones *et al.*, Selective clearance of glycoforms of a complex glycoprotein pharmaceutical caused by terminal N-acetylglucosamine is similar in humans and cynomolgus monkeys., *Glycobiology* **17**, 529–40 (2007).

49. R. Keck *et al.*, Characterization of a complex glycoprotein whose variable metabolic clearance in humans is dependent on terminal N-acetylglucosamine content., *Biologicals* **36**, 49–60 (2008).

50. H. Kogelberg *et al.*, Clearance mechanism of a mannosylated antibody-enzyme fusion protein used in experimental cancer therapy., *Glycobiology* **17**, 36–45 (2007).

51. L. Liu *et al.*, The Impact of Glycosylation on the Pharmacokinetics of a TNFR2:Fc Fusion Protein Expressed in Glycoengineered Pichia Pastoris., *Pharm. Res.* (2012), doi:10.1007/s11095-012-0921-3.

52. E. Ezan, F. Bitsch, Critical comparison of MS and immunoassays for the bioanalysis of therapeutic antibodies., *Bioanalysis* **1**, 1375–88 (2009).

53. W. Wang *et al.*, Impact of methionine oxidation in human IgG1 Fc on serum half-life of monoclonal antibodies., *Mol. Immunol.* **48**, 860–6 (2011).

54. H. Li, M. d'Anjou, Pharmacological significance of glycosylation in therapeutic proteins., *Curr. Opin. Biotechnol.* **20**, 678–84 (2009).

55. L. Huang, J. Lu, V. J. Wroblewski, J. M. Beals, R. M. Riggin, In vivo deamidation characterization of monoclonal antibody by LC/MS/MS., *Anal. Chem.* **77**, 1432–9 (2005).

56. K. R. Anumula, New HPLC Assay for Glycosyltransferases Based on Derivatization with Anthranilic Acid and Fluorescence Detection., *Glycobiology* **22**, 912–917 (2012).

57. M. Melmer *et al.*, HILIC analysis of fluorescence-labeled N-glycans from recombinant biopharmaceuticals., *Anal. Bioanal. Chem.* , 905–914 (2010).

58. M. Melmer, T. Stangler, A. Premstaller, W. Lindner, Comparison of hydrophilic-interaction, reversed-phase and porous graphitic carbon chromatography for glycan analysis., *J. Chromatogr. A* **1218**, 118–23 (2011).

59. B. D. Prater, H. M. Connelly, Q. Qin, S. L. Cockrill, High-throughput immunoglobulin G N-glycan characterization using rapid resolution reverse-phase chromatography tandem mass spectrometry., *Anal. Biochem.* **385**, 69–79 (2009).

60. L. R. Ruhaak *et al.*, Hydrophilic interaction chromatography-based high-throughput sample preparation method for N-glycan analysis from total human plasma glycoproteins., *Anal. Chem.* **80**, 6119–26 (2008).

61. K. R. Anumula, S. T. Dhume, High resolution and high sensitivity methods for oligosaccharide mapping and characterization by normal phase high performance liquid chromatography following derivatization with highly fluorescent anthranilic acid., *Glycobiology* **8**, 685–94 (1998).

62. L. a Gennaro, J. Delaney, P. Vouros, D. J. Harvey, B. Domon, Capillary electrophoresis/electrospray ion trap mass spectrometry for the analysis of negatively

charged derivatized and underivatized glycans., *Rapid Commun. Mass Spectrom.* **16**, 192–200 (2002).

63. R. Haselberg, V. Brinks, a Hawe, G. J. de Jong, G. W. Somsen, Capillary electrophoresis-mass spectrometry using noncovalently coated capillaries for the analysis of biopharmaceuticals., *Anal. Bioanal. Chem.* **400**, 295–303 (2011).

64. M. Nakano *et al.*, Capillary electrophoresis-electrospray ionization mass spectrometry for rapid and sensitive N-glycan analysis of glycoproteins as 9-fluorenylmethyl derivatives., *Glycobiology* **19**, 135–43 (2009).

65. L. a Gennaro, O. Salas-Solano, On-line CE-LIF-MS technology for the direct characterization of N-linked glycans from therapeutic antibodies., *Anal. Chem.* **80**, 3838–45 (2008).

66. L. a Gennaro, D. J. Harvey, P. Vouros, Reversed-phase ion-pairing liquid chromatography/ion trap mass spectrometry for the analysis of negatively charged, derivatized glycans., *Rapid Commun. Mass Spectrom.* **17**, 1528–34 (2003).

67. I. Ritamo, J. Räbinä, S. Natunen, L. Valmu, Nanoscale reversed-phase liquid chromatography-mass spectrometry of permethylated N-glycans., *Anal. Bioanal. Chem.* **405**, 2469–80 (2013).

68. M. Wuhrer, C. a M. Koeleman, A. M. Deelder, C. H. Hokke, Normal-phase nanoscale liquid chromatography-mass spectrometry of underivatized oligosaccharides at low-femtomole sensitivity., *Anal. Chem.* **76**, 833–8 (2004).

69. H. Kalay *et al.*, Online nanoliquid chromatography-mass spectrometry and nanofluorescence detection for high-resolution quantitative N-glycan analysis., *Anal. Biochem.* **423**, 153–162 (2012).

# Chapter 2

## *Reversed-phase liquid-chromatographic mass spectrometric N-glycan analysis of biopharmaceuticals*

Published in *Analytical and Bioanalytical Chemistry*, 2013, 405:2481-2493, doi: 10.1007/s00216-012-6690-3, *Fabian Higel, Uwe Demelbauer, Andreas Seidl, Wolfgang Friess & Fritz Sörgel*

### Abstract

*N*-Glycosylation is a common post-translational modification of monoclonal antibodies with a potential effect on the efficacy and safety of the drugs; detailed knowledge about this glycosylation is therefore crucial. We have developed a reversed-phase liquid chromatographic–mass spectrometric method, with different fluorescent labels, for analysis of *N*-glycosylation, and compared the sensitivity and selectivity of the methods. Our work demonstrates that anthranilic acid as fluorescent label in combination with reversed-phase liquid chromatography–mass spectrometry is an advantageous method for identification and quantification of neutral and acidic N-glycans. Our results show that mass spectrometry-based quantification correlates with quantification by fluorescence. Chromatographic discrimination between several structural glycan isomers was achieved. The sharp peaks of the eluting anthranilic acidlabeled N-glycans enabled on-line mass spectrometric analysis of even low-abundance glycan species. The method is broadly applicable to N-glycan analysis and is an orthogonal analytical method to the widely established hydrophilicinteraction liquid chromatography of 2-aminobenzamidelabeled N-glycans for characterization of N-glycans derived from biopharmaceuticals.

Keywords: Anthranilic acid, 2-aminobenzamide, Mass spectrometry, N-glycosylation, Reversed-phase chromatography, Monoclonal antibody

## 2.1. Introduction

Recombinant protein drugs are the most complex active pharmaceutical ingredients. Monoclonal antibodies (mAbs), glycoproteins with a molecular mass of approximately 150kDa are one important class. Glycosylation has attracted interest because many investigations have shown that such modification may have an effect on the safety and efficacy of these therapeutic protein drugs (*1*–*5*). In general, IgGs have one conserved *N*-glycosylation site on each heavy chain at their Fc part, usually at approximate position 297 of the heavy chain, and several mAbs carry a second *N*-glycosylation site in their variable region. The heterogeneity of the N-glycans attached to these sites is very high, far more than a dozen different glycans can be found (*6*). Identification and quantification of the glycans in this mixture is difficult, and Structural isomers of several glycans make discrimination even more difficult (*7*–*9*). A comprehensive analytical approach is therefore required. *N*-glycosylation can be studied after enzymatic release of the glycans by use of peptide *N*-glycosidase F (PNGaseF), by liquid chromatography, mass spectrometry (MS) (*10*) or by a combination of both technologies (*9*–*14*)**.** Structural analysis of underivatized or labeled N-glycans is usually performed by MALDI-MS or by use of porous graphitized carbon (PGC) liquid chromatography in combination with on-line ESI $MS^2$ (*15*–*17*).

Underivatized N-glycans have no light-absorbing properties. They can be derivatized with a fluorophore (*18*) for quantitative analysis by HPLC. Labeling with a fluorescent dye via reductive amination is widely used (*12*, *18*). This derivatization results in high sensitivity and, because every N-glycan carries only one label, irrespective of size or branching, quantitative information can be obtained from the intensity of the fluorescence signal. The tag not only enables UV or fluorescence detection - it also improves ionization and fragmentation of the labeled N-glycan in ESI-MS (*19*, *20*).

For characterization of N-glycans derived from biopharmaceuticals 2-aminobenzamide (2-AB) is routinely used as label (*19*, *21*, *22*), typically with separation and quantification by HILIC (Hydrophilic interaction liquid chromatography) with fluorescence detection (*23*). HILIC results in high resolution and selectivity for many glycan isomers (*24*). However the small injection volume of aqueous samples necessary, solvent conditions that are essential because of the solubility of the glycans, leads to reduced sensitivity in on-line MS detection and the buffered mobile phase may lead to ion suppression.

In contrast with this, the mobile phases used for RP HPLC usually consist only of water, an organic solvent and an acid; they are, therefore highly MS compatible. In addition, there are almost no limitations with regard to injection volumes of aqueous solutions, which results in high sensitivity. It has been shown that RP LC-MS of 2-AB or ANTS derivatized oligosaccharides can be performed and used to characterize the *N*-glycosylation pattern of mAbs (*13*, *14*, *25*, *26*).However, 2-AB as fluorescent tag adds only weak hydrophobicity to

the hydrophilic glycan which necessitates use of a shallow and long chromatography gradient. Furthermore, labeled acidic glycans elute early and are poorly separated (*13*). This limitationwas solved by Melmer et al. (*24*) by addition of an ion pairing reagent. However, use of an ion-pairing reagent again leads to ion suppression and thus reduced MS sensitivity. For analysis of negatively charged N-glycans containing sialic acids labeling with a negatively charged tag, for example 2-aminobenzoic acid (2-AA) or 8-aminonaphthalene-1,3,6-trisulfonic acid(ANTS) and MS detection in negative ionization mode is frequently used (*14*, *27–29*). *Prien et al.* separated oligomannose structures (especially Mannose 5 isomers) by RP LC after 2-AA derivatization and analyzed them by use of MS in negative mode (*28*). The ability to separate complex N-glycan mixtures or isomers, for example the G1F N-glycans with either 1,3 or 1,6 galactosylation, highly abundant in most mAbs, has not been reported for any N-glycan RP-LC approach.

To provide solutions for the above mentioned limitations of current N-glycan analytical methods we have developed and optimized an RP LC-MS method with positive ionization for characterization of complex *N*-glycosylation profiles. The method was designed to characterize acidic and neutral N-glycans in a single LC-MS approach. We compared the sensitivity and selectivity of 2-AB and 2-AA as fluorescent labels and showed that our newly developed 2-AA RP LC-MS method has advantageous sensitivity and selectivity for a variety of structural isomers analysis of which has not yet been reported in literature. By comparing results from quantitative MS and from FLD we also demonstrated that quantification of mAb glycans by these methods leads to very similar results. The method is versatile and can be used to address various questions in glycobiology or glycomics, from basic screening of N-glycan composition, because of the grouping of the N-glycan types to detailed analysis of low-abundance glycan species. Furthermore our results show that even complex and highly sialylated N-glycans can be investigated. This flexibility and versatility make the method broadly applicable to analysis of N-glycans and it can be applied with little effort to analysis of many (glyco)protein or in proteomics and/ or glycomics laboratories, because the combination of RP LC and MS is a routine application in such laboratories.

## 2.2. Materials and Methods

### 2.2.1. Materials

PNGase F was from New England Biolabs (Frankfurt am Main, Germany). Acetonitrile (ACN) and acetic acid were from Merck (Darmstadt, Germany). Formic acid, DMSO and Sodiumcyanoborohydride was from Fluka (Sigma, Munich, Germany). Sephadex® G-10 columns were custom made by GE Healthcare (Vienna, Austria). Amicon Ultra 30-K filter devices were from Millipore (Schwalbach, Germany). The mAb glycan standard was prepared at Sandoz. Monoclonal antibodies 1-3 were obtained from in-house development at Sandoz. The acidic N-glycan standards were from Thera Proteins (Barcarena, Portugal).

### 2.2.2. Methods

#### 2.2.2.1. Enzymatic N-glycan release by use of PNGaseF

Desalted mAb (1 mg) was used. The N-glycans (15 nmol) were released by incubating the samples with PNGaseF overnight (17 h) at 37°C. The N-glycans were separated from the proteins by use Amicon 30 K filter devices and were brought to dryness by use of a speedvac.

#### 2.2.2.2. Fluorescence labeling of released N-glycans or N-glycan standards

$Na[BH_3(CN)]$ and either 2-AA or 2-AB were dissolved in 70:30 (% *v/v)* DMSO-acetic acid to furnish concentrations of 63 and 50 mg $mL^{-1}$, respectively. Labeling solution (15 µL) and deionized water (10 µL) were added either to 15 nmol enzymatically released and dried glycans or to 250 pmol lyophilized N-glycan standard. The Labeling reaction was performed at 37°C for 17 h.
Excess label was removed by gel filtration on G-10 columns. Columns were conditioned with 10 ml $H_2O$. Samples were diluted to 100 µl with deionized water then applied to the column. After rinsing the column with 700 µl $H_2O$ the purified fluorescence labeled N-glycans were eluted with 600 µl $H_2O$.

#### 2.2.2.3. Reversed Phase HPLC of labeled N-Glycans

Liquid chromatography was performed with an Agilent 1200 Series chromatograph on a Waters Acquity UPLC BEH130 $C_{18}$ (2.1 mm x 150 mm 1.7-µm particle) column. Analysis of 2-AA labeled glycans was performed with a gradient prepared from 1.0 % formic acid in $H_2O$ (component A) and 50 % ACN in 1.0 % formic acid in $H_2O$ (component B). The column was equilibrated with 4 % B. After injection of up to 100 µL sample the mobile phase composition

was held at 4 % B for 2 min. The proportion of B was then raised in four steps to 28%, first to 10 % over 27 min, then to 11.5 % over 10 min, then to 14 % over 8 min and finally to 28 % over 19 min. The column was regenerated by increasing to 90 % B over 4 min, followed by isocratic elution for 2 min. The column was then re-equilibrated at 8 % B for 5 min. Oven temperature was 50 °C and the flow-rate was 0.30 mL $min^{-1}$. Fluorescence detection was performed with an excitation wavelength of 250 nm and an emission wavelength of 425 nm. Analysis of 2-AB labeled glycans was performed with a gradient prepared from 0.5 % formic acid in $H_20$ (component A) and 0.5 % formic acid and 5 % ACN in $H_20$ (component B). The column was equilibrated with 25 % B. After injection the mobile phase was held at 25 % B for 2 minutes, eluent B was increased to 55 % over 60 minutes and then increased to 61 % over 24 minutes. The composition was held for 2 minutes and then initial condition was reached after 2 minutes and held for additional 5 minutes. Oven temperature was 40°C and the flow rate was 0.3 ml $min^{-1}$ Fluorescence detection was performed with an excitation wavelength of 250 nm and an emission wavelength of 428 nm

#### 2.2.2.4. Mass Spectrometry

The HPLC was directly coupled to a 3D ion trap ESI-MS (Bruker AmaZon). The ion trap was operated in Enhanced Resolution Mode with a capillary potential of 4 kV. The capillary temperature was set to 250 °C with a nebulizer pressure of 2 bar and a dry gas flow of 6 l/min. $MS^2$ spectra were generated by use of the Auto $MS^2$ mode and Collision Induced Dissociation (CID).

## 2.3. Results and discussion

### 2.3.1. LC-MS of 2-AB labeled N-glycans

Our RP LC-MS method entails use of two structurally closely similar chemical labels, 2-AB and 2-AA. In a first step an RP LC-MS method for 2-AB labeled N-Glycans was developed. Because 2-AB labeled N-glycans are weakly retained on C18 columns, a mobile phase gradient with a low organic solvent content was used. The separation was optimum under the mobile phase conditions decribed in the section “Reversed-phase HPLC of labeled N-glycans. A fluorescence chromatogram obtained from the 2-AB RP-LC-MS method for the mAb glycan standard is shown in Figure 1. The glycans elute in groups. To reduce the run time the mobile phase composition was adapted. Use of formic acid instead of acetic acid improved retention and led to sharper peaks. A run time of 95 min was sufficient for analysis of the N-glycans of a mAb. A shorter gradient and the resulting reduction of run time led to loss of resolution, because of the low hydrophobicity of the labeled N-glycans.

The first compounds eluting between 16-30 min from the column are the high-mannose glycans, in the order with high to low number of mannose residues (Figure 1, green). The acidic hybrid and complex glycans (Figure 1, pink) overlap with the oligomannose group from approximately 22-26 min. The next glycans to elute are the hybrid N-glycans lacking the core fucose at the terminal GlcNAc (Figure 1, orange), eluting from 28-36 min. The complex bi-antennary 2-AB glycans elute in the middle of the chromatogram (Figure 1, blue, 42-48 min.) immediately before the acidic hybrid glycans with core fucose. Hybrid (Figure 1, orange, 57-71 min.) and acidic complex (Figure 1, pink 48-66 min.) 2-AB glycans, both groups with a fucose residue attached to their core, co-elute. The group with the most abundant glycans in most mABs, the complex type glycans with core-fucose, elute at the end of the chromatogram with a retention time of 74-88 min. Sialic acid-containing 2-AB labeled glycans elute as sharp peaks before their corresponding neutral glycans.

Labeled oligomannose and hybrid structures elute from high to low number of monosaccharides whereas complex type 2-AB glycans, including the acidic variants, elute from low to high number of monosaccharide units. Several 2-AB glycans elute with similar retention time and could not be separated. The 2-AB labeled glycans were identified by MS and $MS^2$ by use of the ion-trap mass spectrometer. Table 1 contains the MS data for the identified glycans and the respective glycan structures are drawn in Figure 3 with the appropriate nomenclature.

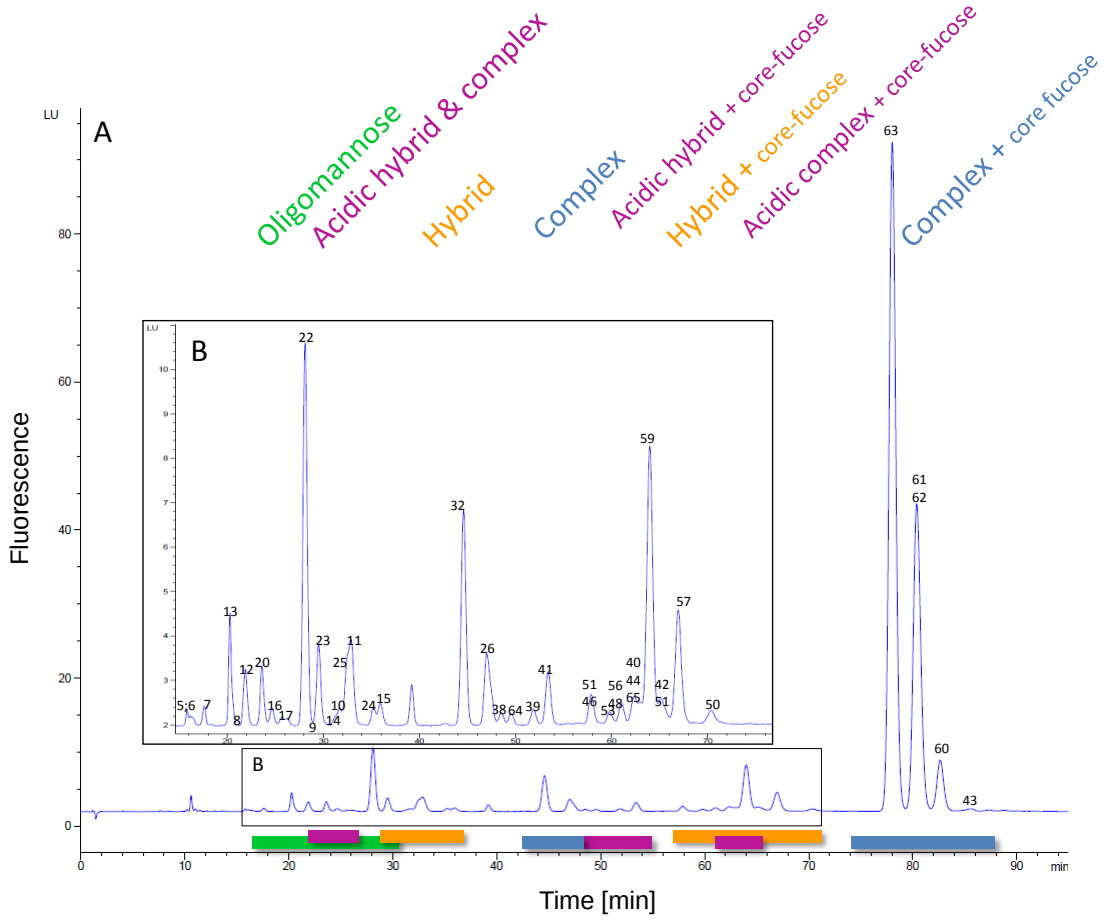


**Figure 1: Fluorescence chromatogram obtained from separation of 2-AB *N*-glycans on a RP column. The magnified view (B) of the chromatogram shows the smaller peaks of less abundant *N*-glycans. The numbered peaks were identified by use of MS and $MS^2$. Stacked numbering indicates co-elution of *N*-glycans. MS data of the identified peaks are listed in Table 1. The 2-AB glycans elute in different groups depending to their type. Oligomannose (green) glycans elute first, followed by acidic hybrid and complex type (pink) and neutral hybrid glycans (orange). Acidic hybrid with core fucose (pink) elute after complex glycans (blue). Neutral hybrid structures (orange) co-elute between approximately 57 and 86 min with acidic complexes followed by complex 2-AB glycans (blue), with all three groups carrying a core fucose.**

### 2.3.2. Separation of 2-AA labeled N-glycans

As an alternative to 2-AB labeled glycans 2-AA labeled glycans were also tested using the developed 2-AB method. Most 2-AA glycans remained on the column after the 95-min gradient, only the oligomannose structures eluted late. Because of this stronger retention of the 2-AA labeled glycans the mobile phase had to be adapted to enable optimum separation. In contrast with 2-AB, 2-AA is negatively charged at neutral pH. Mobile phase pH was therefore reduced to provide sufficient protons for efficient ionization in positive MS mode. Use of 1 % formic acid and an ACN content of component B increased by a factor of 10 compared with the 2-AB method to 50 % enabled optimum separation and good ionization. Higher signal intensity was observed with positive-ionization MS compared with negative ionization mode. The resulting run-time was 78 min. As observed for the 2-AB method a shorter gradient resulted in substantial loss of resolution.

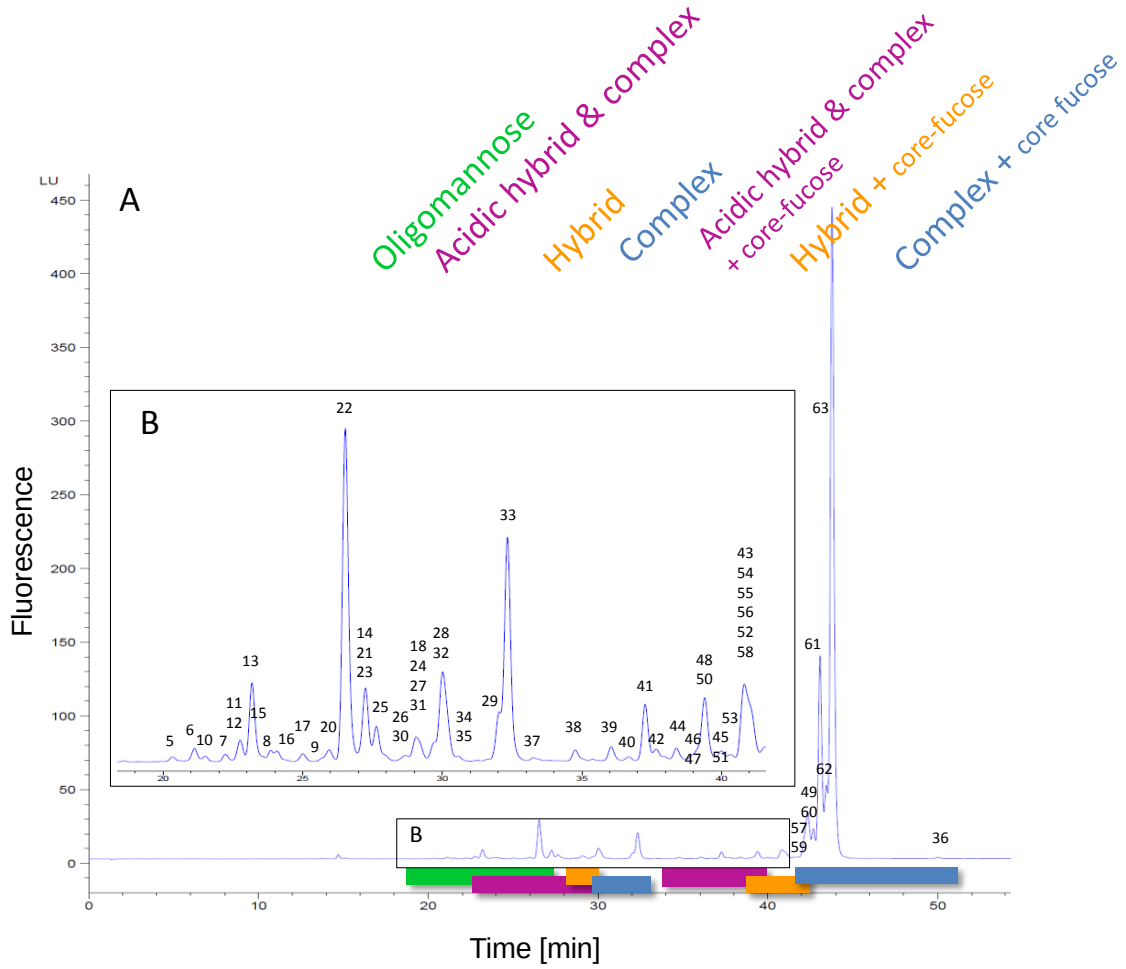


**Figure 2: RP chromatogram obtained from the mAb glycan standard showing the grouping of the eluting 2-AA *N*-glycans. (A) High Mannose structures elute first (green), followed by non-fucosylated hybrid (orange) and complex glycans (blue). Fucosylated hybrid (orange) and complex structures (blue) elute last in the chromatogram. Acidic glycans elute immediately before their appropriate neutral glycans (pink). (B) Magnified view of the region between 18 and 42 min showing the less abundant glycans. The identified glycans are numbered and the appropriate masses are listed in Table 1. Stacked numbering indicates co-elution of *N*-glycans. The glycan structures are depicted in Figure 3**

Figure 2 shows a fluorescence chromatogram obtained from the 2-AA labeled mAb glycan standard; it is similar that from of the 2-AB method (Figure 1). The labeled glycans elute in different groups, highlighted with different colors in Figure 2. High-mannose structures are the first group eluting from high number to small number of monosaccharide residues, for example from M9 to M5 (green, 19-27 min). Sialic acid containing non-fucosylated hybrid and complex variants (pink, 23-30 min) are then followed by the neutral non-fucosylated hybrid variants (orange, 28-31 min). Complex structures lacking the core fucose (blue, 30-34 min) elute before sialic acid containing hybrid glycoforms and sialic acid containing complex forms (pink, 34-40 min), both with core fucosylation. Bi-secting structures co-elute with the latter. Neutral core-fucosylated hybrid glycans (orange, 39-42 min) elute before the most abundant core fucosylated complex variants in mAbs, the bi-antennary N-glycans (blue, 42-51 min).

This grouping is similar to that of our 2-AB approach and to those of previous investigations (*13*). Sialic acid containing non-fucosylated hybrid and complex variants elute after the high mannose and before the neutral non-fucosylated hybrid group. The same order is observed for the core fucosylated hybrid and complex glycoforms. Again, the same sharp peak shape was obtained for the eluting sialic acid containing 2-AA glycans as for neutral glycans without the need for an ion-pairing reagent. Compared with the 2-AB method, the peaks were sharper (e.g. the peak width of peak 63 is 0.72 min. (2-AB) compared with 0.25 min (2-AA) and more condensed. Because of the greater number of separated glycan structures more partially resolved peaks are present in the chromatogram.

### 2.3.3. Identification of N-glycans by use of positive mode ESI-MS and MS2

So far, 2-AA has been used almost exclusively with negative ionization MS (*27*, *29*), because of the negative charge of the acid group. The acidic mobile phase used in this investigation favors proton adducts and resulted in good ionization efficiency in positive ionization mode. We observed higher signal intensities for positive ionization than for negative ionization. The high formic acid content of the mobile phase also led to formation of formic acid clusters. 2-AA N-glycans were identified from their mass derived from mass spectra and from the mass of appropriate fragments generated by CID. All identified 2-AB and 2-AA N-glycans identified in the mAb glycan standard, with their observed and calculated masses, are listed in Table 1. Some glycan structures occur several times in course of the chromatogram. These may be structural isomers or bisecting or tri-antennary variants with the same mass that cannot be distinguished because no linkage information is obtained by use of this LC-MS approach.

**Table 1: 2-AA and 2-AB labeled glycans from mAb glycan standard identified by ion-trap MS and $MS^2$. Observed and theoretical mass are shown for each assigned glycan.For *N*-glycan isomers only one mass is shown. The peak numbers correspond to the appropriate peak numbering in the chromatograms and to the structures in Figure 3.**

| Peak | 2-AA Glycans | | 2-AB Glycans | | N-Glycan |
|---|---|---|---|---|---|
| | Observed Mass | Theoretical Mass | Observed Mass | Theoretical Mass | |
| 5 | 1841.602 | 1841.645 | 1840.689 | 1840.661 | M8 |
| 6,7,8,9 | 1679.541 | 1679.592 | 1678.604 | 1678.608 | M7 |
| 10 | 1031.406 | 1031.381 | 1030.425 | 1030.397 | M3 |
| 11 | 1234.470 | 1234.460 | 1233.489 | 1233.476 | M3G0 |
| 12 | 2027.716 | 2027.709 | 2026.739 | 2026.725 | SM5G1 |
| 13,14 | 1517.592 | 1517.539 | 1516.573 | 1516.555 | M6 |
| 15 | 1396.550 | 1396.513 | 1395.54 | 1395.529 | M3G1 |
| 16 | 1855.655 | 1865.656 | 1865.678 | 1864.672 | SM4G1 |
| 17,18,19 | 1703.619 | 1703.603 | 1702.615 | 1702.619 | SM3G1 |
| 20,21 | 1193.457 | 1193.433 | 1192.49 | 1192.449 | M4 |
| 22 | 1355.525 | 1355.486 | 1354.533 | 1354.502 | M5 |
| 23,24 | 1558.617 | 1558.566 | 1557.582 | 1557.582 | M5G0 |
| 25 | 1720.647 | 1720.618 | 1719.643 | 1719.634 | M5G1 |
| 26,27,28,29 | 1599.618 | 1599.592 | 1598.612 | 1598.608 | G1 |
| 30 | 1720.647 | 1720.618 | 1719.643 | 1719.634 | M6G0 |
| 31 | 1558.592 | 1558.566 | 1557.576 | 1557.582 | M4G1 |
| 32,33 | 1437.586 | 1437.539 | 1436.565 | 1436.555 | G0 |
| 34 | 1687.579 | 1687.608 | - | 1686.624 | SM3G1 |
| 35,36 | 1786.675 | 1786.677 | 1785.708 | 1785.693 | G0F+GN |
| 37 | 1583.710 | 1583.597 | 1582.648 | 1582.613 | G0F |
| 38 | 2173.726 | 2173.767 | 2172.78 | 2172.783 | SM5G1F |
| 39 | 2011.693 | 2011.714 | 2010.754 | 2010.73 | SM4G1F |
| 40 | 2376.763 | 2376.846 | 2375.787 | 2375.862 | SG3F |
| 41 | 1849.705 | 1849.661 | 1848.692 | 1848.677 | SM3G1F |
| 42,43 | 2214.754 | 2214.793 | 2213.818 | 2213.809 | SG2F |
| 44,45 | 2052.732 | 2052.740 | 2051.768 | 2051.756 | SG1F |
| 46 | 1948.741 | 1948.729 | 1947.804 | 1947.745 | G1F+NG |
| 47 | 2028.702 | 2028.729 | - | 2027.745 | M6G1F |
| 48,49 | 1907.689 | 1907.703 | 1906.775 | 1906.719 | G2F |
| 50 | 1866.679 | 1866.676 | 1865.698 | 1865.692 | M5G1F |
| 51,52 | 1704.609 | 1704.624 | 1703.644 | 1703.64 | M5G0F |
| 53 | 1866.650 | 1866.676 | 1865.668 | 1865.692 | M6G0F |
| 54 | 1583.533 | 1583.597 | 1582.608 | 1582.613 | M3G0F+N |
| 55 | 1704.609 | 1704.624 | 1703.643 | 1703.64 | M̄4G1F |
| 56,57 | 1542.566 | 1542.571 | 1541.582 | 1541.587 | M3G1F |
| 58 | 2069.748 | 2069.756 | - | 2068.772 | G3F |
| 59 | 1380.553 | 1380.518 | 1379.569 | 1379.534 | M3G0F |
| 60 | 1907.690 | 1907.703 | 1906.746 | 1906.719 | G2F |
| 61,62 | 1745.610 | 1745.650 | 1745.655 | 1744.666 | G1F |
| 63 | 1583.709 | 1583.597 | 1582.607 | 1582.613 | G0F |

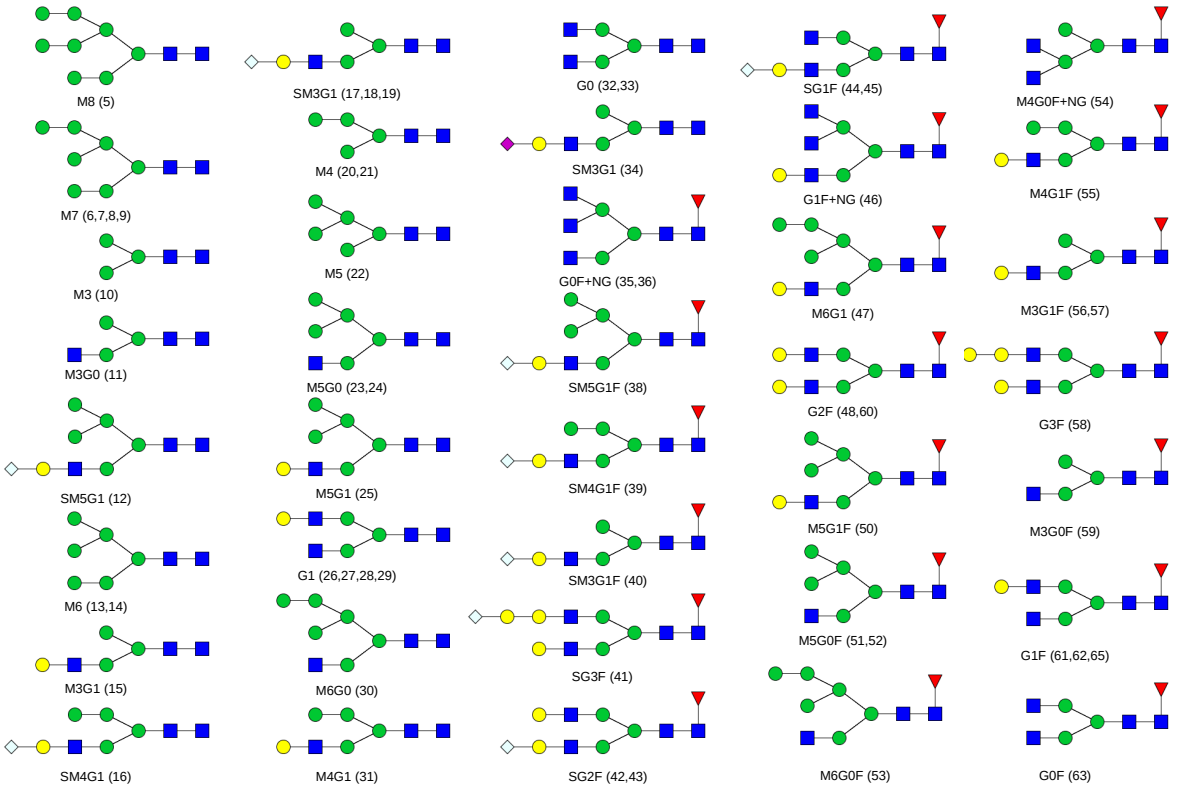


**Figure 3: Symbol structures of the identified *N*-glycans. Numbering is in aqccordance with the peak numbering for the *N*-glycans in the fluorescence chromatograms and in Table 1. For structures with multiple peak assignments only one possible isomer is drawn. Symbols: ▼ L-Fucose, ■ *N*-Acetyl-D-glucosamine, ● D-Mannose, ○ D-Galactose, ◇ *N*-Glycoyl-neuraminic acid, ◆ *N*-Acetyl-neuraminic acid.**

The charge states of the labeled glycans increase with increasing mass. Glycans with a mass < 1200 Da occur almost exclusively as $[M+H]^{1+}$ ions, whereas glycans with mass > 1200 Da are doubly charged $[M+2H]^{2+}$, singly charged $[M+H]^{1+}$ ions, also are present for glycans of mass < 1500 Da. For mass ranges > 1800 Da, the N-glycans begin to ionize as triply charged $[M+3H]^{3+}$ ions with the exception of oligomannose type glycans which usually furnish doubly charged ions. Adduct ions are present for all charge states and the oligomannose glycans tend to have the highest affinity for adduct formation. Doubly and triply charged ions occur as mixed adducts too. $[M+Na]^{1+}$, $[M+K]^{1+}$ , $[M+H+Na]^{2+}$, $[M+2Na]^{2+}$ and $[M+H+K]^{2+}$ are the most abundant adduct ions. On-line MS detection provides more information than is required for identification N-glycans solely on the basis of their mass and fragments, because co-eluting 2-AA N-glycans can be identified and quantified by use of the extracted ion chromatograms (EICs) of the appropriate *m/z* values.

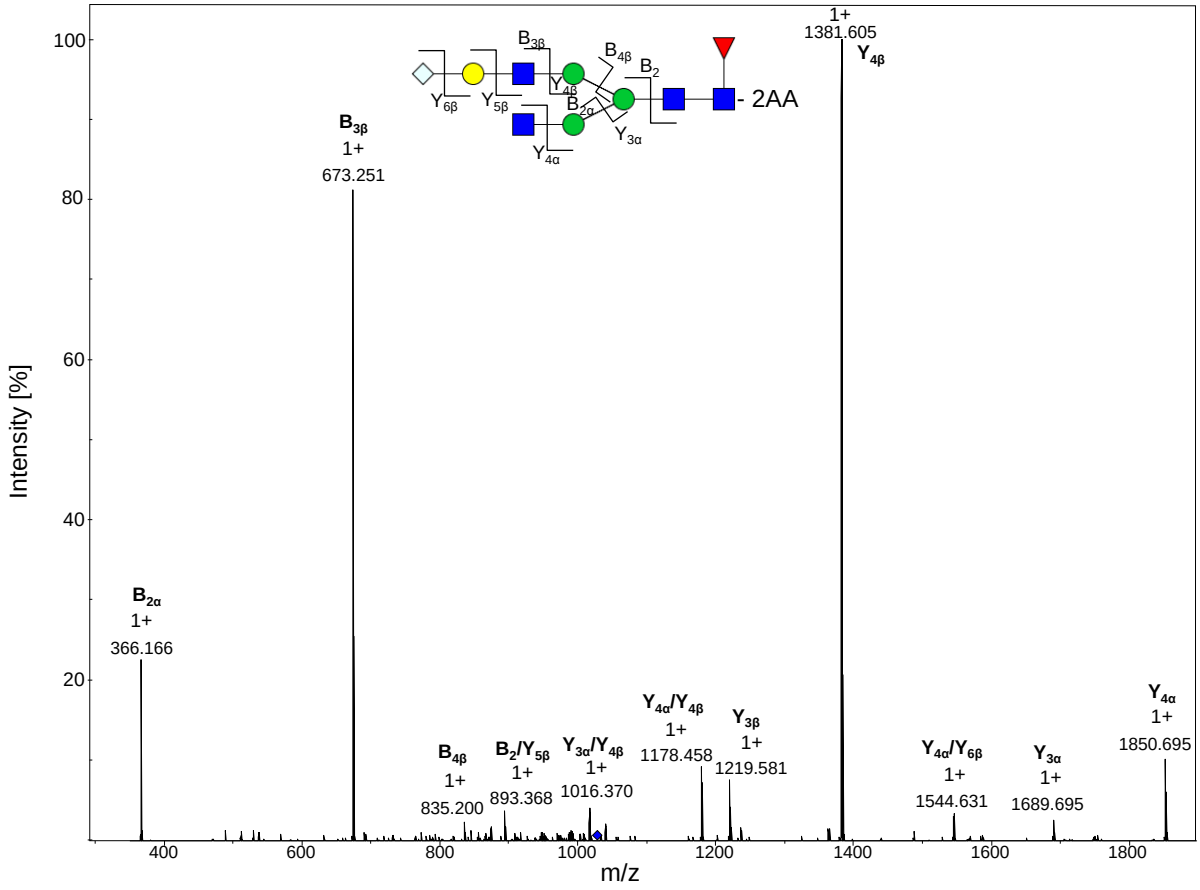


**Figure 4: $MS^2$ spectrum of the 2-AA labeled SG1F glycan from mAb3 at *m/z* 1027.9. The dissociated bonds of the $[M+2H]^{2+}$ ion are depicted and the assigned B and Y ions are labeled in the spectrum. Dissociation of two bonds is indicated by a slash.**

Figure 4 and Figure 5 show the $MS^2$ spectra obtained after fragmentation of different *N*-glycoyl-neuraminic acid containing 2-AA glycans. The fragments were labeled in accordance with the nomenclature of Domon and Costello (*30*). The spectra were acquired on-line by use of positive ionization ESI-MS and CID fragmentation. Each of the SG1F 2-AA glycan fragments (Figure 4) can be explained by the dissociation of a single bond as expected from use of CID in ion-traps. The $MS^2$ spectrum at *m/z* 1027.9 is dominated by B and Y ions. The fragmentation pattern of the sialic acid containing SM5G1F (Figure 5) is slightly different. In the $MS^2$ spectrum of the $[M+2H]^{2+}$ ion at *m/z* 1088.4 only B ions are observed derived from the GlcNAc containing branch, but not from the mannose containing branch of the hybrid structure. The fragments $B_{3\alpha}$ and $Y_{6\alpha}$ with *m/z* 528 and 366 respectively can be explained by loss of the terminal sialylation.

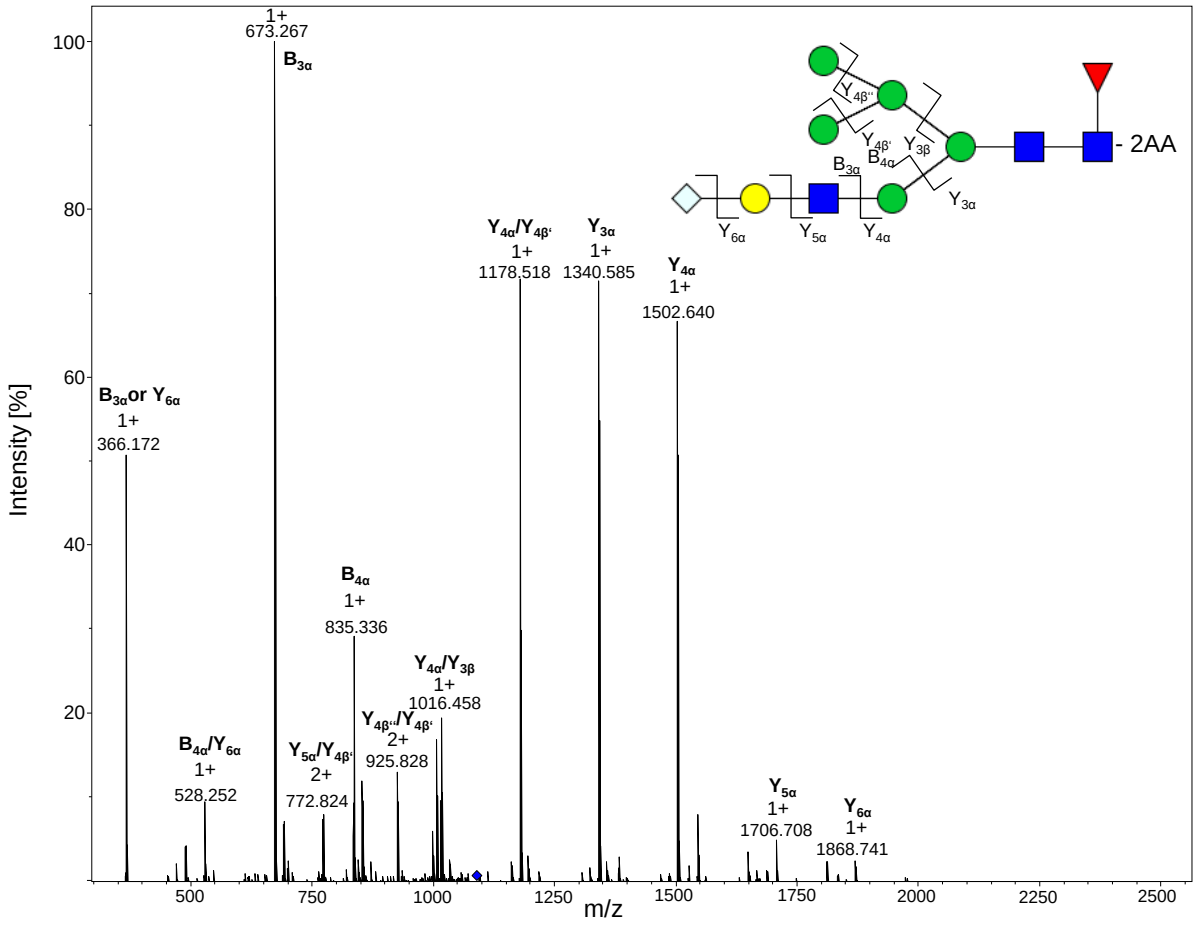


**Figure 5: MS$^2$ spectrum of the 2-AA labeled SM5G1F glycan from mAb3 at *m/z* 1088.4. Singly charged B and Y ions resulting from the $[M+2H]^{2+}$ ion are shown. B ions were exclusively from the α-branch containing a GlcNAc that is able to carry a charge. Dissociation of two bonds is indicated by a slash.**

Figure 6 shows the MS² spectrum at *m/z* 1035.9 of the rare G3F glycan which accounts for less than 0.01% of the glycans. B ions are observed for both branches of the glycan because both contain a GlcNAc. This 2-AA glycan co-elutes with the two overlapping and more abundant M3G0F and G2F peaks, but it can be identified and quantified by use of on-line MS detection. To check the performance of the method for more complex sialic acid glycans we labeled and analyzed six acidic glycan standards (Figure 8 and also the section “Selectivity of the two approaches”). The bi-antennary glycans ionized as described above. For the tri and the tetra-antennary glycans we observed mainly $[M+3H]^{3+}$ and $[M+4H]^{4+}$ ions. Loss of terminal sialic acids was minimal and we observed almost no in-source fragmentation. Only loss of an antenna was monitored for the tetra-antennary N-glycan.

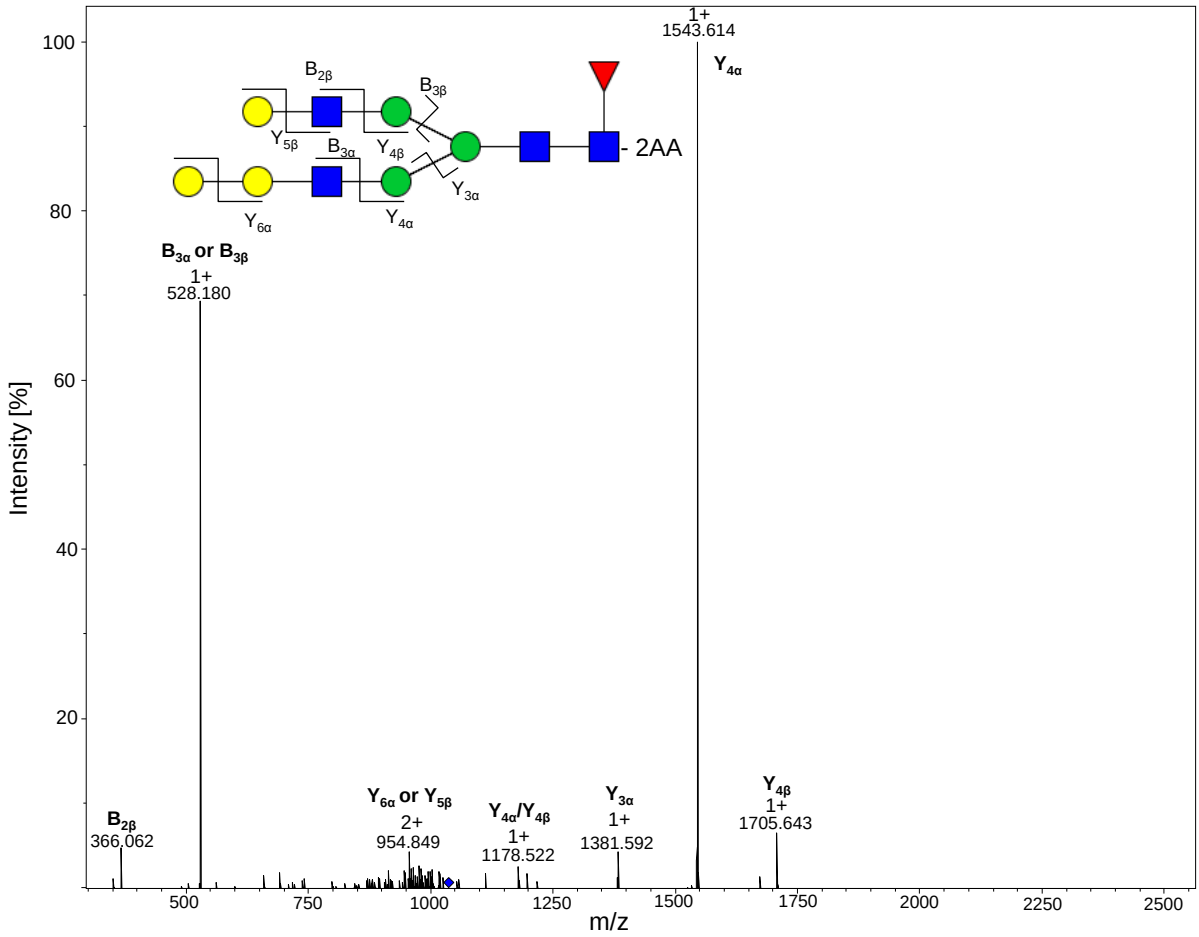


**Figure 6: $MS^2$ spectrum of the 2-AA labeled G3F *N*-glycan from mAb3. The dissociated bonds of the $[M+2H]^{2+}$ ion are depicted and the assigned B and Y ions are labeled in the spectrum. The glycan accounts for <0.01 % of the glycans of mAb3. Dissociation of two bonds is indicated by a slash.**

### 2.3.4. Selectivity of the two approaches

As mentioned in the “Introduction”, the complexity of glycosylation is not only because of the multitude of different N-glycan variants with different monosaccharide composition. It is also because of the existence of structural isomers with different linkage types. To obtain a glycan-map as comprehensive as possible it is important to separate these isomers. Separation of oligomannose isomers, for example, has been investigated and described in several publications (*8*, *13*, *28*).

Figure 7 shows the EIC of the M7 isomers of mAb2 for the 2-AB (Figure 7a) and 2-AA (Figure 7b) labeled glycans. Four different isomers are observed for this high mannose glycan. The linkage could not be deduced with the reducing end derivatization used. The selectivity of the two methods is identical for the high-mannose structures; by comparison of the areas of peaks 3 and 4, however, we deduced that the order of elution might have changed because the ratio of the peak areas was inverted for the two labels (approx. 1.6 for 2-AA peaks 3:4 and approx. 1.6 for 2-AB peaks 4:3).

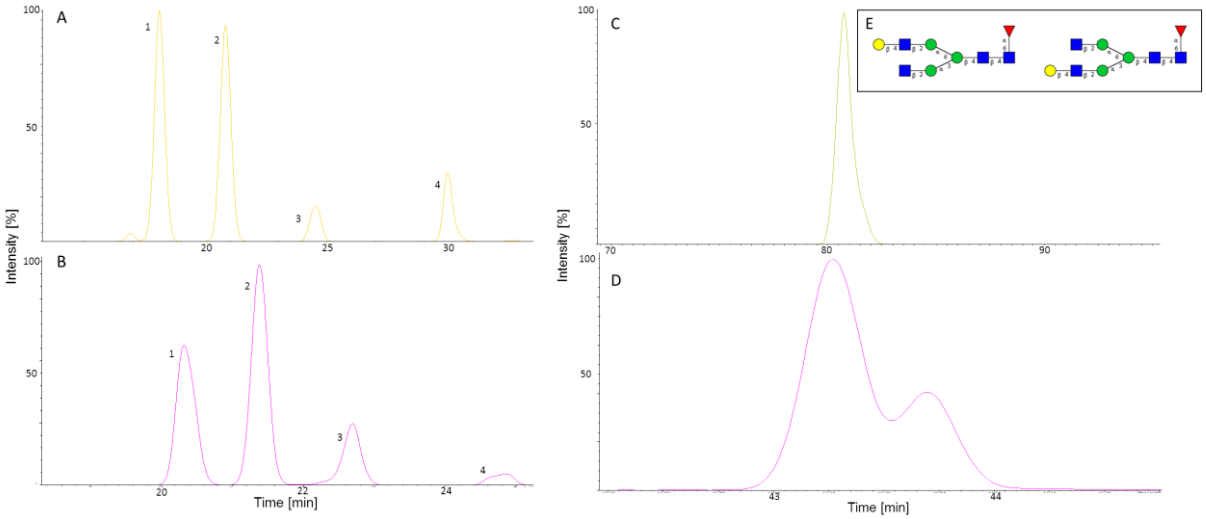


**Figure 7: EICs of four structural M7 isomers (a;b) and G1F isomers (c;d) from mAb2. (a) EIC of 2-AB labeled *N*-glycans. (b) EIC for the 2-AA labeled glycans. Although selectivity is identical for the M7 isomers in both approaches, comparison of the peak areas reveals the order of elution changed for peaks 3 and 4. Selectivity is different for the G1F isomers. The 2-AB labeled G1F elutes as one peak (c), whereas the 2-AA labeled glycans (d) are separated into the two isomers. The terminal galactose residue (e) can be either linked to the α1,6 or the α1,3 branch of the bi-antennary *N*-glycan.**

G1F isomers are usually highly abundant structural isomers on mAbs and IgG (Figure 7e) with the terminal galactose residue at the α1,3 or α1,6 branch (*6*). So far separation of these two isomers has been achieved by use of HILIC and porous graphitized carbon liquid chromatography only (*24*). In Figure 7 it is clearly apparent that the combination of 2-AA as label and the RP chromatography conditions chosen is capable of separating these isomers whereas the 2-AB RP method is not. Figure 7c shows the EIC of the G1F 2-AB glycan which elutes as one peak because separation could not be achieved during method development. Figure 7d illustrates the selectivity of the 2-AA method toward the complex N-glycans. From quantitative data obtained by HILIC chromatography we could deduce that the first, larger peak is that of the α1,6 isomer and the second smaller peak is that of the α1,3 isomer.

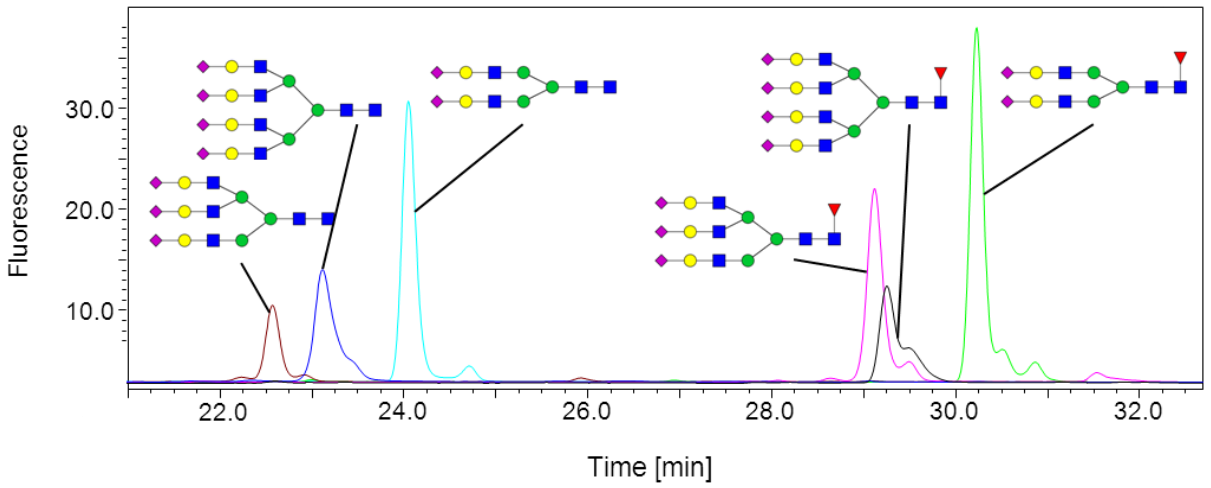


**Figure 8: Overlay of fluorescence chromatograms derived from six different 2-AA labeled sialic *N*-glycan standards.The appropriate structures are depicted. The grouping into non-fucosylated (three peaks on the left) and fucosylated (three peaks on the right) glycans is obvious.**

We also evaluated the performance of our 2-AA method with more highly branched N-glycans with additional sialic acids. Six N-glycan standards with two, three and four antennae were labeled. Each glycoform is present with and without a core-fucose. All antennae carry one terminal N-acetyl sialic acid. Overlays of the chromatograms, with the appropriate glycan structure, are shown in Figure 8. The acidic N-glycans elute in accordance with the overall grouping (Figure 2) and the separation between fucosylated and non-fucosylated glycans is obvious.

### 2.3.5. High sensitivity as a result of large injection volume

The possibility of using large injection volumes of aqueous samples in RP LC enables detection and identification by fluorescence detection or mass spectrometry, of N-glycan variants which occur only at very low levels. Compared with HILIC in which only few microliters of an aqueous sample can be injected, this circumstance is of huge advantage because the labeled and purified N-glycans are eluted in 600 µl $H_2O$ in the last step of our sample preparation procedure. The sample can be injected without any additional concentration steps. N-glycans accounting for less than 0.01 % of total mAb N-glycans, for example G3F (shown in Figure 6) can be easily detected and identified by ion-trap MS resulting in a high sensitivity glycan map of the analyzed mAb.

### 2.3.6. Analysis of different glycosylated mAbs

We analyzed the glycosylation pattern of three different mAbs by use of the 2-AA RP LC-MS method to demonstrate the flexibility and versatility of the method for mAb N-glycan characterization. The fluorescence chromatograms are shown in Figure 9-11. These mAbs were chosen because of their different glycan content. The *N*-glycosylation pattern of mAb1 (Figure 9) is indicative of the smallest amount of high-mannose structures but the largest amount of non-fucosylated complex glycans. Moreover it is the only mAb with both N-acetyl neuraminic acid and *N*-glycoyl neuraminic acid. It consists of 2 % high-mannose structures and <1 % hybrid structures without core fucose and 7 % are complex structures lacking the core fucose. Hybrid and complex N-glycans with α1,6 core fucose account for <1 % and 90 % respectively. Approximately 2 % of the N-glycans carry a terminal sialic acid.

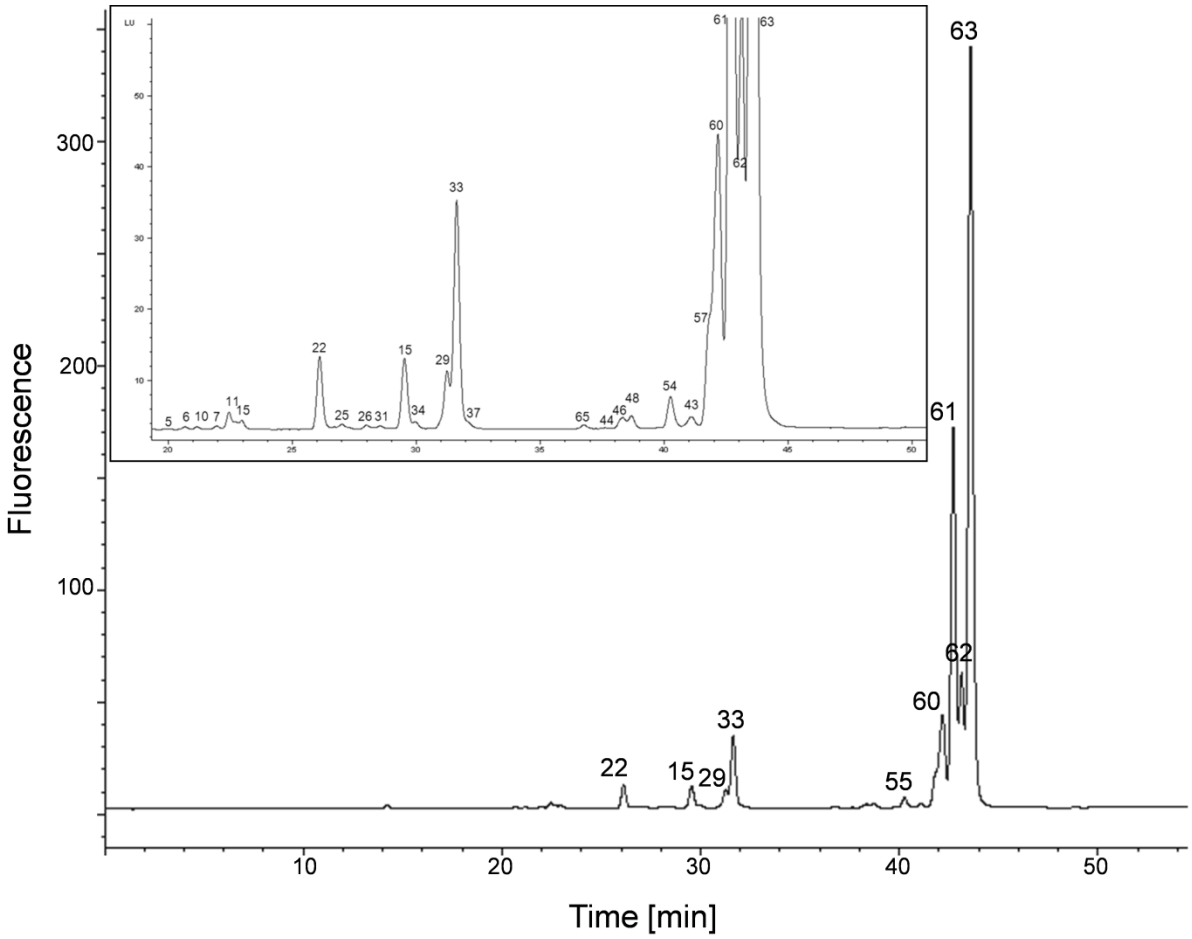


**Figure 9: RP FLD chromatogram obtained from mAb1 *N*-glycans after labeling with 2-AA. Peaks identified by MS and MS$^2$ are numbered and are listed in Table 1. The appropriate 2-AA glycans are shown in Figure 3. The magnified view (small window) of the chromatogram shows the smaller peaks.**

mAb2 (Figure 10) has the highest amount of different oligomannose glycans and carries no sialylation. High-mannose structures account for 7 % of all glycans. Non-fucosylated hybrids account for <1 % and non-fucosylated complex types account for 2 % of the glycans. Hybrid and complex glycoforms with core fucose account for 1 % and 90% respectively. Relative amounts of glycans obtained from either fluorescence or MS results are listed, as examples, in Table 2. FLD data were obtained from integration of the peaks. Quantification by MS was performed by use of extracted ion chromatograms for the appropriate glycans. In general the comparison shows there is good correlation between FLD and MS results, demonstrating the accuracy of the methods. Co-eluting structures 50, 52, 59 and 60 could be quantified individually by MS. The differences between MS and FLD detection for peaks 62 and 63 can be explained by the overlapping of the two peaks. For FLD quantification the peaks were split resulting in a higher peak area for peak 62 whereas for MS detection the peaks could be quantified individually by use of their EICs. In the sum the peak areas are equal. There are

larger differences between the EIC and FLD values for some glycan species of minor abundance; these result from larger relative integration errors of the EIC and FLD signals.

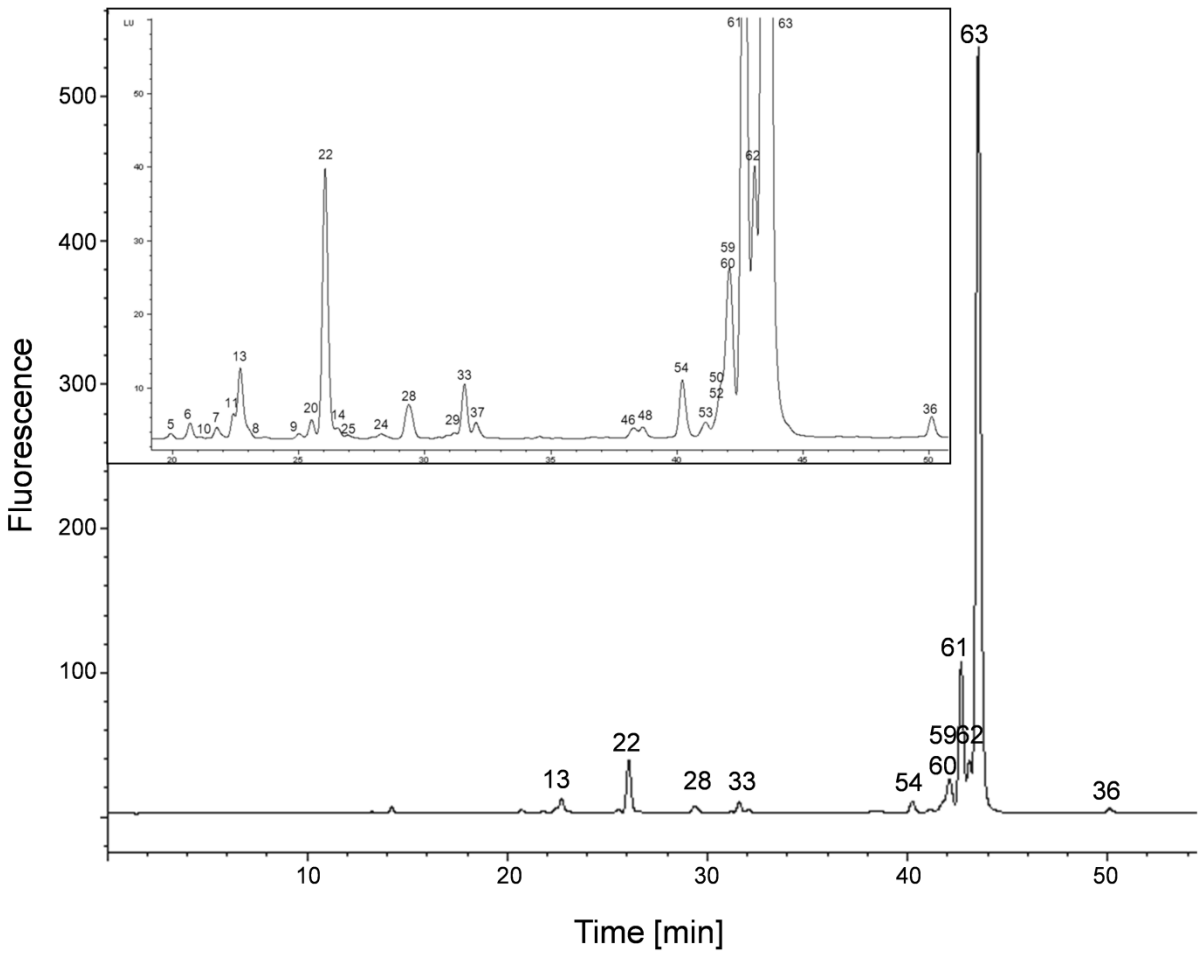


**Figure 10: RP FLD chromatogram obtained from mAb2 *N*-glycans after labeling with 2-AA. Peaks identified by MS and $MS^2$ are numbered and are listed in Table 1. The appropriate 2-AA glycans are shown in Figure 3. The magnified view (small window) of the chromatogram shows the smaller peaks. Stacked numbering indicates co-elution of *N*-glycans. Quantitative data obtained from FLD and MS for mAb2 are listed in Table 2.**

mAb3 (Figure 11) has the most complex *N*-glycosylation pattern of the antibodies analyzed. It is characterized by a large amount of hybrid structures and by oligomannose and several sialic acid moieties carrying glycans. The glycosylation consists of 5 % oligomannose structures and 5 % non fucosylated hybrid structures. Complex variants account for 4 % of all glycans. Fucosylated hybrid glycans account for 5 %. Complex fucosylated glycans account for 85 % and the sialylation level is rather high at 5 % for this mAb. The relative glycan composition of the three mAbs was calculated by using the peak area from the fluorescence chromatogram of the RP LC runs; for unresolved or coeluting glycans the EIC was used for integration. The N-glycan structures assigned to each numbered peak are illustrated in Figure 3.

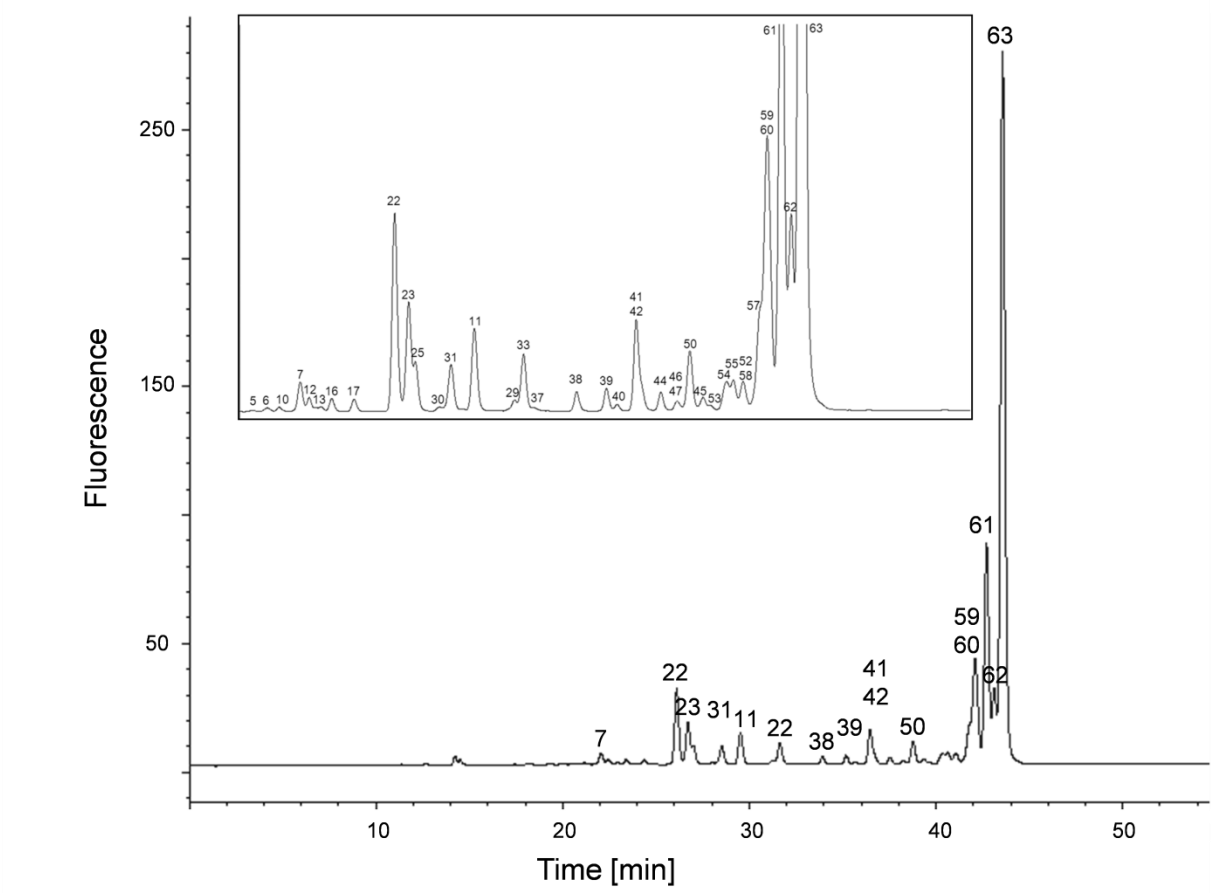


**Figure 11: RP FLD chromatogram obtained from mAb3 *N*-glycans after labeling with 2-AA. Peaks identified by MS and $MS^2$ are numbered and are listed in Table 1. The appropriate 2-AA glycans are shown in Figure 3. The magnified view (small window) of the chromatogram shows the smaller peaks. Stacked numbering indicates co-elution of *N*-glycans.**

### 2.3.7. Qualification of the method

The method was qualified to demonstrate its robustness and reliability. Sample preparation including deglycosylation by use of PNGaseF, N-glycan separation by ultrafiltration, N-glycan labeling using 2-AB and the gel filtration step to remove excess label is a standard company procedure which has been reported elsewhere (*23*). Reproducibility of fluorescence labeling by 2-AA was monitored by performing the two labeling reactions in parallel and by comparing the relative amounts of glycans. Robustness and linearity were assessed by testing different column batches and by analyzing dilutions of analyte (e.g. mAb1 total peak area $R^2 = 0.9992$) respectively. Intra assay precision was monitored by repeated sample preparation and analysis by the same operator. For example, for relative quantification of mAb2 glycans by fluorescence coefficient of variation (%CV) values were calculated (e.g. peaks 22 (1.24 %), 63 (1.17 %) and total glycan area (5.42 %)). All HPLC and MS experiments were conducted with qualified instruments.

**Table 2: Comparison of fluorescence and MS data of 2-AA labeled mAb2. Relative amounts of glycans derived from the fluorescence signal (upper panel) and the MS data (lower panel) are listed for the appropriate peak number.**

| Peak# | 5 | 6 | 10 | 7 | 13 | 11 | 8 | 9 | 20 | 22 | 14 | 25 | 28 | 29 |
|---|---|---|---|---|---|---|---|---|---|---|---|---|---|---|
| FLD | 0.07 | 0.22 | 0.02 | 0.17 | 1.29 | 0.15 | 0.02 | 0.05 | 0.22 | 4.08 | 0.11 | 0.02 | 0.72 | 0.06 |
| MS | 0.08 | 0.22 | 0.03 | 0.15 | 1.12 | 0.26 | 0.07 | 0.08 | 0.27 | 4.37 | 0.14 | 0.03 | 0.66 | 0.17 |
| **Peak#** | **33** | **37** | **46** | **48** | **54** | **53** | **61** | **62** | **63** | **36** | **50** | **52** | **59** | **60** |
| FLD | 0.83 | 0.01 | 0.23 | 0.20 | 0.96 | 0.12 | 12.96 | 2.73 | 70.06 | 0.32 | 4.27 | | | |
| MS | 1.20 | 0.10 | 0.05 | 0.08 | 0.79 | 0.08 | 12.95 | 5.29 | 67.43 | 0.26 | 0.15 | 0.18 | 2.42 | 1.37 |

## 2.4. Conclusion

This glycan-mapping method using RP HPLC of 2-AB or 2-AA labeled N-glycans in combination with fluorescence detection and on-line ion-trap mass spectrometry enables high sensitivity and high-resolution N-glycan analysis. The 2-AA method enables analysis of neutral and acidic N-glycans with positive ESI MS. Compared with the RP LC-MS of 2-AB labeled N-glycans more structural isomers can be separated in a shorter analysis time. In particular separation of the highly abundant and isobaric G1F isomers was achieved. Additionally, the 2-AA chromatogram of the mAb glycan standard (Figure 2) also contains more peaks and partially resolved peaks, because of the greater selectivity and resolution of the method. This selectivity of the reversed-phase chromatography in combination with 2-AA labeling enables separation of a variety of structural isomers of different types of N-glycans and, more important, separates the N-glycans into seven different groups, oligomannose,

hybrid and complex without core fucosylation, hybrid and complex with core fucosylation and two sialic acid-containing groups again with and without the core fucose residues; this enables rapid screening of the glycan composition. The ability to separate N-glycans with multiple sialic acids and up to four antennae shows the versatility of the method. Retention of 2-AA on the reversed phase is better than that of 2-AB; this may result from the greater hydrophobicity of the protonated carboxyl group of the 2-AA label in the acidic mobile phase. The better retention and separation results in sharper peaks and because of the higher sensitivity in fluorescence detection of 2-AA (*19*, *31*), analysis of rare glycan species becomes possible. In addition, focusing of the analyte on the column leads to a more concentrated sample entering the ionization chamber of the mass spectrometer and enables efficient ionization and more sensitive MS detection. Fragmentation of the mostly $[M+2H]^{2+}$ ions by CID produces the mainly occurring B and Y ions providing information about the N-glycan structure. We observed good ionization of the 2-AA labeled N-glycans in positive ESI-MS and even for sialylated structures the MS signal was intense and on-line $MS^2$ data were obtained. Because of the high resolution of the liquid chromatography and the sensitive MS detection, the high complexity of mAb *N*-glycosylation can be investigated in detail. The large injection volume even enables the detection and quantification N-glycans of very low abundance. Analysis of three mAbs with different glycosylation patterns showed the flexibility of the method for mAb N-glycan characterization. Furthermore, our data show that relative quantification with FLD data is comparable with quantification by MS for the labeled mAb N-glycans; this was somewhat expected, because the molecular composition of the glycans is similar and the masses are distributed over a relatively small range. The low hydrophobicity of the labeled glycans, which enables good separation, also makes MS quantification more accurate, because the ACN content changes slowly and conditions in the ionization chamber of the mass spectrometer during analyte elution are almost identical. Co-eluting glycans could also be quantified individually by use of MS data. For samples containing N-glycans with a larger size distribution, however, the comparability must be evaluated individually. To summarize,, our 2-AA RP LC-MS approach can be used as a robust method which is orthogonal to the widely established HILIC of 2-AB glycans or MALDI MS of labeled neutral and acidic N-glycans derived from mAbs and other glycoproteins. In this work we demonstrated the strength and versatility of RP LC with on-line MS detection for analysis of *N*-glycosylation.

## 2.5. References

1. C. H. Chung *et al.*, Cetuximab-induced anaphylaxis and IgE specific for galactose-alpha-1,3-galactose., *The New England journal of medicine* **358**, 1109–17 (2008).

2. A. G. Morell, G. Gregoriadis, I. H. Scheinberg, J. Hickman, G. Ashwell, The role of sialic acid in determining the survival of glycoproteins in the circulation., *The Journal of biological chemistry* **246**, 1461–7 (1971).

3. R. L. Shields *et al.*, Lack of fucose on human IgG1 N-linked oligosaccharide improves binding to human Fcgamma RIII and antibody-dependent cellular toxicity., *The Journal of biological chemistry* **277**, 26733–40 (2002).

4. R. Jefferis, Glycosylation as a strategy to improve antibody-based therapeutics., *Nature reviews. Drug discovery* **8**, 226–34 (2009).

5. C. Liu *et al.*, Assessment of the quality and structural integrity of a complex glycoprotein mixture following extraction from the formulated biopharmaceutical drug product., *Journal of pharmaceutical and biomedical analysis* **54**, 27–36 (2011).

6. G. C. Flynn, X. Chen, Y. D. Liu, B. Shah, Z. Zhang, Naturally occurring glycan forms of human immunoglobulins G1 and G2., *Molecular immunology* **47**, 2074–82 (2010).

7. D. J. Ashline *et al.*, Carbohydrate structural isomers analyzed by sequential mass spectrometry., *Analytical chemistry* **79**, 3830–42 (2007).

8. J. M. Prien, D. J. Ashline, A. J. Lapadula, H. Zhang, V. N. Reinhold, The high mannose glycans from bovine ribonuclease B isomer characterization by ion trap MS., *Journal of the American Society for Mass Spectrometry* **20**, 539–56 (2009).

9. S. Maslen, P. Sadowski, A. Adam, K. Lilley, E. Stephens, Differentiation of isomeric N-glycan structures by normal-phase liquid chromatography-MALDI-TOF/TOF tandem mass spectrometry., *Analytical chemistry* **78**, 8491–8 (2006).

10. D. J. Harvey, Structural determination of N-linked glycans by matrix-assisted laser desorption/ionization and electrospray ionization mass spectrometry., *Proteomics* **5**, 1774–86 (2005).

11. C. Huhn, M. H. J. Selman, L. R. Ruhaak, A. M. Deelder, M. Wuhrer, IgG glycosylation analysis., *Proteomics* **9**, 882–913 (2009).

12. K. R. Anumula, Anumula Anal Biochem 1994.pdf, *Analytical biochemistry* **220**, 275–283 (1994).

13. X. Chen, G. C. Flynn, Analysis of N-glycans from recombinant immunoglobulin G by on-line reversed-phase high-performance liquid chromatography/mass spectrometry., *Analytical biochemistry* **370**, 147–61 (2007).

14. L. a Gennaro, D. J. Harvey, P. Vouros, Reversed-phase ion-pairing liquid chromatography/ion trap mass spectrometry for the analysis of negatively charged, derivatized glycans., *Rapid communications in mass spectrometry : RCM* **17**, 1528–34 (2003).

15. D. J. Harvey, Collision-induced fragmentation of underivatized N-linked carbohydrates ionized by electrospray., *Journal of mass spectrometry : JMS* **35**, 1178–90 (2000).

16. M. Pabst *et al.*, Isomeric analysis of oligomannosidic N-glycans and their dolichol-linked precursors., *Glycobiology* **22**, 389–99 (2012).

17. D. J. Harvey, L. Royle, C. M. Radcliffe, P. M. Rudd, R. a Dwek, Structural and quantitative analysis of N-linked glycans by matrix-assisted laser desorption ionization and negative ion nanospray mass spectrometry., *Analytical biochemistry* **376**, 44–60 (2008).

18. J. Bigge *et al.*, Nonselective and efficient fluorescent labeling of glycans using 2-amino benzamide and anthranilic acid, *Analytical biochemistry* **230**, 229–238 (1995).

19. D. J. Harvey, Derivatization of carbohydrates for analysis by chromatography; electrophoresis and mass spectrometry., *Journal of chromatography. B, Analytical technologies in the biomedical and life sciences* **879**, 1196–225 (2011).

20. E. Lattová, S. Snovida, H. Perreault, O. Krokhin, Influence of the labeling group on ionization and fragmentation of carbohydrates in mass spectrometry., *Journal of the American Society for Mass Spectrometry* **16**, 683–96 (2005).

21. M. Pabst *et al.*, Comparison of fluorescent labels for oligosaccharides and introduction of a new postlabeling purification method., *Analytical biochemistry* **384**, 263–73 (2009).

22. L. R. Ruhaak *et al.*, Glycan labeling strategies and their use in identification and quantification., *Analytical and bioanalytical chemistry* **397**, 3457–81 (2010).

23. M. Melmer *et al.*, HILIC analysis of fluorescence-labeled N-glycans from recombinant biopharmaceuticals., *Analytical and bioanalytical chemistry* , 905–914 (2010).

24. M. Melmer, T. Stangler, A. Premstaller, W. Lindner, Comparison of hydrophilic-interaction, reversed-phase and porous graphitic carbon chromatography for glycan analysis., *Journal of chromatography. A* **1218**, 118–23 (2011).

25. W. Morelle, A. Page, J.-C. Michalski, Electrospray ionization ion trap mass spectrometry for structural characterization of oligosaccharides derivatized with 2-aminobenzamide., *Rapid communications in mass spectrometry : RCM* **19**, 1145–58 (2005).

26. B. D. Prater, H. M. Connelly, Q. Qin, S. L. Cockrill, High-throughput immunoglobulin G N-glycan characterization using rapid resolution reverse-phase chromatography tandem mass spectrometry., *Analytical biochemistry* **385**, 69–79 (2009).

27. J. M. Prien, B. D. Prater, Q. Qin, S. L. Cockrill, Mass spectrometric-based stable isotopic 2-aminobenzoic acid glycan mapping for rapid glycan screening of biotherapeutics., *Analytical chemistry* **82**, 1498–508 (2010).

28. J. M. Prien, B. D. Prater, S. L. Cockrill, A multi-method approach toward de novo glycan characterization: a Man-5 case study., *Glycobiology* **20**, 629–47 (2010).

29. D. J. Harvey, Collision-induced fragmentation of negative ions from N-linked glycans derivatized with 2-aminobenzoic acid., *Journal of mass spectrometry : JMS* **40**, 642–53 (2005).

30. B. Domon, C. E. Costello, A systematic nomenclature for carbohydrate fragmentations in FAB-MS/MS spectra of glycoconjugates, *Glycoconjugate Journal* **5**, 397–409 (1988).

31. K. R. Anumula, S. T. Dhume, High resolution and high sensitivity methods for oligosaccharide mapping and characterization by normal phase high performance liquid chromatography following derivatization with highly fluorescent anthranilic acid., *Glycobiology* **8**, 685–94 (1998).

# Chapter 3

## *Small scale affinity purification and high sensitivity reversed phase nanoLC-MS N-glycan characterization of mAbs and fusion proteins*

Published in *mAbs* 2014 May 21; 6(4), doi: 10.4161/mabs.29263; Fabian Higel, Andreas Seidl, Uwe Demelbauer, Fritz Sörgel, Wolfgang Frieß

### Abstract

N-glycosylation is a complex post-translational modification with potential effects on the efficacy and safety of therapeutic proteins and known influence on the effector function of biopharmaceutical monoclonal antibodies (mAbs). Comprehensive characterization of N-glycosylation is therefore important in biopharmaceutical development. In early development, e.g. during pool or clone selection, however, only minute protein amounts of multiple samples are available for analytics. High sensitivity and high throughput methods are thus needed. An approach based on 96-well plate sample preparation and nanoLC-MS of 2-anthranilic acid or 2-aminobenzoic acid (AA) labeled N-glycans for the characterization of biopharmaceuticals in early development is reported here. With this approach, 192 samples can be processed simultaneously from complex matrices (e.g., cell culture supernatant) to purified 2-AA glycans, which are then analyzed by reversed phase nanoLC-MS. Attomolar sensitivity has been achieved by use of nanoelectrospray ionization, resulting in detailed glycan maps of mAbs and fusion proteins that are exemplarily shown in this work. Reproducibility, robustness and linearity of the approach are demonstrated, making use in a routine manner during pool or clone selection possible. Other potential fields of application, such as glycan biomarker discovery from serum samples, are also presented.

**Keywords:** oligosaccharide, N-glycosylation, fusion protein, therapeutic antibody, mass spectrometry, nanoLC, biomarker discovery

## 3.1. Introduction

N-glycosylation, a complex post-translational modification of proteins, is of central importance in the research and development of therapeutic proteins. Of all approved recombinant biopharmaceuticals, e.g., monoclonal antibodies (mAbs), protein hormones, ~40% are glycoproteins.(*1*) Characterization of N-glycosylation is important during biopharmaceutical process development because N-glycosylation may affect the safety or efficacy of a protein drug.(*2*–*6*) For mAbs, these effects are based on structural properties derived from the CH2 domain glycosylated at $Asn^{297}$. Size and charge of attached N-glycans as well as terminal sugar moieties influence complement-dependent cytotoxicity (CDC) and antibody-dependent cell-mediated cytotoxicity (ADCC) potency of IgGs and thereby the overall efficacy. For example, lack of core fucose increases ADCC by improving binding to FcγRIIIa. Increased ADCC activity could be correlated with product safety, i.e., serious infections during TNF-targeted treatment in rheumatoid arthritis patients.(*7*) Moreover, lack of terminal galactose residues and the resulting terminal GlcNAc residues increase CDC by modulating binding to C1q.(*8*) Therefore, it is crucial to analyze the glycan pattern of a biopharmaceutical as early as possible during development to be able to modify the drug candidate, for example by glyco-engineering. Alterations of IgG N-glycosylation have been linked with aging and a variety of diseases, and distinct N-glycans are regarded as potential biomarkers because the interactions of IgGs and Fc-receptors influence and modulate immune responses.(*9*–*16*)

N-glycosylation analysis is sophisticated because of the numerous N-glycan variants that may be attached to the protein molecules and the huge differences in their relative amounts. For example, recombinant human IgG antibodies contain up to 60 different N-glycans with relative amounts of individual N-glycans ranging from 0.02% for an oligomannose structure to more than 70% for the most abundant N-glycan, reflecting differences that cover three orders of magnitude.(*17*) Technologies frequently used for N-glycan analysis are CE, HPAEC-PAD, HPLC, MALDI and ESI-MS and various combinations of these technologies.(*18*) LC-MS is an advantageous combination as LC is able to separate glycan mixtures, after which glycan variants can be individually identified and quantified by on-line MS. However, for various analytical applications, conventional LC-MS is not sufficiently sensitive, especially for cases where sample amount is strongly limited. During early biopharmaceutical development (e.g., pool or clone selection), only minute amounts of recombinant protein from microtiter plates are usually available for protein and glycan analysis.

N-glycan biomarker discovery in patients or healthy individuals is another scenario where sample amount is typically very limited. In proteomics, similar limitations have been

circumvented by reducing the dimensions of the analytical system, for example by use of nanoLC-MS. Literature reports of approaches for N-glycan analysis by use of nanoLC-MS are rare. Several investigations reported feasibility of nanoESI or nanoLC for glycan analysis.(*19*–*23*) Using a separation-free direct infusion nanoESI approach, Prien et al. quantified 2-$^{13}[C_6]$-AA and 2-$^{12}[C_6]$-AA labeled N-glycans relatively, and demonstrated the usefulness of nanoESI for 2-AA glycan analysis.(*22*) Wuhrer et al. miniaturized HILIC-MS to nanoscale for oligosaccharide analysis, analyzing underivatized N-glycans with femtomolar sensitivity.(*19*) Avoiding glycan derivatization shortens sample preparation, but the benefit of improved MS detection due to the label is lost.(*19*, *24*) Kalay et al. have used normal-phase nano scale HPLC-MS with on-line fluorescence to analyze 2-AB N-glycans.(*20*) However, their approach resulted in long and time consuming gradients to achieve a good chromatographic resolution. Ritamo et al. recently published on glycoanalysis utilizing nano-reversed phase chromatography (RPC).(*21*) A nanoLC system was used to separate permethylated N-glycans, achieving separation for various structural isomers on a nano RP-column. Permethylation of N-glycans is an orthogonal approach to labeling. But it requires the use of toxic reagents and also the formation of side products is rather likely which makes routine utilization questionable. Gong et al used multiplex tandem mass tag labeling for the quantification of neutral IgG N-glycans. They could demonstrate that their approach is suitable for the quantification of major N-glycans and highly reproducibly with linearity over several orders of magnitude.(*23*) However, their short PNGaseF incubation and sample preparation at elevated temperatures might result in incomplete deglycosylation and the loss of sialic acids.(*25*–*27*) It has been reported previously that RP-LC with on-line MS is broadly applicable for analysis of differently reducing-end labeled N-glycans.(*17*, *28*, *29*) For RP- LC-MS, we have demonstrated that anthranilic acid (2-AA) as label is advantageous for glycan analysis.(*17*) The tag not only improves ionization by contribution of an additional charge carrying residue to the N-glycan, it also improves separation of labeled glycans on RP. The combination of 2-AA labeling with RP separation offers the additional advantage that N-glycans are separated according to their glycan type (high mannose, hybrid and complex), whether they carry a fucose residue at their core N-acteylglucosamine or not and according to their charge caused by terminal sialylation.

Based on these findings we report in this manuscript a new RP nanoLC-MS approach to analyze minute amounts of glycoproteins with high sensitivity. The presented 96-well based sample preparation work-flow is simple, offers high throughput and can be applied during early biopharmaceutical development as a routine or to discover clinical relevant changes of N-glycosylation with high sensitivity. The method has high resolving power and separates many N-glycan structural isomers including multiple branched and acidic variants. In addition, 2-AA labeled glycans can be identified by $MS^n$ of the ion-trap mass spectrometer.

An overall sensitivity for a single N-glycan on column of ~ 400 attomol (amol) was observed with the recently introduced MS source. Furthermore, we demonstrate that the method is feasible for N-glycan characterization of minute amounts of mAbs, as well as for N-glycan biomarker discovery. This is shown by comparing the N-glycosylation of an Fc containing therapeutic protein from different cell clones and the method's broad applicability is demonstrated by glycan analysis of IgGs from human serum. The approach is versatile and due to the use of RPC it should be applicable in many analytical laboratories already working with nanoLC-MS with little effort.

## 3.2. Material and Methods

### 3.2.1. Materials

PNGaseF (Roche; 11365177001). Acetonitrile (1.00030.2500) and acetic acid (1.00063.1000) were from Merck. Formic acid (94318), picolineborane, RNase B (R1153) and DMSO (41647) were from Sigma. Protein A Sepharose (17-1297-03), Protein G Sepharose (17-0618-05) and Sephadex® G-10 96-well plats (custom made) were from GE Healthcare. AcroPrep™ Advance Omega™ 10K 96-well filter plates (518-0032) were from Pall. Human serum was from Lonza. MAbs and cell culture supernatants were obtained from in-house development at Sandoz. G0F glycan standard was from Dextra. Complex and acidic N-glycan standards were from TheraProtein.

### 3.2.2. Methods

#### 3.2.2.1. Purification of IgGs from human serum or cell culture supernatant

Protein G and Protein A Sepharose were used to purify IgG from human pooled serum or cell culture supernatant. A centrifuge with a rotor for 96-well plates (Eppendorf) was used to force liquid through the filter-plates. Serum or cell culture supernatant was applied to a 96-well filter-plate well containing Protein A or Protein G Sepharose, respectively.

#### 3.2.2.2. Enzymatic N-glycan release by use of PNGaseF

After intensive washing of immobilized IgGs or fusion proteins with PBS N-glycans were enzymatically released with use of PNGaseF and incubation over-night at 37°C. Released N-glycans were separated from remaining proteins by ultrafiltration using 10K filter plates. Purified N-glycans were brought to dryness in a vacuum centrifuge (Christ RVC 2-25).

#### 3.2.2.3. Fluorescence labeling of released N-glycans or N-glycan standards

Picolineborane and 2-AA were dissolved in 70% DMSO / 30% acetic acid (v/v) to obtain concentrations of 100 mg/ml and 50 mg/ml, respectively. Labeling solution (15 µl) and deionized $H_2O$ (10 µl) were added to either dried N-glycans or lyophilized N-glycan standards. The labeling reaction was performed at 37 °C for 17 h. Excess label was subsequently removed by gel filtration in Sephadex™ G-10 96-well plates. Columns were equilibrated with $H_2O$ (800 µl). Samples were filled up to 100 µl with deionized $H_2O$ and the sample was applied to the column. After washing with 100 µl of $H_2O$, 2-AA labeled N-glycans were finally eluted with 150 µl of $H_2O$.

#### 3.2.2.4. NanoLC of labeled N-Glycans

NanoLC (Thermo/Dionex Ultimate 3000) was set-up in “direct injection onto a nano column” mode according to the manufacturer manual. Column compartment with a RP-column (Dionex Acclaim Pepmap 25cm; 75µm I.D.) was held at 40 °C. Mobile phase A consisted of 0.5% formic acid. Mobile Phase B consisted of 0.5% formic acid in 50% ACN. The column was equilibrated with 2% B at a flow rate of 300 nl/min. With a user-defined injection routine, 1-4 µl sample were stacked between loading solution (0.1% formic acid, 1% ACN in ultrapure $H_2O$) in a 20 µl sample loop. Sample loop was switched for 5-15 min, depending on the injected sample volume, in-line to allow the sample to enter the flow, after which the sample loop was switched back to load position to avoid additional gradient delay. Prior to the next injection sample, the loop was washed with loading solution. After sample injection, mobile phase B was raised to 30% over 60 min, then to 95% over 5 min. After holding at 95% B for 5 min, the column was finally re-equilibrated with 2% B for 15 min. Eluting 2-AA N-glycans were detected at 254nm using the variable wavelength detector (Dionex Ultimate 3000 VWD-3400RS with a 3 nl flow cell).

#### 3.2.2.5. Mass Spectrometry

The outlet of the nanoLC was directly coupled to an ion trap ESI-MS (Bruker AmaZon) equipped with a recently marketed on-line nano source (Bruker CaptiveSpray NanoBooster™). The ion trap was operated in Enhanced Resolution Mode with a capillary voltage of 1.7 kV. Source temperature was set to 200 °C and a dry gas flow of 3 l/min was used to heat the nano source. $MS^2$ and $MS^3$ spectra were generated with the Auto $MS^2$ mode, Auto $MS^3$ mode and Collision Induced Dissociation (CID). Ion charge control was set to a target value of 2x105 and a maximal accumulation time of 200 ms.

## 3.3. Results

### 3.3.1. Method development

N-glycosylation analysis of glycoproteins can be performed in different ways by LC-MS: the intact proteins, proteolytic digests or released N-glycans can be analyzed. Released glycans can be derivatized to even the ionization efficiency and thereby to improve the accuracy of quantification. This approach provides excellent coverage of the N-glycosylation pattern. We reported previously a method to identify and quantify 2-AA labeled N-glycans by ion-trap MS after RPC.(*17*) The method is selective for many N-glycan isomers and its robustness and reproducibility have been demonstrated. However, the method was developed to analyze N-glycans of mAbs in advanced development stages, not for early development when limited sample amounts are available and higher sensitivity is required. Thus, we have started to develop a nanoLC-MS method.

Our approach used glycans released from RNase B (Figure S1 and Table S1), a model protein for N-glycosylation analysis. RNase B N-glycans were prepared as described in the methods section, and the labeled and purified N-glycans were analyzed by nanoLC-MS. The nanoLC was configured in “direct injection on a nano column” mode because highly hydrophilic 2-AA N-glycans like the high mannose type glycans did not bind properly to the trapping column, and were therefore underrepresented in setups that included a pre-concentration step with a trapping column. The user defined injection routine allows injection volumes from 1 to 4 µl without major gradient delay. This is achieved by, depending on the chosen injection volume, switching the sample loop between 5 to 15 min into the flow to ensure that the entire sample leaves the loop before switching it back to loading position. Because of the direct injection, samples must be highly purified to avoid salt plugs entering the nanospray chamber of the MS, which may damage the emitter tip and shorten its lifetime. The chosen acidic mobile phases resulted in high selectivity for many glycan isomers on RP and improved ionization of glycans in the positive ionization mode. The portion of formic acid in the mobile phase could be lowered to 0.5% compared with 1% for the LC-MS method, which may be due to the more efficient ionization in the nano spray. The 2-AA glycans occurred mostly as double $[M+2H]^{2+}$ charged ions, 2-AA N-glycans smaller than 1500 Da occurred as single $[M+H]^{1+}$ charged ions. In addition along with protonated ions, mixed adduct ions with sodium (e.g., $[M+H+Na]^{2+}$) or potassium (e.g., $[M+H+K]^{2+}$) were also present. The 2-AA glycans were identified by MS, $MS^2$ and $MS^3$. In addition to RNase B, the method was tested with multiply branched and sialylated glycans to cover all types of glycans. Therefore, several N-glycan standards were labeled with 2-AA and analyzed (Figure S2). All types of N-glycans can be identified and quantified with this new approach, which is in agreement with our previously reported RP LC-MS approach. (*17*) High mannose glycans

elute first, followed by non-fucosylated hybrid and complex variants, then fucosylated hybrid and complex glycans. The overall chromatographic resolution is higher for the nanoLC approach compared with the LC-MS approach.

As described in the introduction, the amount of sample available can be very limited at various stages of biopharmaceutical development, especially during early development phases like pool or clone selection. During clone selection, numerous samples in complex matrices (cell culture supernatant) must be analyzed, making affinity purification necessary. Therefore, sample preparation had to be adapted to increase throughput and include affinity purification steps. 96-well plate-based sample preparation is a viable option, the success of which has already been demonstrated for glycoprotein analytics.(*10*, *15*, *30*) We selected a centrifugation-based 96-well filter plate sample preparation because we had observed inhomogeneous flow through the small scale columns in the filter plate wells on a vacuum manifold. Protein A Sepharose, which is commercially available and state-of-the-art for downstream processing of Fc-part containing biopharmaceuticals (mAbs and fusion proteins), F was used as affinity resin. The schematic work-flow is illustrated in Figure 1. Deglycosylation with PNGaseF was performed “on-column”. After washing of bound mAb, N-glycans were released by incubation of the Protein A-mAb complex with PNGaseF at 37 °C followed by elution with $H_2O$, which resulted in higher glycan yields than mAb elution followed by PNGaseF digestion in solution. PNGaseF was subsequently removed by ultrafiltration. Glycans were dried by vacuum centrifugation and 2-AA labeling was performed via reductive amination by use of the non-toxic reductive agent picoline borane.(*31*) Excess label was removed by small scale gel filtration, which was performed in custom-made 96-well plates with Sephadex G-10 resin. The last step is a downscaled procedure based on a previously published purification approach.(*17*, *27*) This purification is highly efficient because it separates labeled N-glycans from excess 2-AA in a single centrifugation step.

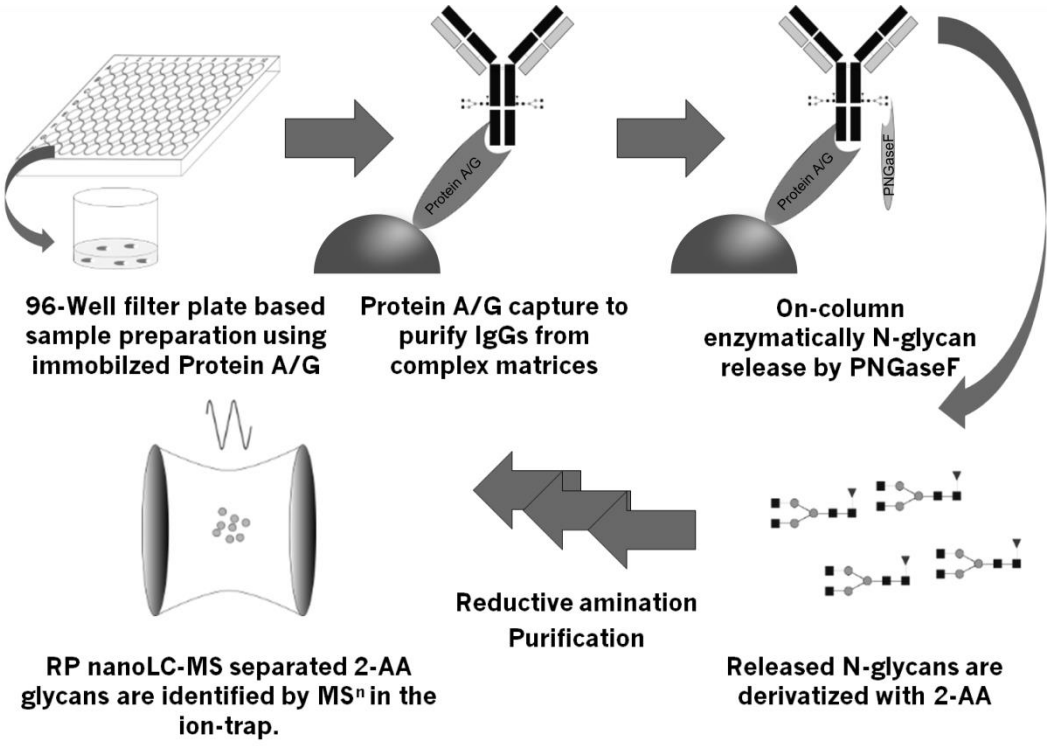


**Figure 1: Schematic work-flow. Up to 2x 96 samples can be handled simultaneously. Immobilized Protein A or Protein G is used to capture mAbs, Fc-containing fusion proteins or other IgGs with high specificity. Immobilized target is then highly efficiently deglycosylated with the use of PNGaseF. Released N-Glyans are labeled with 2-AA via reductive amination after ultrafiltration to remove remaining proteins. Labeled and purified 2-AA glycans are identified and quantified by RP nanoLC-MS by use of an ion-trap mass spectrometer.**

### 3.3.2. Qualification of the approach

Several parameters, e.g., sensitivity, robustness, linearity, reproducibility, were investigated to qualify the nanoLC-MS method. Different column batches were tested and the method was executed on different days and by different operators. To determine overall sensitivity and linearity of the method N-glycan standard G0F was labeled with 2-AA as described in the methods section and serial dilutions were prepared to obtain concentrations ranging from ~ 2.2 pmol/µl to 200 amol/µl. One µl of each dilution was injected. EIC peak areas of 2-AA G0F were used for data interpretation (Figure S3 A). Example MS spectra are shown in Figure S4. EICs of the four smallest amounts that are still in the linear range are shown in magnified view (Figure S3 B). Peak areas were plotted against glycan amount (Figure S3 C and Figure S3 D) and linearity was evaluated by linear regression with $R^2$=0.9988, indicating good linear correlation between 2.2 pmol and 800 amol. Injections with 600 and 400 amol 2-AA G0F were still detected, but were not in the linear range. The 200 amol 2-AA G0F injections were not detected anymore. The overall detection limit was thus ~ 400 amol 2-AA G0F glycan on column, and the lower limit of quantification (LLOQ) was 800 amol. Subsequently, the complete method including sample preparation was validated.

Reproducibility and robustness were assessed, for example, by comparing results of two different operators (Table S2). With the determined sensitivity, it is possible to analyze all N-glycans of an IgG using less than 1 µg protein. Varying ionization efficiencies among different N-glycan types was reported previously, especially differences between neutral and sialylated glycans. (*24*) In an earlier work we demonstrated that quantification by fluorescence and MS is identical for neutral N-glycans. (*17*) To further qualify our quantification by MS for acidic N-glycans, we compared the quantitative MS data of three N-glycans, the neutral G2F structure and the single and double sialylated glycans SG2F and S2G2F obtained from a fusion protein with high sialylation to the percentages obtained from the highly sensitive UV-cell in the same nanoLC-MS run (Figure S5). The SG2F glycan has a lower percentage when determined by MS (MS: 44%; UV: 52%) which might be due to loss of the sialic acid as a small G2F peak is visible under the SG2F peak (Figure S5A). However, for the double sialylated structure S2G2F, the quantity relative to G2F is identical for MS and UV quantification. These findings show that relative quantification by MS is possible and reliable with the developed method, especially for the intended relative comparison of different pools or clones with the same method.

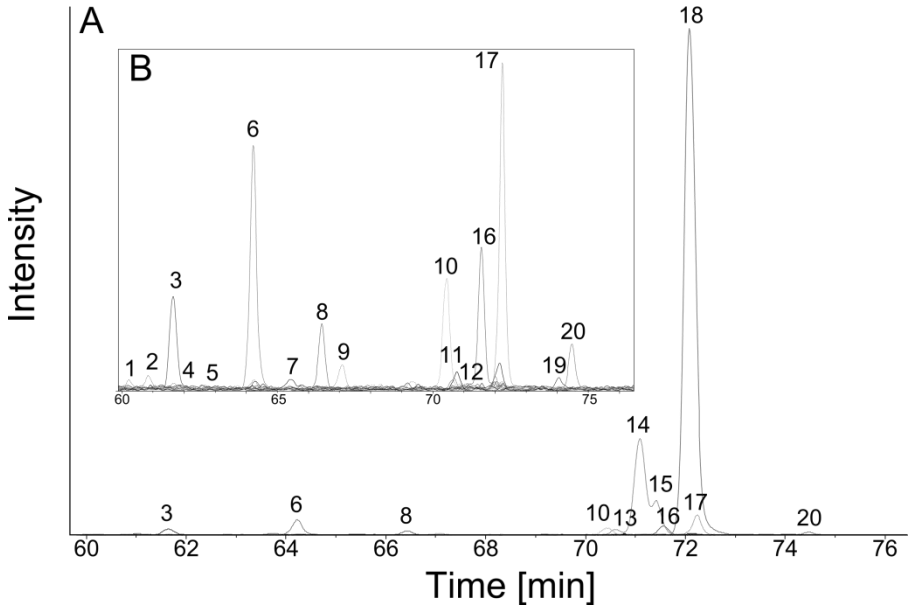


**Figure 2: NanoLC-MS glycan map of a monoclonal antibody. 1.6 pmol of 2-AA labeled N-glycans corresponding to ~ 120 ng antibody were used for analysis. EICs of the 2-AA labeled N-glycans are depicted. Complete glycan map (A) and magnified view (B) are shown. Peaks are numbered in elution order. Identified glycans are listed in Table 1, glycan structures are depicted in Figure S6.**

### 3.3.3. Glycan mapping of a monoclonal antibody

We then demonstrated the feasibility of the method for characterization of therapeutic glycoproteins. The N-glycosylation pattern of a mAb was analyzed. Sample preparation was successfully performed with less than 1 µg mAb from a drug product formulation. Approximately 1.6 pmol 2-AA labeled N-glycans, corresponding to 800 fmol or 120 ng mAb were finally injected after sample preparation. The resulting EIC is shown in Figure 2. The most abundant oligosaccharides are complex type N-glycans, G0F followed by the two G1F isomers with 1,3 and 1,6 galactosylation, respectively. Minor abundant species are shown in magnified view (Figure 2B). Identified N-glycans and relative N-glycan composition of the mAb are listed in Table 1. The absolute N-glycan amounts range from ~ 640 amol for a M7 isomer to 1.1 pmol for the most abundant G0F glycan, again showing the huge differences in relative glycan amounts and the resulting requirements to the method in terms of linearity and sensitivity. Listed structures in Table 1 are deduced from their mass and from $MS^2$, as well as from $MS^3$ data. For example, the peaks 13, 14 and 15 have the same mass and are not distinguishable by $MS^2$ or $MS^3$. Peaks 13 and 14 correspond to G1F with the terminal galactose residue on the 1,3 arm or 1,6 arm, respectively, and the separated peak 15, also named G1F, might be a truncated bi-secting or tri-antennary variant with the same number of sugar moieties, but not a third G1F isomer. As described above, the elution order of 2-AA glycans is similar to the pattern obtained by RP LC-MS. More hydrophilic oligomannose structures elute first, followed by non-fucosylated complex variants. Hybrid structures elute before complex type structures as observed for fucosylated glycan structures. Assigned glycan structures are shown in Figure S6.

**Table 1: 2-AA glycans observed in the glycan map of a monoclonal antibody. Glycan structures were identified from their mass and their fragmentation by MS/MS. Theoretical and by ion-trap MS measured values are given. Composition of the N-glycans with their respective portion is depicted on the right.**

| Glycan map – monoclonal antibody | | | | |
|---|---|---|---|---|
| | Mass | | | |
| # | Measured | Calculated | Structure | Portion |
| **1** | 1679.45 | 1679.59 | M7 | 0.07% |
| **2** | 1679.46 | 1679.59 | M7 | 0.12% |
| **3** | 1517.53 | 1517.54 | M6 | 0.84% |
| **4** | 1679.47 | 1679.59 | M7 | 0.04% |
| **5** | 1679.46 | 1679.59 | M7 | 0.06% |
| **6** | 1355.46 | 1355.49 | M5 | 2.13% |
| **7** | 1599.49 | 1599.59 | G1 | 0.07% |
| **8** | 1437.48 | 1437.54 | G0 | 0.55% |
| **9** | 1031.34 | 1031.38 | M3 | 0.23% |
| **10** | 1907.57 | 1907.70 | G2F | 0.95% |
| **11** | 1948.57 | 1948.73 | A3G1F | 0.55% |
| **12** | 1866.53 | 1866.68 | M5G1F | 0.15% |
| **13** | 1745.52 | 1745.65 | G1F | 13.39% |
| **14** | 1745.61 | 1745.65 | G1F | 4.45% |
| **15** | 1745.56 | 1745.65 | G1F | 1.02% |
| **16** | 1542.50 | 1542.57 | M3G1F | 1.02% |
| **17** | 1380.36 | 1380.52 | M3G0F | 2.41% |
| **18** | 1583.58 | 1583.60 | G0F | 71.52% |
| **19** | 1786.57 | 1786.68 | G0FB | 0.10% |
| **20** | 1948.59 | 1948.73 | G1FB | 0.33% |

### 3.3.4. Application during early biopharmaceutical development

Central goal of our investigation was a glycan characterization approach that can be used in a routine manner during clone selection. In early stages of biopharmaceutical development, protein producing cells (clones) are cultivated in microtiter plates in a few hundred microliters of medium and titers around 1 mg/ml. The aim of this procedure is to identify a clone with appropriate characteristics, for example, distinct protein and glyco-variants and a high titer. Clones must be analyzed comprehensively, but characterization is difficult because as many different aspects of the biopharmaceutical candidate as possible have to be analyzed, hence only minute amounts can be used for each analysis. With the presented work-flow, it is possible to characterize N-glycosylation patterns during clone selection employing only minute amounts of protein. Different clones of an Fc-part containing fusion protein from early development were used to demonstrate the feasibility.

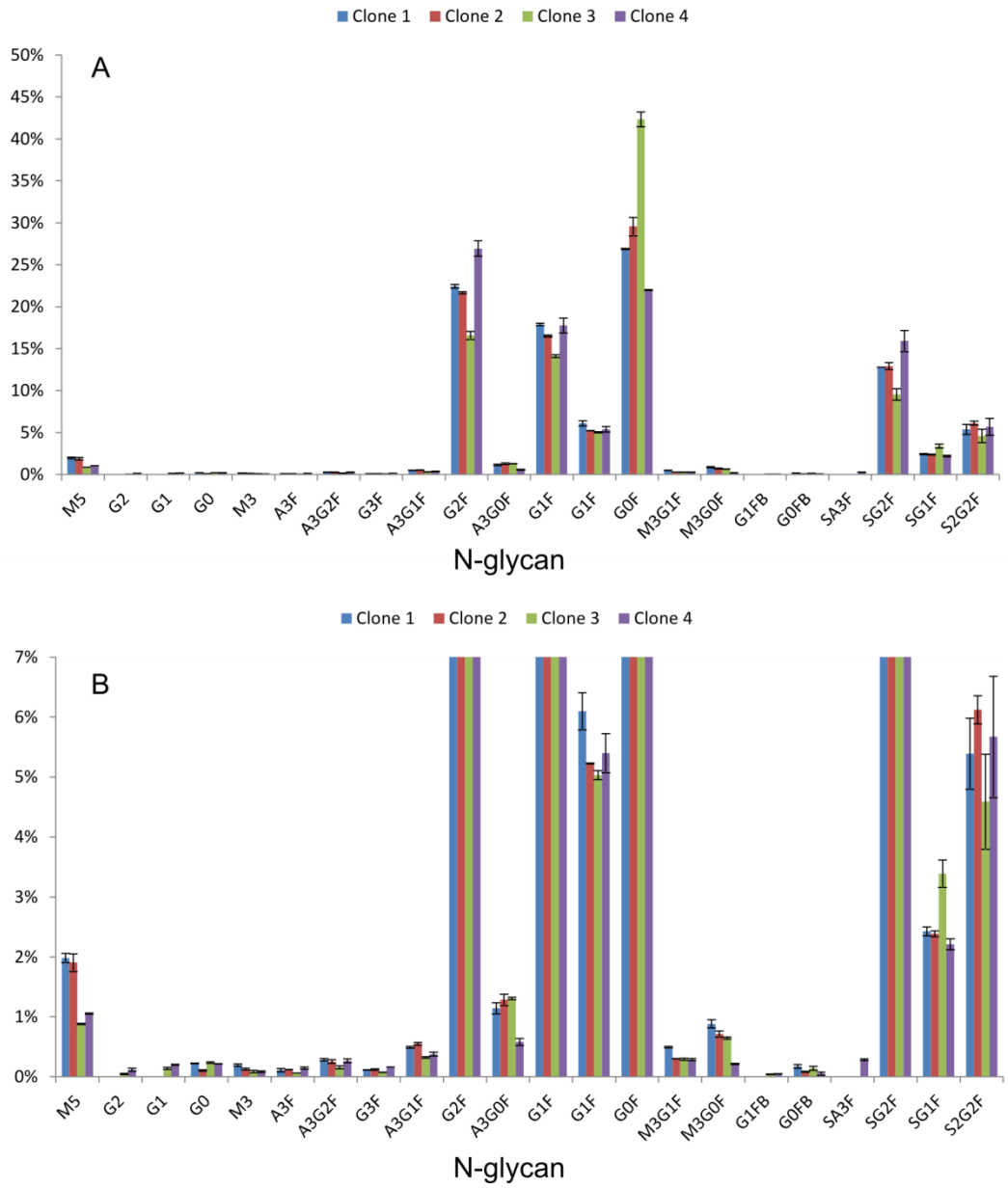


**Figure 3: Glycan map of four Fc containing therapeutic proteins derived from clone selection phase determined by nanoLC-MS after small scale sample preparation. Clones 1-4 are shown exemplarily. A) Percentages of the different glycoforms are shown. Error bars indicate variability of the method. Glycosylation pattern of the four clones is similar. B) Magnified view shows the minor abundant N-glycans**

Cell culture supernatants from different clones with concentrations between 0.3 mg/ml and 1.7 mg/ml were analyzed. Sample preparation was performed with immobilized Protein A as described in the methods section and shown in Figure 1. Supernatant (5 µl) from each clone sample containing between 1.5 µg and 8 µg fusion protein, respectively, was mixed with 45 µl PBS before sample preparation. Between 0.27 and 1.5 pmol glycans were injected from each sample, depending on the titer. Detailed glycan maps of four different clones based on EICs are shown exemplarily in Figure 3. Small differences between the clones can be observed, which demonstrates the need for a sensitive, precise and accurate method to

differentiate the clones. Major abundant N-glycans are present in all four clone samples. Some minor abundant N-glycans are absent in some clones and some structures are present only in one clone sample, e.g., SA3F is exclusively present in clone 4. Relative distribution of N-glycan types is also comparable. Clone 1 and clone 2 have 2% oligomannose structures and clone 3 and clone 4 have 1% oligomannose structures. Clone 1 has 47.9% terminal galactosylation and 20.6% terminal sialic acids. Clone 2 has 44.8% terminal galactosylation and 21.4% terminal sialic acids. Clone 3 has slightly less terminal galactosylation and sialylation with 36.9% and 17.5%, respectively. Clone 4 has the highest portion of terminal galactosylation (51.7%) and terminal sialylation (24.1%). These results demonstrate that this robust nanoLC-MS methodology can be used to characterize N-glycans in very early biotechnological development. To further qualify the approach the glycan maps obtained with the newly developed 96-well approach are compared to glycan maps from the same clones after conventional downstream processing (DSP) using Protein A columns. Sample preparation including glycan labeling was performed as described earlier.(*17*) Figure 4 shows the correlation plots of glycan maps. The N-glycan pattern are highly similar to the one obtained using the 96-well-based approach. The plots show the linear correlation of the two methods. These findings further demonstrate the potential of the developed approach in biopharmaceutical development.

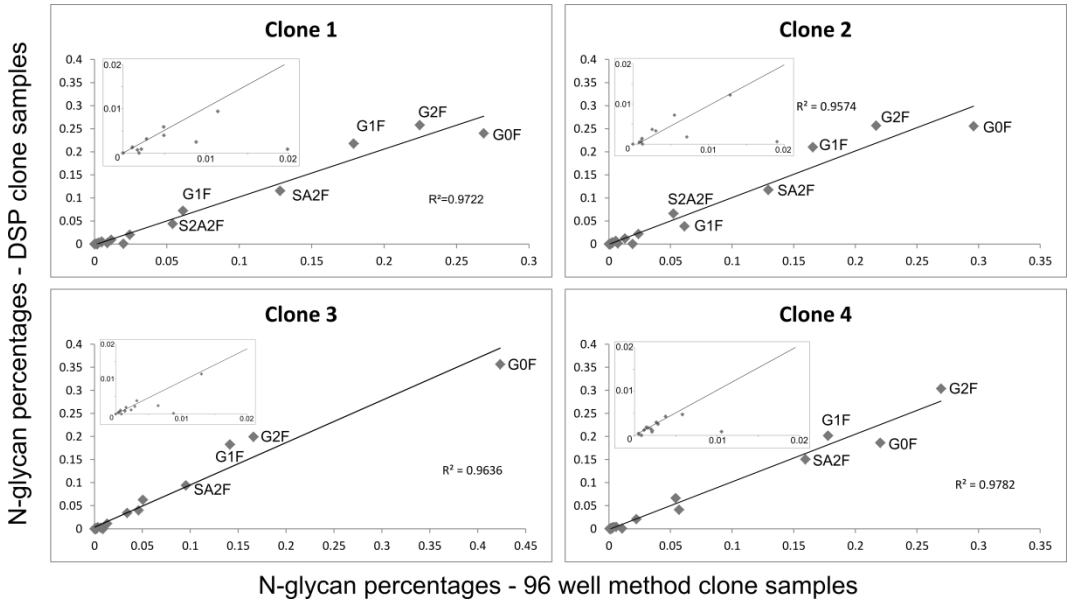


**Figure 4: Correlation plots comparing glycan maps of four clones after downstream processing to glycan maps obtained with the newly developed 96-well based nanoLC-MS analysis. Most abundant N-glycans are labeled and linear correlation coefficients are depicted. Insets show the minor abundant N-glycans.**

### 3.3.5. Investigation of serum IgG N-glycans

Application of this new approach is not limited to characterization of biopharmaceutical products and product candidates. Due to its high reproducibility, application in biomarker discovery investigations is possible. Changes in N-glycosylation of glycoproteins such as IgGs have been connected to various diseases and aging in several investigations.(*13–16*) As described in the introduction, terminal galactosylation or fucosylation influence interactions between IgG molecules and Fc-receptors, which in turn affects immune response. This may influence progression, prognosis or outcome of certain diseases. The presented work-flow can be used to screen large populations of patients or healthy subjects for significant differences in their respective N-glycosylation. The high resolving power of the nanoLC-MS method and the order of 2-AA N-glycan elution from the RP column according to their glycan type (e.g., oligomannose, hybrid and complex with and without fucosylation or acidic glycans) allow rapid semi-automatic interpretation of the nanoLC-MS runs. To demonstrate applicability of the method for glycan biomarker discovery, human IgG N-glycosylation was investigated. IgGs were purified from 5 µl of pooled human serum with an estimated IgG concentration of 10 mg/ml with immobilized Protein G Sepharose. In contrast to the above described experiments, the resin was changed from Protein A to Protein G, which allows selective purification of all IgG subclasses 1, 2, 3 and 4. Protein A has no affinity to IgG3 and variable affinity to IgA and IgM, and it is therefore of limited use for this specific study. After Protein G affinity isolation and subsequent sample preparation, a total amount of ~ 4 pmol 2-AA labeled glycans was analyzed by nanoLC-MS.

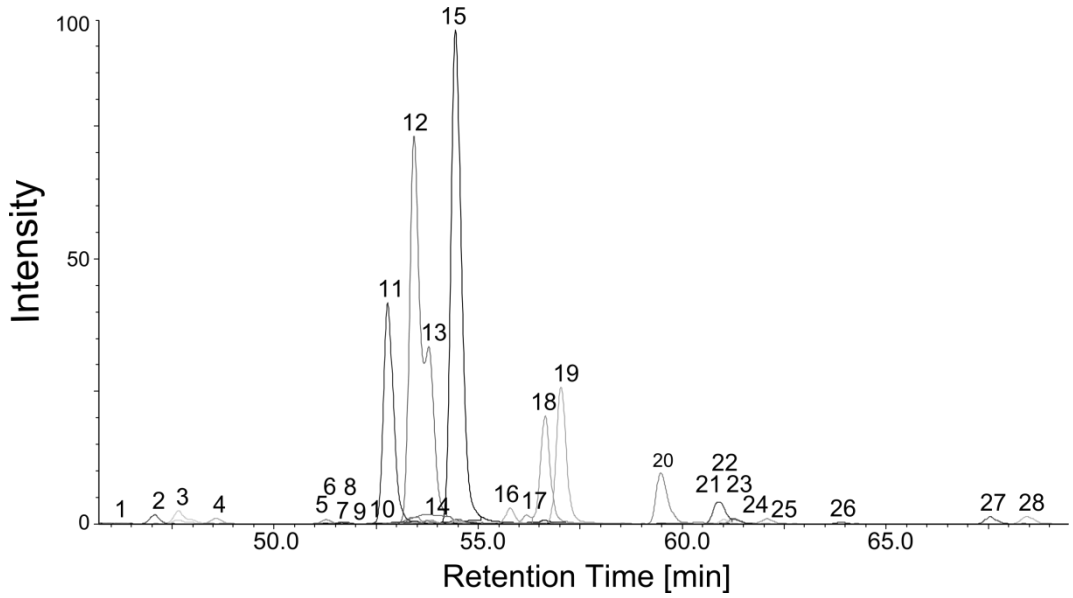


**Figure 5: Glycan map of human serum IgGs. (A) EICs of the various 2-AA labeled N-glycans are shown. Peak numbering is according to elution order. Table 2 lists the identified glycans and their relative amount and Figure S6 shows the glycan structures.**

Resulting chromatograms based on the EICs of the 2-AA N-glycans are shown in Figure 5. A total of 28 different glycoforms were identified and quantified. Detected glycans, relative glycan composition and the retention time relative to most abundant G0F glycans are listed in Table 2; appropriate glycan structures are shown in Figure S6. The majority of detected N-glycans carry a core fucose, and a small portion carries one to two terminal sialic acids. Complex biantennary glycans carrying a core fucose are the most abundant glycans, comprising more than 70%. Double fucosylated glycan species as G1F2 or G2F2 (Figure S7) were also found during our investigations and were identified by $MS^2$ by their signature fragments. These findings correspond to previous reports.(*32*)

**Table 2: 2-AA labeled N-glycans identified from human serum IgGs. Assigned N-glycans identified by MS, $MS^2$ and $MS^3$ are listed. Relative retention time to most abundant G0F and the portion is depicted, as well as the portion for each glycoform.**

| Glycan Map – Human serum IgGs | | | |
|---|---|---|---|
| **#** | **Rel. Ret.Time** | **Structure** | **MS (Mean %)** |
| **1** | 0.85 | M5 | 0.06% |
| **2** | 0.86 | G2 | 0.52% |
| **3** | 0.88 | G1 | 0.99% |
| **4** | 0.89 | G0 | 0.38% |
| **5** | 0.94 | G3F | 0.01% |
| **6** | 0.94 | G1B | 0.21% |
| **7** | 0.95 | G2F | 0.07% |
| **8** | 0.95 | G0B | 0.12% |
| **9** | 0.95 | G2F2 | 0.01% |
| **10** | 0.96 | G1F2 | 0.01% |
| **11** | 0.97 | G2F | 12.69% |
| **12** | 0.98 | G1F | 22.29% |
| **13** | 0.99 | G1F | 9.31% |
| **14** | 0.99 | SG2 | 0.24% |
| **15** | 1.00 | G0F | 30.08% |
| **16** | 1.02 | G2FB | 0.82% |
| **17** | 1.03 | G1FB | 0.43% |
| **18** | 1.04 | G1FB | 6.38% |
| **19** | 1.05 | G0FB | 8.09% |
| **20** | 1.09 | SG2F | 3.39% |
| **21** | 1.12 | SG1F | 1.60% |
| **22** | 1.12 | SA3G2F | 0.24% |
| **23** | 1.12 | SG1F | 0.23% |
| **24** | 1.12 | SM3G1F | 0.36% |
| **25** | 1.14 | S2G2 | 0.36% |
| **26** | 1.17 | SA3G1F | 0.11% |
| **27** | 1.24 | S2G2F | 0.45% |
| **28** | 1.26 | S2A3G2F | 0.55% |

With the use of relative retention times and separated 2-AA N-glycans in groups, rapid screening of the N-glycan type composition can be done semi-automatically by integration of the appropriate region of the chromatogram. For example, content of sialic acid-containing and core fucosylated 2-AA glycans can be quantified by integration of peaks between 1.09 and 1.26 relative retention times. With the same methodology, e.g., the degree of fucosylation, which has been associated with certain types of cancer, can be determined. (*33*) The approach is not limited to IgGs. By adjusting sample preparation, other target proteins or protein mixtures can be investigated. These results also show that N-glycan biomarker investigation can be performed with the presented approach.

### 3.4. Discussion

Starting with RNase B (Figure S1) and several glycan standards (Figure S2), a new methodology that enables sensitive and selective analysis of less than 1 µg glycoprotein with linearity over several orders of magnitude and high sensitivity for single glycans in the attomolar range has been developed. Compared to a previous publication that reported MS detection of underivatized N-glycans with low femtomolar sensitivity, the presented approach has improved sensitivity, which is most likely due to the applied 2-AA labeling.(*19*) In comparison with the HILIC nanoLC-MS of Kalay et al., a shorter run time with equal or even better chromatographic resolving power was achieved with the RP approach reported here.(*20*)

Using our technology, many glycan isomers could be differentiated and different kinds of samples were successfully analyzed with minimal sample consumption. The feasibility of the approach was demonstrated with N-glycan characterization of 160 ng mAb from a drug product formulation with high sensitivity. High sample throughput has been achieved with this 96-well plate sample preparation. A previously published highly efficient gel filtration step has been successfully miniaturized.(*17*, *27*) This purification step desalts 2-AA glycans efficiently and removes excess label in a single step. Robustness and reproducibility were demonstrated. Requirements for routine use in early biopharmaceutical development are fulfilled, which is shown with the glycan mapping results of clone selection samples. Minor differences in N-glycosylation of a fusion protein from different clones have been detected, which allows early guidance for further development with respect to N-glycosylation. Comparison with glycan maps derived from the same clone samples after conventional downstream processing demonstrated highly similar results.

The nanoLC-MS method has been developed to quantify all types of N-glycans. The formic acid content of the mobile phase was raised to 0.5%. At this concentration sialic acids of N-glycans are mainly protonated and therefore behave like neutral glycans, which enhanced MS intensities in positive ionization mode. Furthermore the used nanoESI source greatly improved and equalized ionization of the labeled N-glycans which was demonstrated by comparing UV to MS data. This ability to identify and quantify all different types of N-glycans, including multiply branched and sialylated variants, facilitates broad application in different areas of glycobiology. One further possible application has been shown exemplarily with the serum IgG glycan biomarker experiment. Results are in good agreement with a previously published investigation by Flynn et al.(*32*)

Compared to other recently published high throughput glycan analysis approaches that are also based on 96-well plate sample preparation, (*34*, *35*) the methodology reported here,

which uses 2-AA instead of 2-AB and RP nanoLC-MS instead of UPLC or MALDI MS, results in an up to ten-fold higher sensitivity based on the initial glycoprotein amounts. Higher coverage of the glycan maps is also achieved due to the ability to reliable quantify minor abundant N-glycans. To summarize, the presented method demonstrates the power of RP nanoLC-MS for N-glycosylation analysis. In combination with the high throughput 96-well plate sample preparation procedure N-glycan characterization can be performed in a routine manner during early biopharmaceutical development. The versatility of the method was demonstrated with several different possible fields of application.

**Acknowledgements**

The authors thank Alexander Rysin for technical assistance and Tilen Praper from Analytical Development/Lek Menges for providing the clone samples.

## 3.5. References

1. G. Walsh, Biopharmaceutical benchmarks 2010., *Nature biotechnology* **28**, 917–24 (2010).

2. C. H. Chung *et al.*, Cetuximab-induced anaphylaxis and IgE specific for galactose-alpha-1,3-galactose., *The New England journal of medicine* **358**, 1109–17 (2008).

3. A. G. Morell, G. Gregoriadis, I. H. Scheinberg, J. Hickman, G. Ashwell, The role of sialic acid in determining the survival of glycoproteins in the circulation., *The Journal of biological chemistry* **246**, 1461–7 (1971).

4. R. L. Shields *et al.*, Lack of fucose on human IgG1 N-linked oligosaccharide improves binding to human Fcgamma RIII and antibody-dependent cellular toxicity., *The Journal of biological chemistry* **277**, 26733–40 (2002).

5. R. Jefferis, Glycosylation as a strategy to improve antibody-based therapeutics., *Nature reviews. Drug discovery* **8**, 226–34 (2009).

6. C. Liu *et al.*, Assessment of the quality and structural integrity of a complex glycoprotein mixture following extraction from the formulated biopharmaceutical drug product., *Journal of pharmaceutical and biomedical analysis* **54**, 27–36 (2011).

7. E. G. Favalli *et al.*, Serious infections during anti-TNFalpha treatment in rheumatoid arthritis patients., *Autoimmunity reviews* **8**, 266–73 (2009).

8. T. S. Raju, Terminal sugars of Fc glycans influence antibody effector functions of IgGs., *Current opinion in immunology* **20**, 471–8 (2008).

9. U. M. Abd Hamid *et al.*, A strategy to reveal potential glycan markers from serum glycoproteins associated with breast cancer progression., *Glycobiology* **18**, 1105–18 (2008).

10. L. R. Ruhaak *et al.*, Hydrophilic interaction chromatography-based high-throughput sample preparation method for N-glycan analysis from total human plasma glycoproteins., *Analytical chemistry* **80**, 6119–26 (2008).

11. J. Bones, S. Mittermayr, N. O'Donoghue, A. Guttman, P. M. Rudd, Ultra performance liquid chromatographic profiling of serum N-glycans for fast and efficient identification of cancer associated alterations in glycosylation., *Analytical chemistry* **82**, 10208–15 (2010).

12. L. R. Ruhaak *et al.*, Plasma protein N-glycan profiles are associated with calendar age, familial longevity and health., *Journal of proteome research* **10**, 1667–74 (2011).

13. R. Malhotra *et al.*, Glycosylation changes of IgG associated with rheumatooid arthritis can activate complement via the mannose-binding protein, *Nature Medicine* **1**, 237–243 (1995).

14. E. Yamada, Y. Tsukamoto, R. Sasaki, K. Yagyu, N. Takahashi, Structural changes of immunoglobulin G oligosaccharides with age in healthy human serum., *Glycoconjugate journal* **14**, 401–5 (1997).

15. M. Wuhrer *et al.*, Glycosylation profiling of immunoglobulin G (IgG) subclasses from human serum., *Proteomics* **7**, 4070–81 (2007).

16. K. Kodar, J. Stadlmann, K. Klaamas, B. Sergeyev, O. Kurtenkov, Immunoglobulin G Fc N-glycan profiling in patients with gastric cancer by LC-ESI-MS: relation to tumor progression and survival., *Glycoconjugate journal* **29**, 57–66 (2012).

17. F. Higel, U. Demelbauer, A. Seidl, W. Friess, F. Sörgel, Reversed-phase liquid-chromatographic mass spectrometric N-glycan analysis of biopharmaceuticals., *Analytical and bioanalytical chemistry* **405**, 2481–93 (2013).

18. K. Mariño, J. Bones, J. J. Kattla, P. M. Rudd, A systematic approach to protein glycosylation analysis: a path through the maze., *Nature chemical biology* **6**, 713–23 (2010).

19. M. Wuhrer, C. a M. Koeleman, A. M. Deelder, C. H. Hokke, Normal-phase nanoscale liquid chromatography-mass spectrometry of underivatized oligosaccharides at low-femtomole sensitivity., *Analytical chemistry* **76**, 833–8 (2004).

20. H. Kalay *et al.*, Online nanoliquid chromatography-mass spectrometry and nanofluorescence detection for high-resolution quantitative N-glycan analysis., *Analytical biochemistry* **423**, 153–162 (2012).

21. I. Ritamo, J. Räbinä, S. Natunen, L. Valmu, Nanoscale reversed-phase liquid chromatography-mass spectrometry of permethylated N-glycans., *Analytical and bioanalytical chemistry* **405**, 2469–80 (2013).

22. J. M. Prien, B. D. Prater, Q. Qin, S. L. Cockrill, Mass spectrometric-based stable isotopic 2-aminobenzoic acid glycan mapping for rapid glycan screening of biotherapeutics., *Analytical chemistry* **82**, 1498–508 (2010).

23. B. Gong *et al.*, N-glycosylamine-mediated isotope labeling for mass spectrometry-based quantitative analysis of N-linked glycans., *Analytical and bioanalytical chemistry* **405**, 5825–31 (2013).

24. L. R. Ruhaak *et al.*, Glycan labeling strategies and their use in identification and quantification., *Analytical and bioanalytical chemistry* **397**, 3457–81 (2010).

25. T. Watanabe, N. Inoue, T. Kutsukake, S. Matsuki, M. Takeuchi, Labeling conditions using a 2-aminobenzamide reagent for quantitative analysis of sialo-oligosaccharides., *Biological & pharmaceutical bulletin* **23**, 269–73 (2000).

26. J. Bigge *et al.*, Nonselective and efficient fluorescent labeling of glycans using 2-amino benzamide and anthranilic acid, *Analytical biochemistry* **230**, 229–238 (1995).

27. M. Melmer *et al.*, HILIC analysis of fluorescence-labeled N-glycans from recombinant biopharmaceuticals., *Analytical and bioanalytical chemistry* , 905–914 (2010).

28. X. Chen, G. C. Flynn, Analysis of N-glycans from recombinant immunoglobulin G by on-line reversed-phase high-performance liquid chromatography/mass spectrometry., *Analytical biochemistry* **370**, 147–61 (2007).

29. B. D. Prater, H. M. Connelly, Q. Qin, S. L. Cockrill, High-throughput immunoglobulin G N-glycan characterization using rapid resolution reverse-phase chromatography tandem mass spectrometry., *Analytical biochemistry* **385**, 69–79 (2009).

30. D. Reusch *et al.*, High-throughput work flow for IgG Fc-glycosylation analysis of biotechnological samples., *Analytical biochemistry* **432**, 82–9 (2013).

31. L. R. Ruhaak, E. Steenvoorden, C. a M. Koeleman, A. M. Deelder, M. Wuhrer, 2-Picoline-Borane: a Non-Toxic Reducing Agent for Oligosaccharide Labeling By Reductive Amination., *Proteomics* **10**, 2330–6 (2010).

32. G. C. Flynn, X. Chen, Y. D. Liu, B. Shah, Z. Zhang, Naturally occurring glycan forms of human immunoglobulins G1 and G2., *Molecular immunology* **47**, 2074–82 (2010).

33. E. Miyoshi, K. Moriwaki, T. Nakagawa, Biological function of fucosylation in cancer biology., *Journal of biochemistry* **143**, 725–9 (2008).

34. H. Stoeckmann, B. Adamczyk, J. Hayes, P. M. Rudd, An automated, high-throughput IgG-antibody glycoprofiling platform., *Analytical chemistry* (2013), doi:10.1021/ac402068r.

35. I. Burnina, E. Hoyt, H. Lynaugh, H. Li, B. Gong, A cost-effective plate-based sample preparation for antibody N-glycan analysis., *Journal of chromatography. A* , 6–11 (2013).

# *Small scale affinity purification and high sensitivity reversed phase nanoLC-MS N-glycan characterization of mAbs and fusion proteins*

## *Supporting Information*

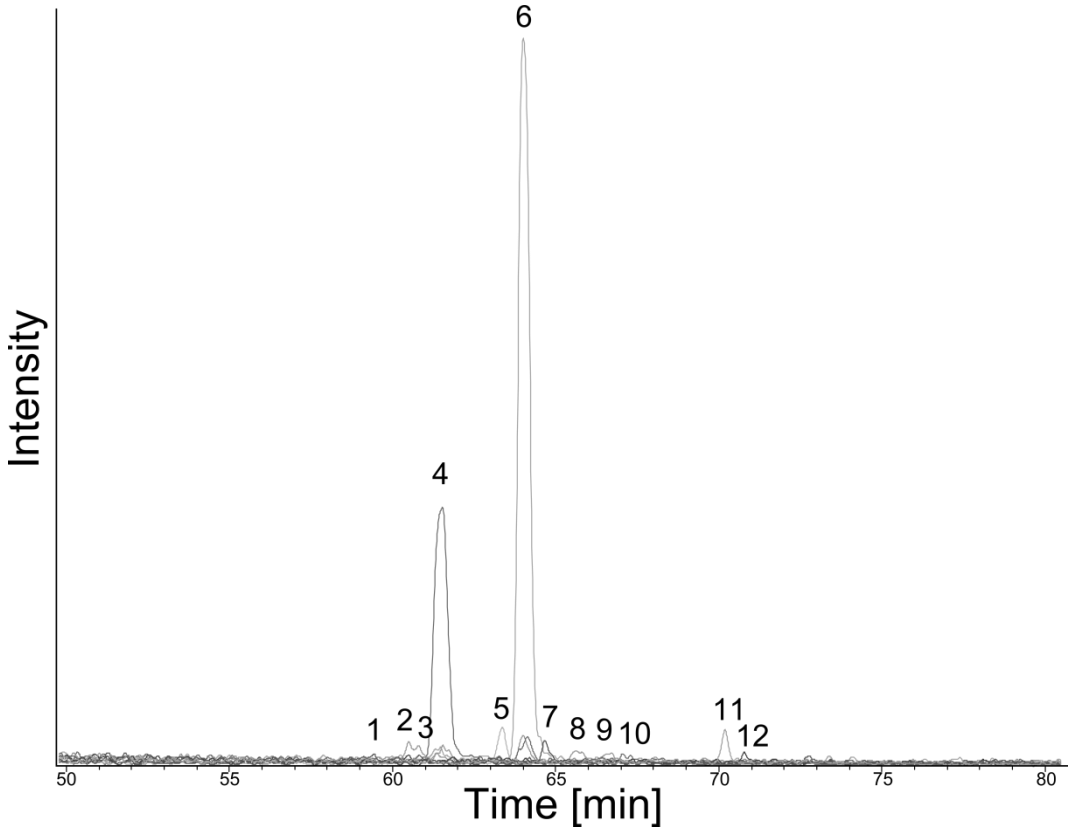


**Figure S1: Extracted Ion chromatograms of 2-AA labeled N-glycans derived from RNAse B. Peaks are numbered by elution order. Identified glycans are listed in Table S1**

**Table S1: RNaseB glycans identified by MS and MS². Figure S1 shows the corresponding chromatogram.**

| # | 1 | 2 | 3 | 4 | 5 | 6 | 7 | 8 | 9 | 10 | 11 | 12 |
|---|---|---|---|---|---|---|---|---|---|---|---|---|
| **Glycan** | M8 | M7 | M7 | M6 | M4 | M5 | G2 | M6G0 | M6 | M5G1 | G2F | G1F |

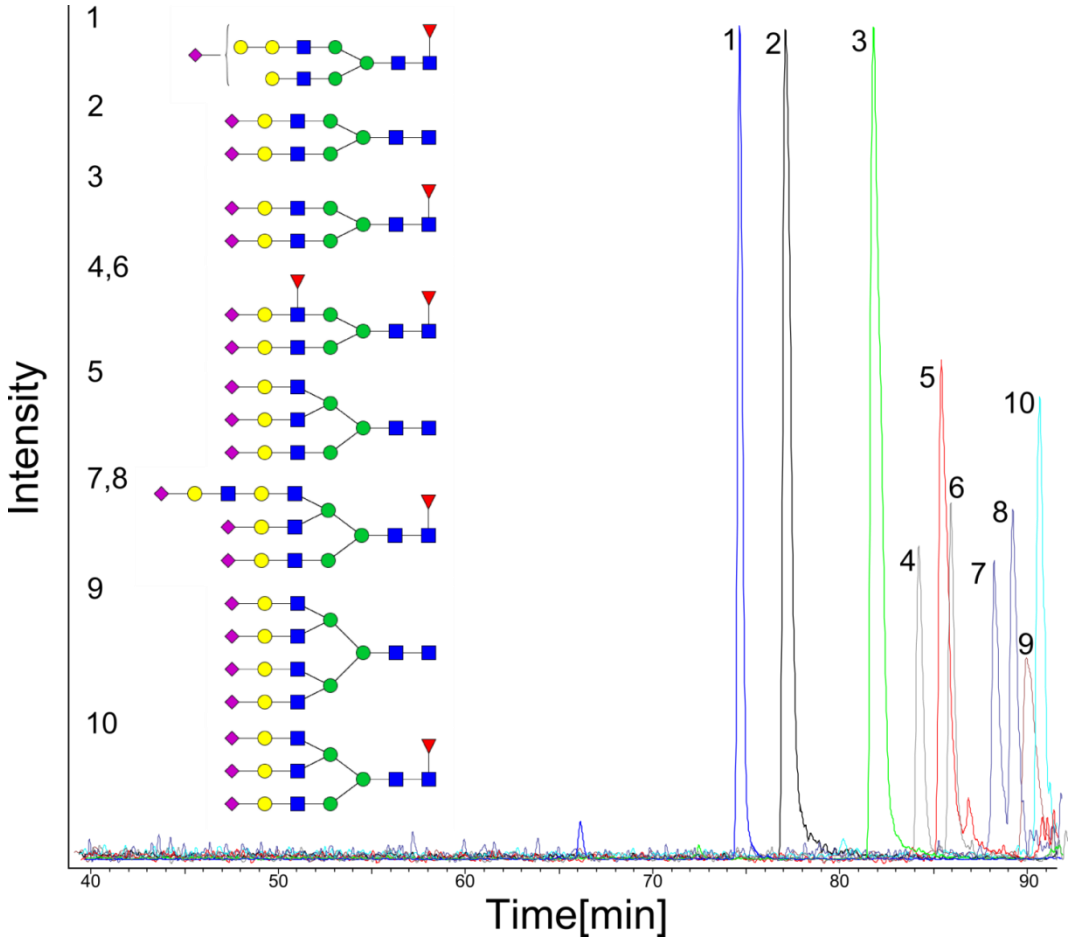


**Figure S2: Analysis of highly acidic and multiply branched N-glycan standards. Overlay of EICs from different 2-AA labled glycan standards is shown. Each standard was analyzed individually. N-glycan structures corresponding to the peak numbering are depicted on the left. For N-glycans with several structural isomers one possible structure is shown.**

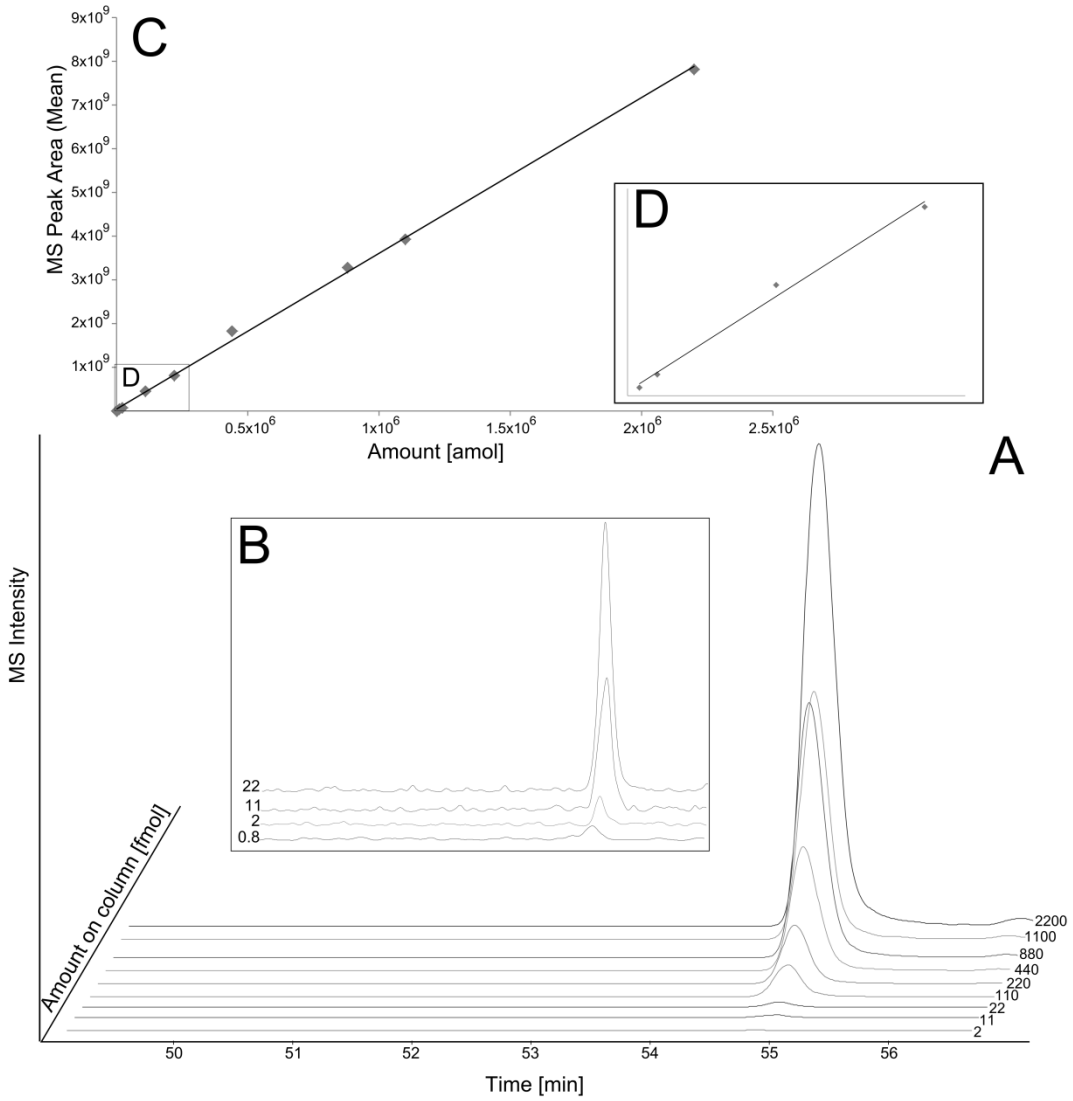


**Figure S3: Determining linearity and limits of the method by use of 2-AA labeled G0F standard in a serial dilution. (A) EICs of injections from 2200 fmol to 2 fmol. Peaks had a constant retention time around 55 minutes. (B) Magnified view of the four lowest amounts. (C) Peak areas of EICs are plotted against the glycan amount on column to show the linear correlation. 800 amol was the lowest amount that fitted the linear regression. 600 and 400 amol were also detectable, but did not fit linear regression. 800 amol is the lowest amount for reliable quantification, the lower limit of quantification. (D) Magnified view of four lowest injection amounts (22 fmol – 0.8 fmol) that fitted into the linear regression.**

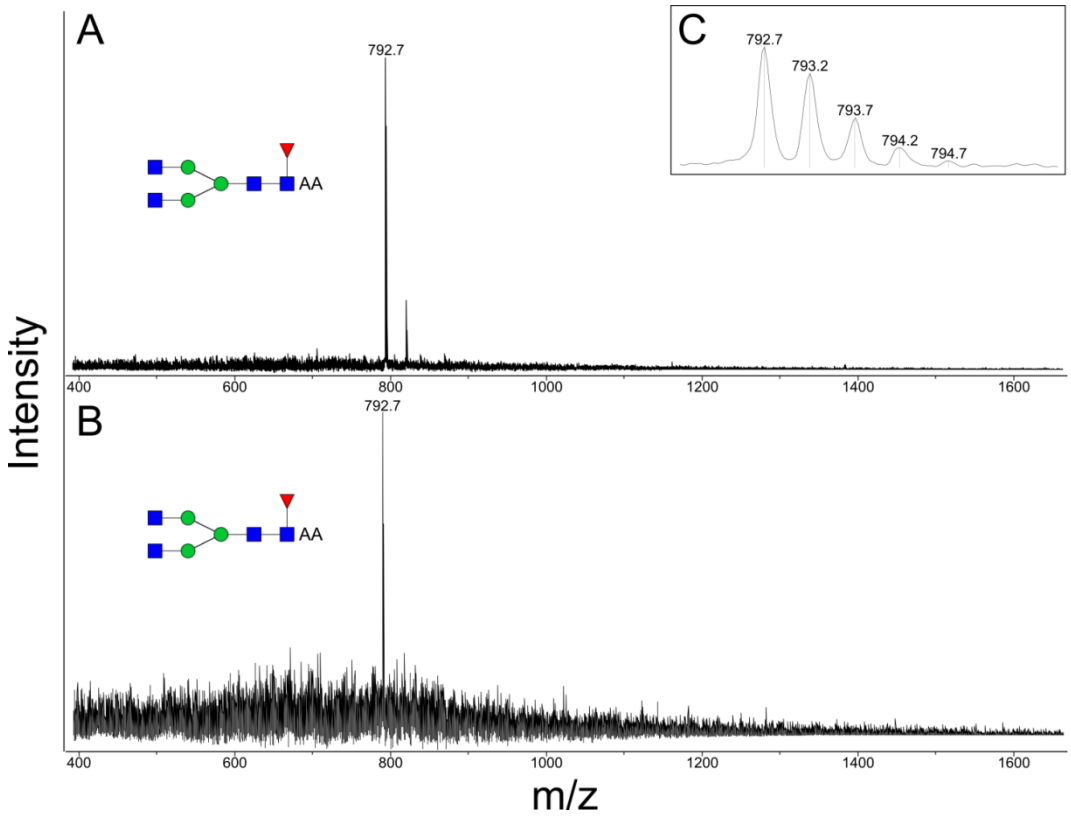


**Figure S4: MS spectra of high and low G0F 2-AA dilutions. (A) MS spectrum of 1.1 pmol injection showing the $[M+H]^{2+}$ ion at 792.7 m/z. (B) MS spectrum of 2.2 fmol injection. $[M+H]^{2+}$ ion at 792.7 m/z is clearly visible with good S/N. (C) Exemplary isotopic pattern of double charged 2-AA G0F at 792.7 m/z.**

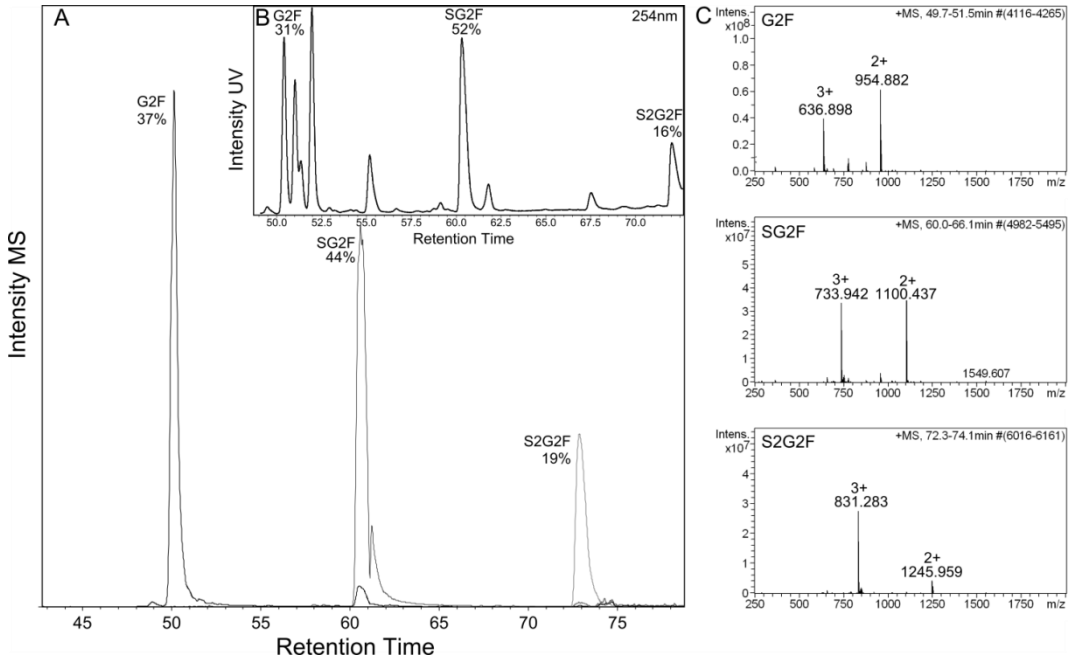


**Figure S5: Comparison of MS quantitation to UV quantitation of neutral and acidic N-glycans. (A) MS quantification based on the EIC peak areas of G2F (neutral), SG2F (one sialic acid) and S2G2F (two sialic acids). (B) UV quantification based on peak areas of the three N-glycans. Only the three labeled peaks of the chromatogram from glycans of a fusion protein were integrated for comparison. (C) Mass spectra of the three analyzed N-glycans.**

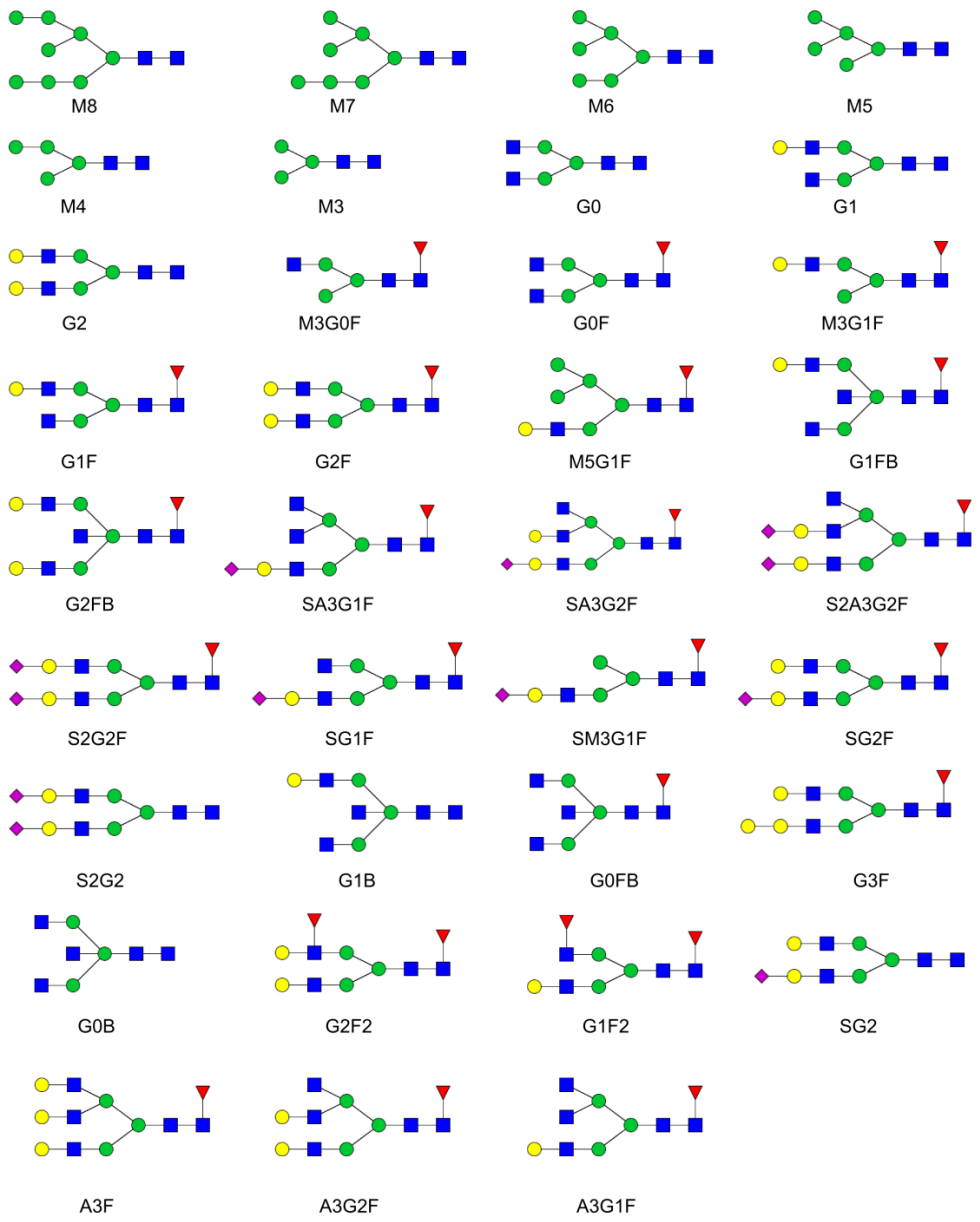


**Figure S6: Glycan structures found in serum IgGs and the monoclonal antibody. N-Acetylglucosamine (blue), Galactose (yellow), Mannose (green), Fucose (red), N-Acetylneuraminic acid (purple). For glycan structures with several isomers only one possible structure is depicted exemplarily.**

**Table S2 Robustness of the developed approach for the glycan map of a monoclonal antibody. Sample preparation and nanoLC-MS was performed by two different operators on different days in the same laboratory on the same nanoLC-MS system. For better comparison relative retention times (Rel. RT) based on most abundant G0F are listed. Rel. RT and relative glycan amounts are in good agreement between the two operators.**

| | Operator 1 | | Operator 2 | |
|---|---|---|---|---|
| **Glycan** | **Rel. RT** | **MS %** | **Rel. RT** | **MS %** |
| M7 (1) | 0,77 | 0,11% | 0,78 | 0,10% |
| M7 (2) | 0,78 | 0,15% | 0,79 | 0,10% |
| M6 | 0,80 | 0,58% | 0,81 | 0,64% |
| M7 (3) | 0,81 | <0,10% | 0,82 | <0,10% |
| M7 (4) | 0,83 | <0,10% | 0,84 | <0,10% |
| M5 | 0,85 | 2,28% | 0,85 | 2,64% |
| G1 | 0,88 | 0,04% | 0,88 | 0,12% |
| G0 | 0,89 | 0,46% | 0,90 | 0,57% |
| M3 | 0,90 | 0,76% | 0,90 | 0,70% |
| G2F | 0,95 | 0,08% | 0,95 | 0,10% |
| M5G1F/M6G0F | 0,95 | 0,05% | 0,95 | 0,06% |
| G2F | 0,97 | 0,73% | 0,97 | 1,08% |
| G1F | 0,97 | 0,52% | 0,97 | 0,64% |
| M5G1F/M6G0F | 0,98 | 0,15% | 0,98 | 0,20% |
| G1F | 0,98 | 11,48% | 0,98 | 13,27% |
| G1F | 0,99 | 3,42% | 0,99 | 4,10% |
| M3G1F | 0,99 | 1,04% | 0,99 | 1,11% |
| G0F | 1,00 | 74,96% | 1,00 | 71,78% |
| M3G0F | 1,00 | 2,73% | 1,00 | 2,27% |
| G1FB | 1,04 | 0,08% | 1,04 | 0,12% |
| G0FB | 1,05 | 0,37% | 1,05 | 0,41% |

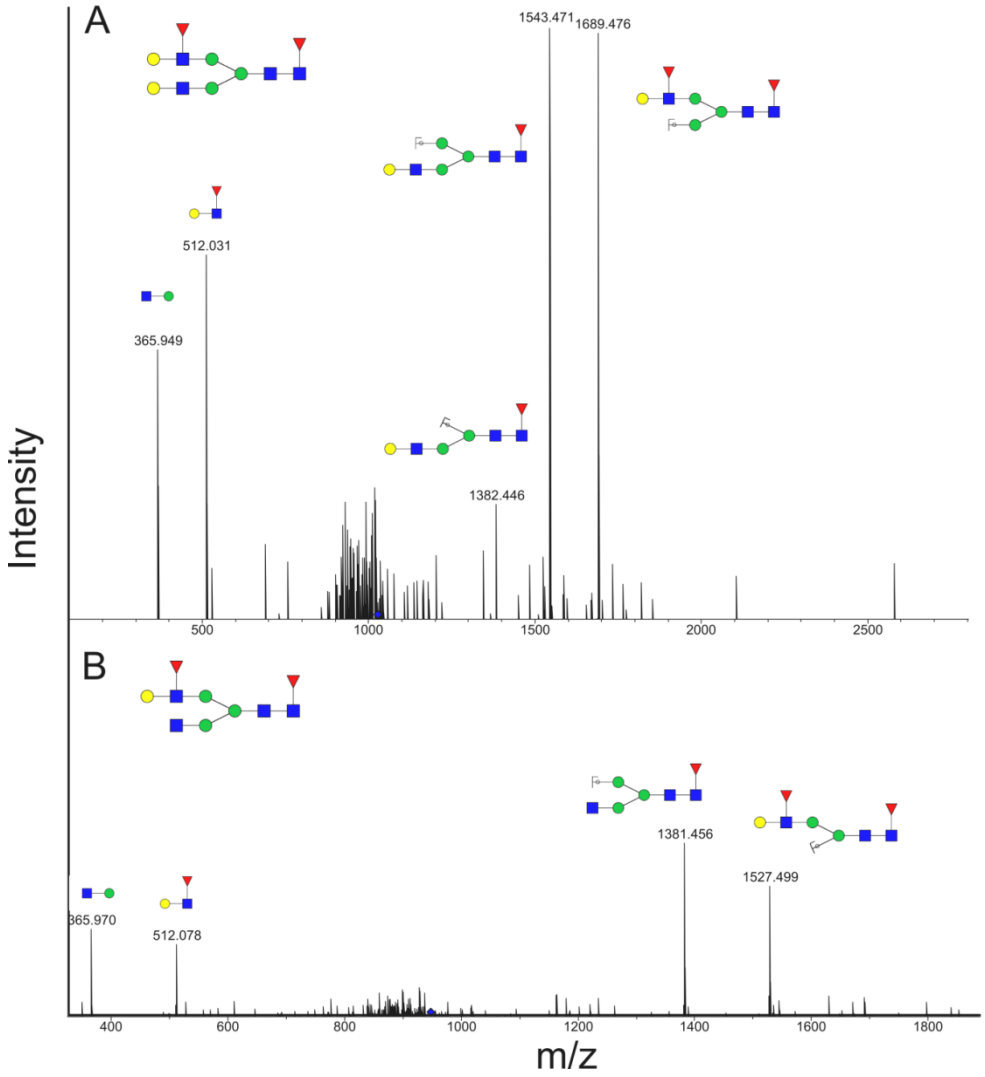


**Figure S7: MS² spectra of two glycans each carrying two fucose residues. (A) MS² of G2F2. Precursor ion was double charged 1027.8 m/z. The glycan can be identified unambiguously due to two signature fragments at 1689 m/z and 512 m/z respectively. (B) MS² of G1F2. Precursor ion was double charged 946.8 m/z. This glycan can be identified according to the fragments at 512 m/z and 1527 m/z.**

# Chapter 4

## *Development and qualification of a high-throughput affinity purification and N-glycan analysis methodology for glycan PK profiling of monoclonal antibodies*


### Abstract

In this chapter the development and qualification of an affinity purification is described. The method was intended to recover monoclonal antibodies from preclinical or clinical serum samples. The affinity purification utilized immobilized antigen columns in 96-well format and a selective elution step of the Fc part from selectively captured mAbs using the IdeS enzyme. The glycosylated antibody fragment was deglycosylated and the N-glycans were labeled with 2-AA and finally analyzed using nanoLC-MS. The incorporation of an internal stable heavy isotope N-glycan standard allowed the differential analysis of individual mAb N-glycans. The sensitive method enabled N-glycan analysis from 50 µl serum samples containing as little as 40 ng mAb. The approach was subsequently qualified in terms of linearity, reproducibility and robustness. The investigation of a simulated decrease of terminal galactosylation of a mAb demonstrated the viability of the developed methodology for the intended N-glycan PK profiling.

## 4.1. Introduction

Affinity purification of biopharmaceuticals from complex matrices is difficult, especially the purification of monoclonal antibodies. In serum there is a constant IgG concentration of approximately 10 mg/ml, the so called baseline concentration (*1*, *2*). The half-life of endogenous IgG is around 23 days which is achieved through a recycling mechanism involving the neonatal Fc receptor (FcRn). This process also applies for mAbs (*3*, *4*). After administration of an IgG biopharmaceutical a baseline concentration increase of approximately 1-3 % occurs depending on the injected amount (*1*). Investigation of N-glycosylation influence on the pharmacokinetics of mAbs in animal and human studies is reported several times in literature (*5*–*12*). For distinct glycoforms enriched IgG fractions were used in some studies (*10*, *12*). However, enrichment might change the protein drug product and may lead to false results. Analysis of N-glycosylation from the complex glycosylated mAb for example by HPLC or MS is therefore advantageous. The mAb has to be purified from the highly complex serum matrix which can be achieved with high affinity using the respective antigen. However, use of 0.5 ml to 1 ml serum are reported due to the low mAb concentration (*5*–*7*). In addition the elution of monoclonal antibodies after binding their respective antigen requires harsh conditions (e.g. very low pH) which could in turn lower the yield (*13*).

To overcome these challenges a comprehensive sample preparation is necessary. In this chapter a 96-well plate based affinity purification is developed to enable processing of large numbers of samples. Immobilized antigen is used to recover the target mAb. Instead of elution via pH shift, the glycosylated Fc part is released with a specific enzyme and the released and derivatized N-glycans analyzed by LC-MS. Quantification of proteins and peptides from serum is often performed using stable heavy isotope internal standards (*14*–*17*). However, since stable heavy isotope labeling of N-glycans is hardly possible the use of stable heavy isotope fluorescence labels like 2-AA is a viable option for N-glycan quantification by mass spectrometry (*18*). The use of stable heavy isotope labeled 2-AA N-glycans as internal standard levels out differences during sample preparation and different ionization efficiencies during mass spectrometric analysis and will be evaluated and implemented in the work-flow.

It is further demonstrated that the developed method enables full mAb N-glycan characterization from 50 µl of serum samples with minimum concentrations of 5-10 µg/ml and analysis of the major glycovariants at concentrations below 1 µg/ml. The developed approach is finally qualified for use with two feasibility studies including linearity, reproducibility and robustness experiments.

## 4.2. Material and Methods

### 4.2.1. Materials

2-Aminobenzoic acid, ethanolamine, formic acid, picoline borane, DMSO, $^{13}C$ aminobenzoic acid were purchased from Sigma (Munich, Germany), PNGaseF from Roche (Penzberg, Germany), acetic acid, acetonitrile and hydrochloric acid from Merck (Darmstadt, Germany), Protein G sepharose, NHS activated sepharose, Sephadex® G-10 96-well plates and 96-well deep well plates from GE Healthcare (Munich, Germany), PBS from Gibco/Life technologies (Darmstadt, Germany) and B-galactosidase from New England Biolabs (Frankfurt, Germany).

Multicreen THS HV filter plates were obtained from Milipore, IdeS (Fabricator™) from Genovis (Lund, Sweden), 96-well plates from Nunc (Thermo Scientific, Germany), AcroPrep™ Advance Omega™ 10 kDa 96-well filter plates from Pall (Dreieich, Germany).

### 4.2.2. Methods

#### 4.2.2.1. Preparation of heavy isotope 2-AA labeled N-glycans

N-glycans of desalted mAb (1 mg) were released with use of PNGaseF overnight (17 h) at 37°C. The N-glycans were separated from the proteins using Amicon 30K filter devices and were brought to dryness in a speedvac. Picoline borane and [$^{13}C$] 2-AA were dissolved in 70:30 (% *v/v)* DMSO-acetic acid to furnish concentrations of 63 and 50 mg $mL^{-1}$, respectively. Labeling solution (15 µL) and deionized water (10 µL) were added to 15 nmol enzymatically released and dried glycans. The labeling reaction was performed at 37°C for 17 h. Excess label was removed by gel filtration on G-10 columns. Columns were conditioned with 10 ml $H_2O$. Samples were diluted to 100 µl with deionized $H_2O$ then applied to the column. After rinsing the column with 700 µl $H_2O$ the purified fluorescence labeled N-glycans were eluted with 600 µl $H_2O$. Purified [13C] 2-AA labeled N-glycans were aliquoted and stored at -20°C until use.

#### 4.2.2.2. Reconstitution of antigen and preparation of stock solution

Recombinant human antigen was reconstituted according to the manufacturer instructions. Antigen was dissolved in $H_2O$ (1 mg/mL) and reconstituted for 2 hours at room temperature.

#### 4.2.2.3. Preparation of 96-well filter plate based affinity columns

The membranes of a 96 well filter plate were wetted with 1mM HCl (100 µL) before addition of 200µL NHS activated sepharose-isopropanol slurry per well. Isopropanol was removed by centrifugation and the columns were washed with 1 mM HCl (150 µL) for four times. Antigen solution (100 µL) was centrifuged into the columns and coupling reaction was allowed to take place for 2 hours at ambient temperature. Affinity columns were washed and remaining NHS

groups were inactivated with use of ethanolamine buffer (150 µL). Finally columns were equilibrated with PBS.

#### 4.2.2.4. Affinity purification of monoclonal antibodies

Serum samples (50 µL) were diluted to 100 µL with PBS and applied to the affinity purification column by centrifugation. Bound mAb was washed six times with PBS to remove serum and unspecific bound proteins. Fabricator solution was centrifuged into the columns to release the glycosylated Fc part of the mAb. Reaction was performed at 37°C for 30 minutes. Released Fc parts were eluted with PBS and PNGaseF with $^{13}$C-2-AA labeled N-glycan standards was added. This mixture was incubated for 17 hours at 37°C. Remaining proteins were removed by ultrafiltration using 96-well plates with 10 kDa membranes. Released N-glycans with glycan standard were dried by vacuum centrifugation.

#### 4.2.2.5. N-glycan labeling

Dried samples containing free reducing end N-glycans and 13C 2-AA labeled glycan standard were dissolved in $H_2O$ (10µL) and 2-AA labeling solution (15 µL; 100 mg/mL picoline borane, 50 mg/mL 2-AA in a 7:3 mixture of DMSO and acetic acid) was added. Labeling reaction took place for 17 hours at 37°C.

#### 4.2.2.6. Gel filtration

Custom made 96-well plate Sephadex G-10 columns were equilibrated with 800µL $H_2O$. Labeled samples were filled up to 100µL with $H_2O$ and applied to the gel filtration columns. 2-AA and 13C 2-AA labeled N-glycans were eluted with $H_2O$ (150 µL). Finally samples were brought to dryness by vacuum centrifugation and were redissolved in 20µL $H_2O$ for nanoLC-MS analysis.

#### 4.2.2.7. Degalactosylation of monoclonal antibodies

mAb was degalactosylated by addition of beta-galactosidase and incubation at 37°C for 1 h after desalting and transferred into PBS. Reaction was stopped by cooling the samples to 4°C.

#### 4.2.2.8. Size Exclusion Chromatography

Size exclusion chromatography (SEC) analysis of proteins was performed with an Agilent 1200 series HPLC with a SEC column (Phenomenex Yarra™ SEC-3000, 4.6 mm x 30cm; 3 µm particle size). Eluent was 150 mM potassium phosphate pH 6.5. Following sample injection elution was performed for 40 min at 0.4 ml/min. Column temperature was 30°C. UV detection was performed at 206 nm, 214 nm and 280 nm.

#### 4.2.2.9. HPLC of intact proteins

Analysis of intact proteins was performed with an Agilent 1200 series HPLC on a C8 reversed phase chromatography column (Agilent Zorbax 300SB-C8, 2.1 x 150mm; 3.5µm particle size). Eluents were 0.05 % formic acid in $H_2O$ (component A) and 0.05 % formic acid in ACN (component B). The system was equilibrated at 26% component B. Following sample injection initial conditions were held for 2 min. Component B was then raised to 60 % over 18 min and to 95% over 4 min. After column regeneration at 95% B for 4 min, the column was re-equilibrated at 26 % for 4 min. Flow rate was 0.35 mL $min^{-1}$ oven temperature was 70°C. UV detection was performed at 206 nm, 214 nm and 280 nm.

#### 4.2.2.10. RP HPLC of 2-AA labeled glycans

Liquid chromatography was performed with an Agilent 1200 Series chromatograph on a Waters Acquity UPLC BEH130 $C_{18}$ (2.1 mm x 150 mm 1.7-µm particle) column. Analysis of 2-AA labeled glycans was performed with a gradient prepared from 1.0 % formic acid in $H_2O$ (component A) and 50 % ACN in 1.0 % formic acid in $H_2O$ (component B). The column was equilibrated with 4 % B. After injection of up to 100 µL sample the mobile phase composition was held at 4 % B for 2 min. The proportion of B was then raised in four steps to 28%, first to 10 % over 27 min, then to 11.5 % over 10 min, then to 14 % over 8 min and finally to 28 % over 19 min. The column was regenerated by increasing to 90 % B over 4 min, followed by isocratic elution for 2 min. The column was then re-equilibrated at 8 % B for 5 min. Oven temperature was 50 °C and the flow-rate was 0.30 mL $min^{-1}$. Fluorescence detection was performed with an excitation wavelength of 250 nm and an emission wavelength of 425 nm. Analysis of 2-AB labeled glycans was performed with a gradient prepared from 0.5 % formic acid in $H_20$ (component A) and 0.5 % formic acid and 5 % ACN in $H_20$ (component B). The column was equilibrated with 25 % B. After injection the mobile phase was held at 25 % B for 2 min, eluent B was increased to 55 % over 60 min and then increased to 61 % over 24 min. The composition was held for 2 min and then initial condition was reached after 2 min and held for additional 5 min. Oven temperature was 40°C and the flow rate was 0.3 ml $min^{-1}$ Fluorescence detection was performed with an excitation wavelength of 250 nm and an emission wavelength of 428 nm.

#### 4.2.2.11. nanoLC-MS of 2-AA labeled glycans

NanoLC (Thermo/Dionex Ultimate 3000) was set-up in “preconcentration” mode according to the manufacturer manual with a pre-concentration column (3 µm particles, 75 µm x 2 cm) and an analytical column (2 µm particles, 75 µm x 25 cm). Column compartment was held at 40°C. Mobile phase of the nano pump consisted of 0.5% formic acid in $H_2O$ (component A)

and 0.5% formic acid in 50% ACN (component B). Mobile phase of the capillary pump consisted of 0.5% formic acid and 1% ACN in $H_2O$ (component C). The analytical column was equilibrated with 2% component B at a flow rate of 300nl/min. The preconcentration column was equilibrated with 100% component C. With a user defined injection routine 8 µl sample were stacked between loading solution (0.1% formic acid, 1% ACN in ultrapure water) in a 20µl sample loop. Sample loop was switched for 2 minutes in-line of the capillary pump flow to allow optimal trapping. Prior to the next injection sample the loop was washed with loading solution. After trapping the pre-concentration column was switched into the nano pump flow and component B was raised to 30% over 60 min, then to 95% over 5 min. After holding at 95% component B for 5 min the column was finally re-equilibrated at 2% component B for 15 min. Column outlet was connected to a UV detector with a 3nl flow-cell.

#### 4.2.2.12. ESI Mass Spectrometry

The HPLC was directly coupled to a 3D ion trap ESI-MS (Bruker AmaZon). The ion trap was operated in Enhanced Resolution Mode with a capillary potential of 4 kV. The capillary temperature was set to 250 °C with a nebulizer pressure of 2 bar and a dry gas flow of 6 l/min. $MS^2$ spectra were generated by use of the Auto $MS^2$ mode and Collision Induced Dissociation (CID).

#### 4.2.2.13. nanoESI Mass Spectrometry

Outlet of the nanoLC was directly coupled to an ion trap ESI-MS (Bruker AmaZon) equipped with an on-line nano source (Bruker CaptiveSpray®). The ion trap was operated in Enhanced Resolution Mode with a capillary voltage of 1.7 kV. Source temperature was set to 200°C and a dry gas flow of 3 l/min was used to heat the source.

## 4.3. Results

### 4.3.1. Development of the approach

In order to achieve the goal of an analytical method for characterization of the pharmacokinetics of individual N-glycan variants of monoclonal antibodies an affinity purification approach had to be established which consumes only minute amounts of serum samples. In addition, the work-flow should be compatible with the existing biopharmaceutical development program as shown in Figure 1. The standard way is shown on the right utilizing immunoassays for the detection and quantification of proteins in (pre)clinical samples. On the left the glycan PK profiling work-flow is depicted schematically. The selected strategy was to purify the target protein and the N-glycans were released and labeled. Samples were then analyzed by LC-MS. All steps of the approach had to be optimized for the intended use and were subsequently qualified.

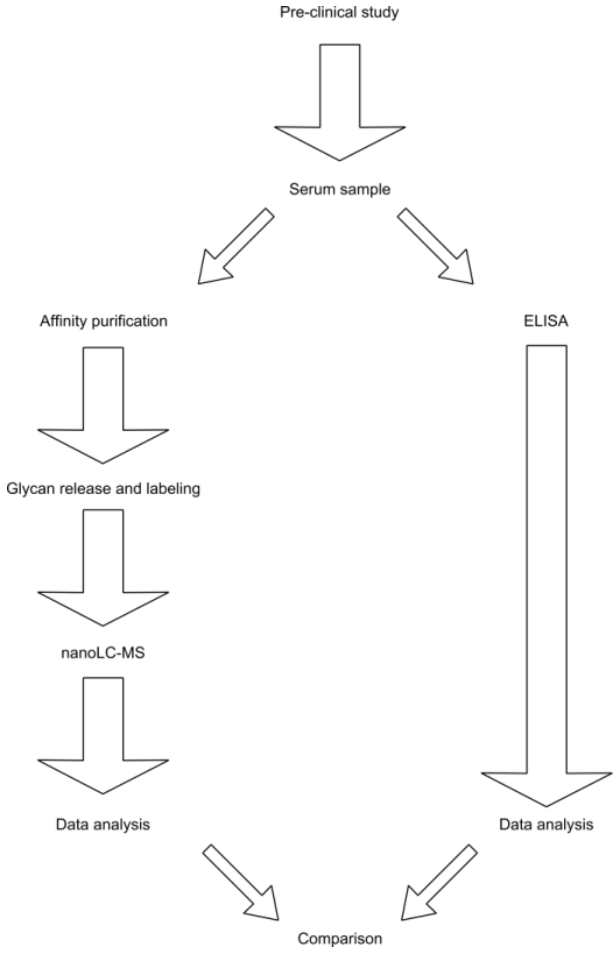


**Figure 1: Simplified work-flow of the (pre)clinical study analysis. Serum concentrations of the biopharmaceuticals are obtained by ELISA. Information about single glyco-variants is obtained by the work-flow shown on the left including affinity purification, glycan release and labeling and nanoLC-MS.**

Immunoassay analysis of (pre)clinical samples provides information about the absolute mAb content. All existing variants are quantified as a mixture providing that all variants can be

detected. In contrast LCMS based glycan PK profiling provides information about individual variants, in this case glyco-variants. However, the information is not quantitative; it is a differential analysis with a constant internal standard. Data from both arms can be combined and interpreted.

Preclinical and clinical studies usually render a high number of samples. To be able to analyze large sets of samples a high-throughput affinity purification method with the use of 96-well filter plates has been developed. High selectivity and sensitivity of affinity purification could be achieved using the binding partner or target protein of the protein of interest, in the case of monoclonal antibodies the antigen. First step for successful and efficient affinity purification was the immobilization of the antigen to a resin, e.g. sepharose with active groups. There were several commercially available sepharose resins, for protein immobilization two frequently used active groups are CNBr or NHS activated sepharose both binding to primary amines of the protein (e.g. lysine residues or the N-terminus). For the antigen immobilization NHS activated sepharose was optimal. The NHS group has an additional spacer arm to the resin which allowed a more efficient binding of mAbs because more potential binding sites were accessible. 5 µg of antigen was used for immobilization which enabled purification of approximately 14 µg of the appropriate mAb.

After resin preparation, antigen immobilization and deactivation of remaining active group as described in the methods section the affinity plates could be used. First experiments were performed utilizing a vacuum device to force the liquid through the columns. However, inhomogeneous flow and contaminations from serum glycoproteins was observed resulting in poor reproducibility. Therefore, the work-flow was optimized using centrifugation which resulted in a highly reproducible procedure.

### 4.3.2. Determination of the maximal mAb binding capacity of the affinity columns

After implementation of the centrifugation work-flow, the coupling efficiency and maximal binding capacity of the affinity columns was determined. Coupling efficiency was evaluated analyzing three types of samples: (i) an aliquot of the antigen solution that was centrifuged into the column as reference, (ii) the direct flow through obtained after centrifuging the coupling solution into the sepharose column and (iii) the eluat after the first washing step collected after the coupling reaction which might contain uncoupled antigen. Figure 2A shows the resulting chromatograms of the direct flow through analysis from two replicates and the reference solution after C8 chromatography of the intact antigen. The sample contained 4 % and 10 % antigen respectively which was centrifuged through the column and not coupled to the resin. Variation between the samples was due to small differences of the

column volume. Coupling was subsequently optimized by adjusting the utilized volumes. Instead of 150 µl only 100 µl containing 5 µg of antigen were applied. Flow through was again analyzed after optimization and antigen could hardly be detected (Figure 2B). The flow through collected after the first washing step did not contain antigen also due to the high excess of free NHS groups compared to antigen that is used.

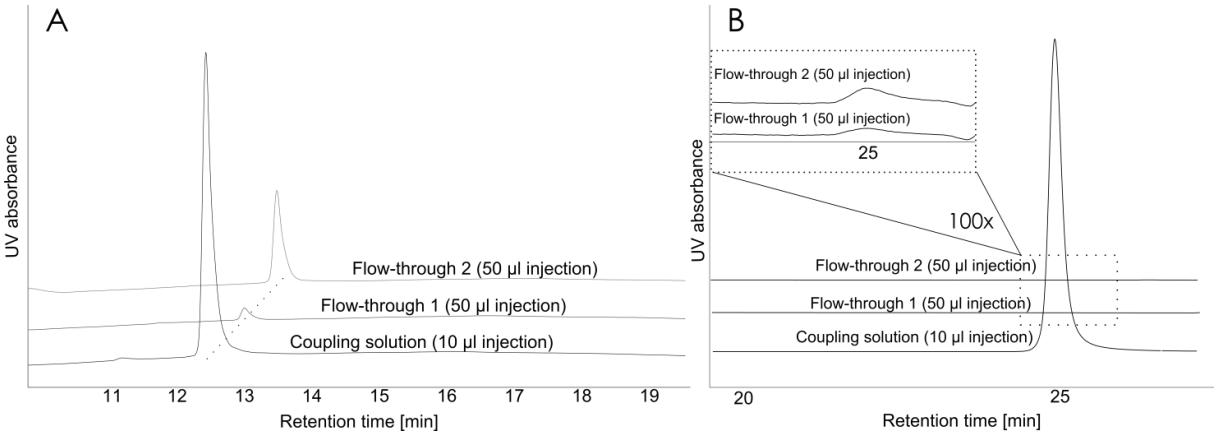


**Figure 2: UV chromatograms of antigen intact protein analysis. A) C8 chromatography. Results of coupling solution containing 0.033 mg mL-1 antigen and flow-through of two samples 1 and 2 are shown. B) SEC analysis. Results of coupling solution containing 0.05 mg mL-1 antigen and flow-through of two samples are shown after optimization of the work-flow. Injection volumes are depicted in inserts.**

### 4.3.3. Proof of concept study

Next step was to test the developed affinity purification method for artificial serum samples. Serum samples were prepared by spiking a mAb into pooled rabbit serum. Dilutions were prepared to simulate concentrations of a typical preclinical study between 5 µg/ml and 85 µg/ml (Figure 3). Bound mAb was washed several times and the glycosylated Fc parts were eluted enzymatically by centrifugation of Fabricator into the column and by incubation of the plates. N-glycans were released by PNGaseF, ultrafiltrated and labeled with 2-AA. The labeled N-glycans were then analyzed by LC-MS (method is described in detail in Chapter 2).

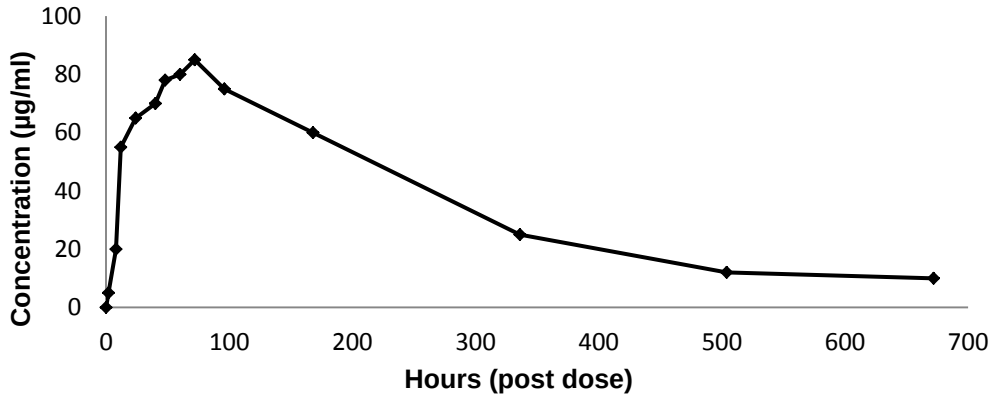


**Figure 3: Exemplary PK profile of a mAb in a preclinical study obtained by ELISA. Dilution series was prepared according to concentrations obtained from the profile.**

However, the MS method was not sensitive enough to detect most of the 2-AA glycans. Consequently, detection and quantification was performed with the fluorescence detector of the HPLC. Results for four N-glycans with different percentages are shown in Figure 4. The results were in good agreement with the N-glycan composition obtained from 2-AA glycan maps of the mAb.

For the MS analysis of all 2-AA N-glycans a more sensitive NanoLC-MS method was developed (see Chapter 3). Results of the nanoLCMS analysis are shown in Figure 5. All N-glycans of the mAb were analyzed successfully. The percentages of G0F, G1F and M3G0F were identical to the fluorescence based quantification. The portion of M5 was smaller when using nanoLC-MS. This might be due to a slightly worse ionization efficiency of high mannose N-glycans. In addition, the variation between the samples was rather high due to small differences in the sample preparation and variation of the nanoLC-MS system lacking internal standards. In order to overcome this issue and to further improve the method an internal standard based on heavy isotopes was included into the work-flow.

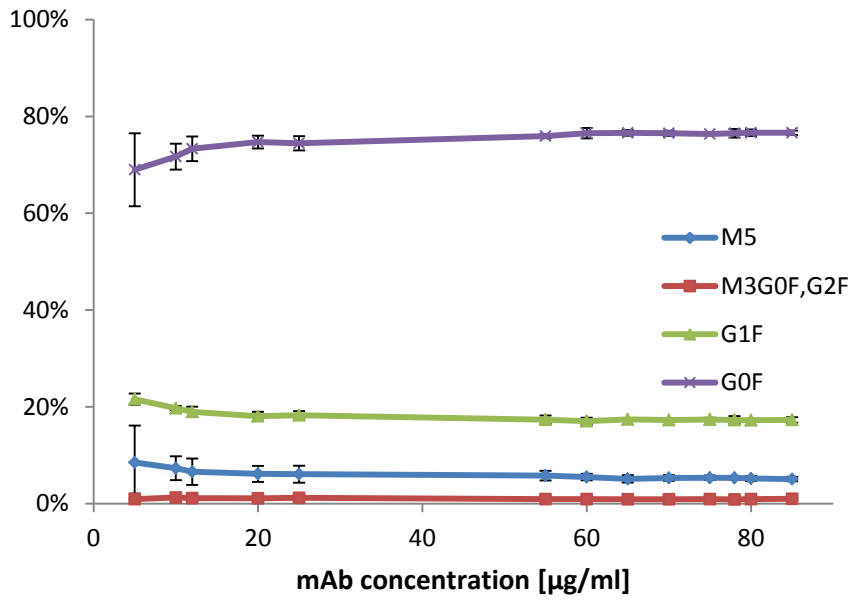


**Figure 4: Relative glycan composition of the proof of concept study obtained by fluorescence detection.**

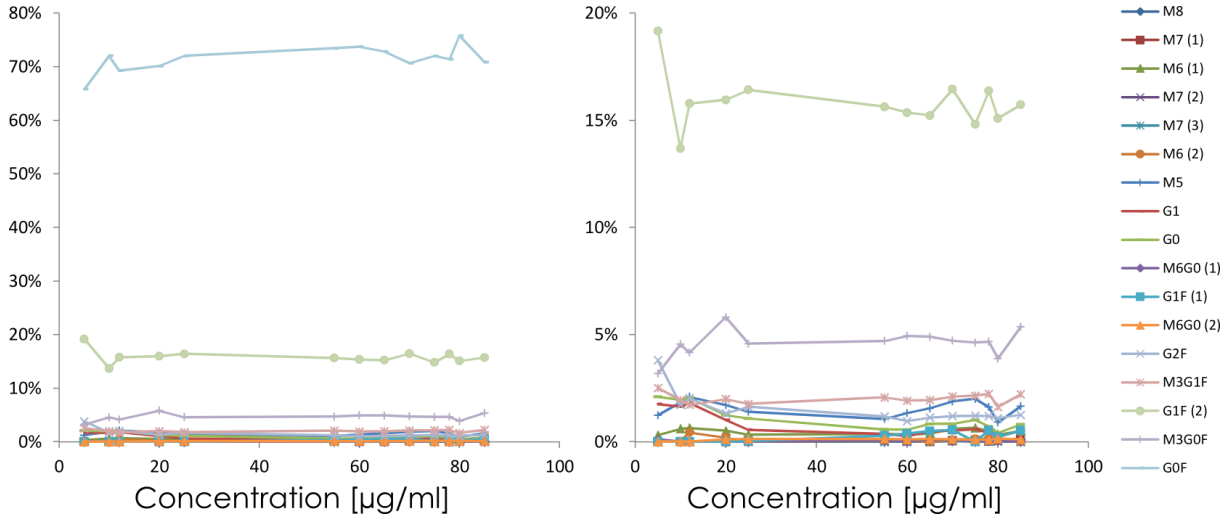


**Figure 5: Results of the proof of concept study. Spiked serum samples were analyzed by nanoLCMS after affinity purification and N-glycan processing.**

### 4.3.4. Differential analysis of N-glycans with heavy isotope 2-AA labeling

Stable heavy isotope containing standards are frequently used for the quantitation of proteins or peptides by MS (*16*, *19*). The standard can either be a peptide or an intact protein containing several $^{13}C$ or $^{15}N$ atoms. Due to the identical chemical properties the respective

standard has the same retention and ionization like the sample but the mass shift enables selective detection and quantification. Quantification or differential analysis of samples is performed against known or constant amounts of this standard.

For N-glycans no stable heavy isotopes are commercially available and the production of multiple standards would be very expensive. The use of a stable heavy isotope containing label however is a viable and simple option to obtain stable heavy isotope variants for N-glycan analysis. $^{13}$C 2-AA is commercially available with very high purity. A general drawback of using a $^{13}$C 2-AA labeled glycan standard is the rather late addition to the work-flow, at the earliest with PNGaseF after the affinity purification. This option reflects glycan release, labeling, purification and most important the nanoLC-MS analysis. Accordingly, the N-glycans of the used mAb were released and labeled with the $^{13}$C 2-AA and used as the internal standard. This proceeding renders a standard for each N-glycan.

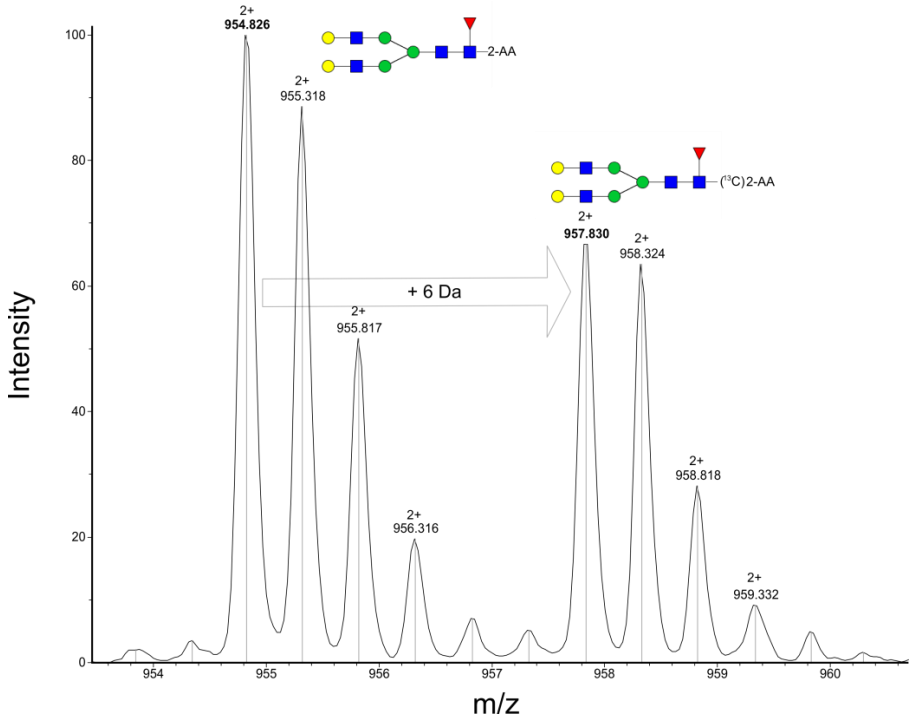


**Figure 6: MS raw spectrum of 2-AA labeled G2F glycan. The two isotopic pattern show the 2-AA labeled G2F (left) and the 6 Da heavier 13C 2-AA labeled G2F (right). The heavy isotope labeled N-glycan serves as internal standard for quantification.**

Figure 6 shows an exemplary profile spectrum of co-eluting 2-AA labeled G2F and its corresponding stable heavy isotope standard with six $^{13}$C atoms resulting in a mass shift of six Daltons. The intensity of the monoisotopic peak of the “light” sample relative to the intensity of the monoisotopic peak of the “heavy” standard was determined giving a “light” to “heavy” ratio (L/H). This ratio was determined for each N-glycan and time point of the

(pre)clinical study individually. Plotting the L/H ratio provided the PK profile for each N-glycan comparable to an ELISA profile.

### 4.3.5. Comparison of mAb glycan map and results from affinity purification

After implementation of the stable heavy isotope 2-AA glycan standard the resulting glycan map after affinity purification and N-glycan processing of mAb spiked samples (100 µg/ml) was compared to conventional glycan analysis of the mAb. The results are depicted in Figure 7. The glycan map obtained from spiked serum samples showed some differences compared to the conventional glycan map. Some less abundant N-glycans with a portion below 0.1 % like the high mannose type structures M7 and M8 or hybrid type structures like one M5G1F/M6G0F and M4G1F/M5G0F isomer were not detected in the glycan maps of the serum samples. Two N-glycans were overrepresented in the serum samples. The percentages of the two bisecting N-glycans G1FB and G0FB were around ten times higher than in the drug product. The N-glycans appeared to be co-purified and were exclusively present when analyzing serum blanks. Additional washing steps (high and low pH, high NaCl or addition of soft detergent) did not lead to an improvement and these two glycans finally had to be excluded from analysis. High mannose glycan M5 percentages were smaller in the serum spiked samples. These results showed that there might be some glycan related impurities (e.g. from the two bi-secting glycans) which were co-purified with the target molecule. To prevent false results, negative and positive, quality control (QC) samples with varying mAb concentrations spiked into serum should be prepared in parallel to each analysis. Furthermore the results showed that N-glycans with very low abundance could not be analyzed with the developed method at preclinically relevant concentrations.

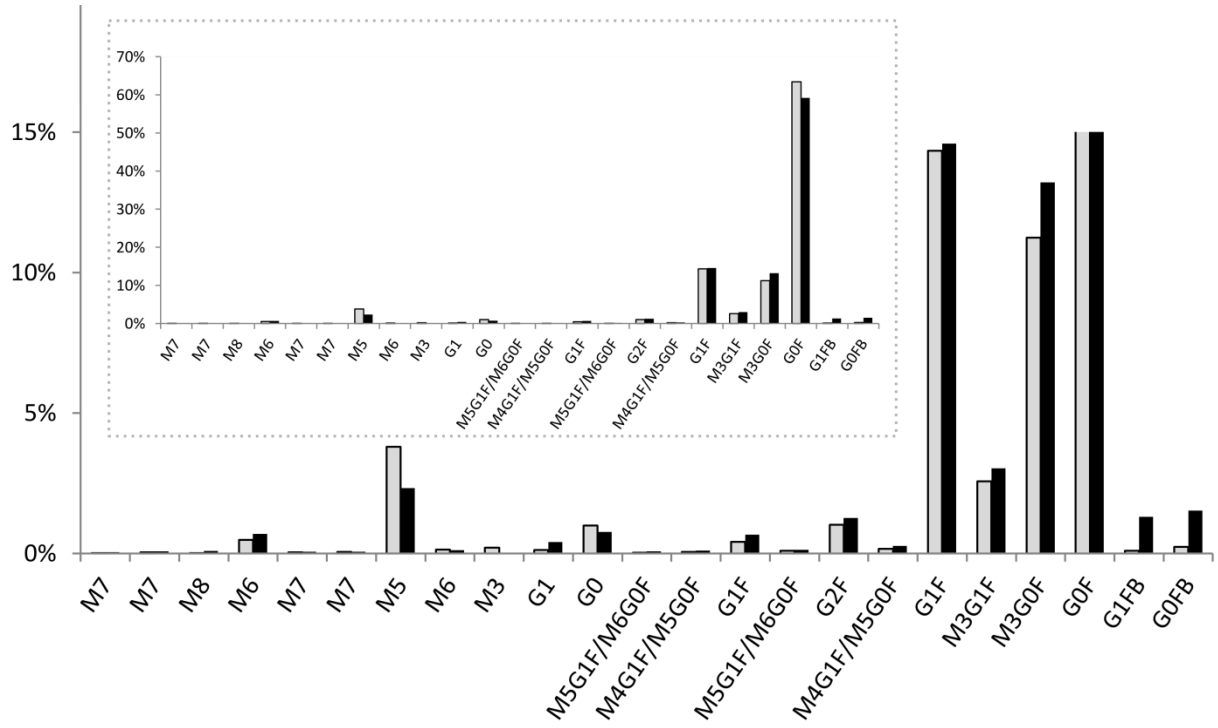


**Figure 7: Comparison of relative glycan composition between drug product derived mAbs (grey) and serum spiked and affinity purified mAb (black). Magnified view and inset with full view are shown.**

### 4.3.6. Linearity of the N-glycan PK profiling method

Linearity of the glycan PK method was determined including the complete work-flow with affinity purification, N-glycan processing and nanoLC-MS from repeated analysis of sample duplicates. Serial dilutions were prepared freshly and for each replicate individually. Serial dilutions contained nine relevant concentration levels (200, 100, 50, 25, 12.5, 6.3, 3.1, 1.6 and 0.8 µg/ml). The L/H ratio was determined for each N-glycan and normalized relative to the signal at 200 µg/ml. These relative L/H ratios were plotted against the respective concentration and under the assumption of linear correlation a linear regression was performed. Table 1 lists the linear range of each N-glycan of the mAb. Previously excluded G1FB and G0FB as well as the not detectable high mannose and hybrid structures are not shown. Linearity was given for regressions with $R^2 > 0.980$.

**Table 1: Linearity of the developed glycan PK profiling method. Linearity was determined for each N-glycan. Linear range with LLOQ, ULOQ and coefficient of determination is depicted.**

| | Linear range [µg/mL] | | Linear correlation |
|---|---|---|---|
| **N-glycan** | LLOQ | ULOQ | $R^2$ |
| M6 | 3.1 | 100.0 | 0.996 |
| M5 | 0.8 | 100.0 | 0.991 |
| G0 | 1.6 | 100.0 | 0.984 |
| M3 | 3.1 | 200.0 | 0.986 |
| M5G1F/M6G0F | 25.0 | 100.0 | 0.979 |
| G2F | 0.8 | 200.0 | 0.985 |
| M5G1F/M6G0F | 12.5 | 100.0 | 0.971 |
| G1F | 0.8 | 100.0 | 0.992 |
| M3G1F | 0.8 | 100.0 | 0.988 |
| M3G0F | 1.6 | 100.0 | 0.995 |
| G0F | 0.8 | 100.0 | 0.992 |

The lower limit of quantification (LLOQ) which is the lowest concentration still fitting to linear regression of major N-glycans was lower than for minor abundant N-glycans. G0F, G1F, M5 and G2F signals were linear to 0.8 µg/ml. To obtain valid glycan maps including all N-glycans the mAb concentration must be as high as the lowest LLOQ. In the present case 25 µg/ml. However the portion of the two M5G1F/M6G0F isomers was around 0.1 – 0.2 % of the total mAb glycan content and thus the potential influence on PK would be limited. The remaining nine N-glycans of the mAb were analyzed between 100 µg/ml and 3.1 µg/ml. Immobilization of 5 µg antigen per affinity column was sufficient to theoretically purify 14 µg mAb or when using a serum sample volume of 50 µl a mAb concentration of 280 µg/ml. In practice the maximal binding capacity should be lower due to a coupling efficiency <100% and saturation effects during the binding step. The observed maximal binding capacity within the linear range of ~5µg mAb (100 µg/ml when using 50 µl sample volume) was therefore in good agreement with the expected values.

In Figure 8 linearity plots of all eleven investigated N-glycans are shown. Relative L/H ratio was plotted against protein concentration. The straight line resulting from linear regression is depicted in each diagram.

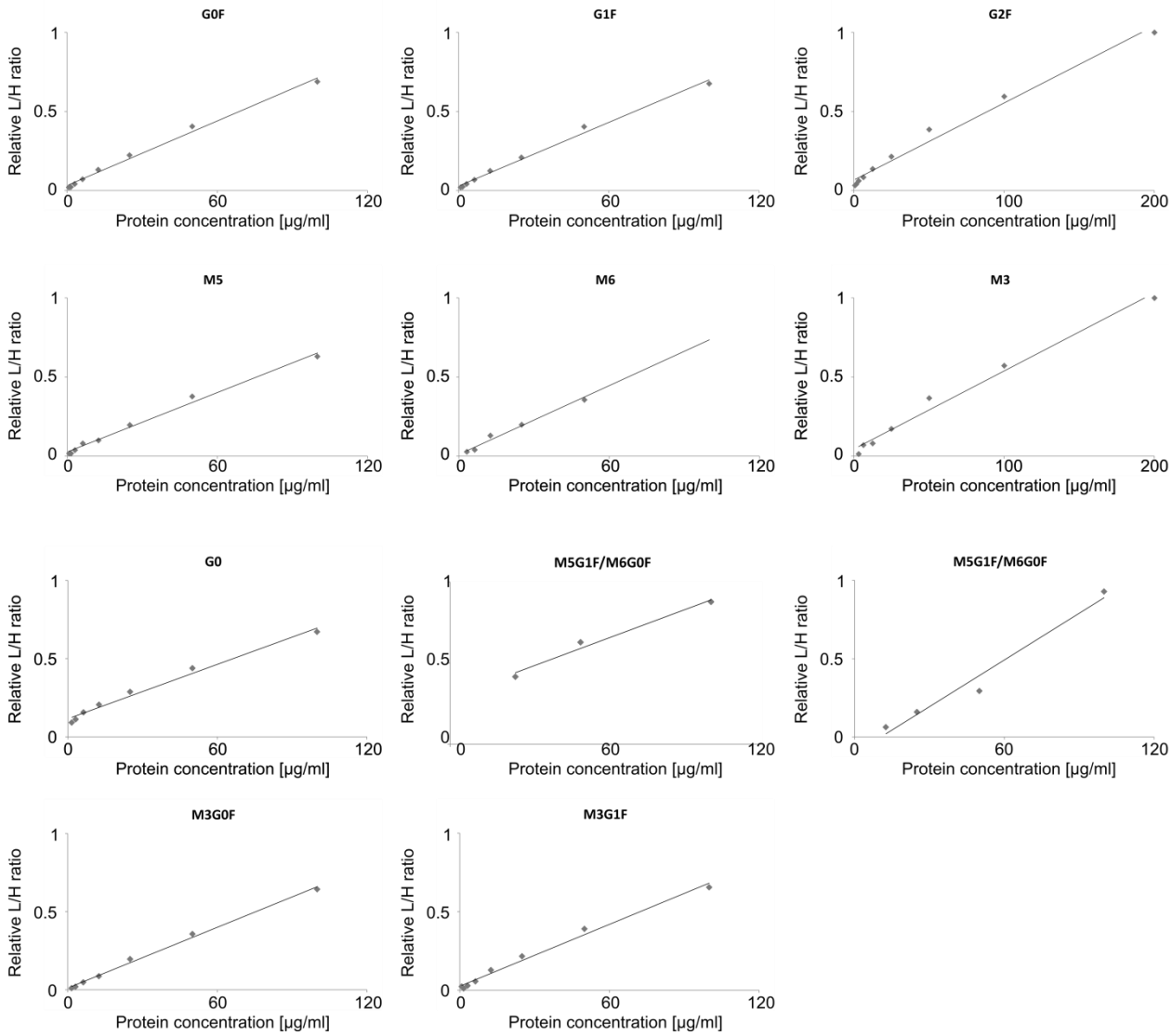


**Figure 8: Linearity plots of the eleven N-glycans of the mAb that could be analyzed with the developed method.**

### 4.3.7. Tracking increasing degalactosylation with the N-glycan PK profiling method

To further qualify the method an artificial change of the N-glycosylation composition was prepared by admixing increasing amounts of degalactosylated mAb to normal glycosylated mAb. The samples were analyzed with the PK profiling method to determine if the change can be observed as well as the minimal change that can be detected. The portions of normal and degalactosylated mAb are listed in Table 2 for each sample. Experiment 1 was the control experiment with eight samples containing only normal mAb. In experiment 2 the portion of degalactosylated mAb was increased to 100%. In experiment 3 and experiment 4 the portion of degalactosylated mAb was increased to 20 % and 5 % respectively. The total mAb concentration was constant at 100 µg/ml.

**Table 2: Experimental set-up of the degalactosylation experiment. Four different dilution series were prepared.**

| | Experiment 1 | | Experiment 2 | | Experiment 3 | | Experiment 4 | |
|---|---|---|---|---|---|---|---|---|
| # | Deglactosylated mAb | normal mAb | Deglactosylated mAb | normal mAb | Deglactosylated mAb | normal mAb | Deglactosylated mAb | normal mAb |
| **1** | 0,00% | 100,00% | 0,00% | 100,00% | 0,00% | 100,00% | 0,00% | 100,00% |
| **2** | 0,00% | 100,00% | 10,00% | 90,00% | 2,50% | 97,50% | 0,63% | 99,38% |
| **3** | 0,00% | 100,00% | 20,00% | 80,00% | 5,00% | 95,00% | 1.30% | 98,75% |
| **4** | 0,00% | 100,00% | 30,00% | 70,00% | 7,50% | 92,50% | 1.88% | 98,12% |
| **5** | 0,00% | 100,00% | 50,00% | 50,00% | 10,00% | 90,00% | 2.50% | 97,50% |
| **6** | 0,00% | 100,00% | 70,00% | 30,00% | 12,50% | 87,50% | 3.75% | 96,25% |
| **7** | 0,00% | 100,00% | 90,00% | 10,00% | 15,00% | 85,00% | 4.38% | 95,63% |
| **8** | 0,00% | 100,00% | 100,00% | 0,00% | 20,00% | 80,00% | 5.00% | 95,00% |

Percentages of terminal galactosylation resulting from summing-up the portions of G2F, G1F and M3G1F for the eight samples of each experiment are shown in Figure 9. The control experiment had a constant portion of approximately 18 %. Experiment 2 showed a constant decrease of terminal galactosylation. A small amount of terminal galactosylation remained in the last sample indicating incomplete degalactosylation.

Experiment 3 showed a decrease from 17.7 % galactosylation to approximately 15 % which was a shift of 15 % relative to the initial portion. Considering an incomplete degalactosylation as seen for experiment 2 this result demonstrated that a relative change of 20 % or 15 % terminal galactosylation can be detected. In experiment 4 with a theoretical change of 5 % a 2.5 % change was observed, but the samples could not be differentiated from the control sample. Thus the decrease of individual N-glycans should be at least 10 – 15 % (relative to initial portion) in order to be detected with the developed approach.

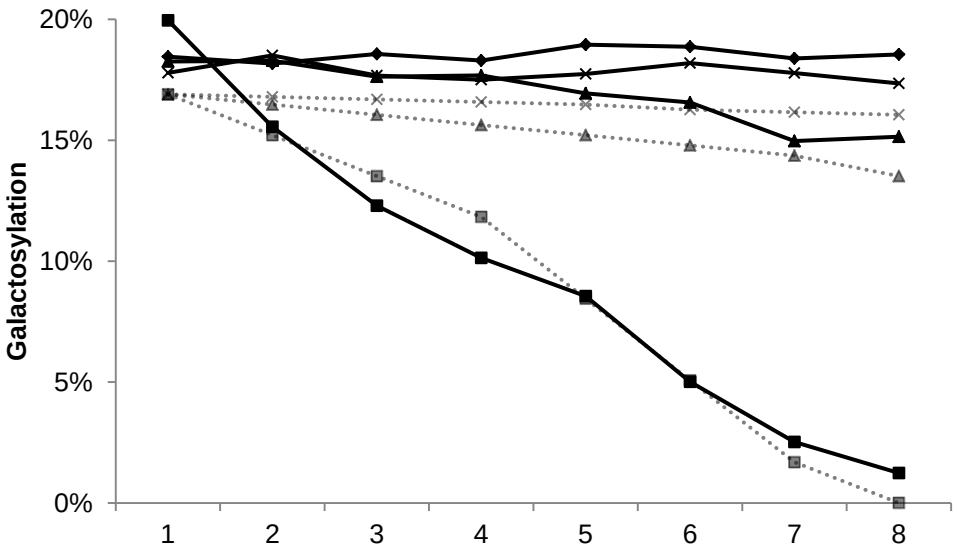


**Figure 9: Galactosylation levels of experiment 1 (diamond), experiment 2 (square), experiment 3 (triangle) and experiment 4 (cross). Dashed line in the same color indicate the theoretical values.**

As a consequence of the decrease in terminal galactose residues an increase of terminal N-acetylglucosamine should be detectable. Terminal GlcNAc was determined by summing-up the percentages of G0F and M3G0F which were also produced by enzymatic removal of galactose residues from G1F, G2F and M3G1F. The results were similar to the quantification of terminal galactosylation (Figure 10). For experiment 2 and 3 the increase of terminal GlcNAc was slightly higher than calculated. Samples from experiment 4 could not be distinguished from the control experiment samples. Thus the developed method was suitable to detect changes with a relative change of at least 10-20% of single N-glycans.

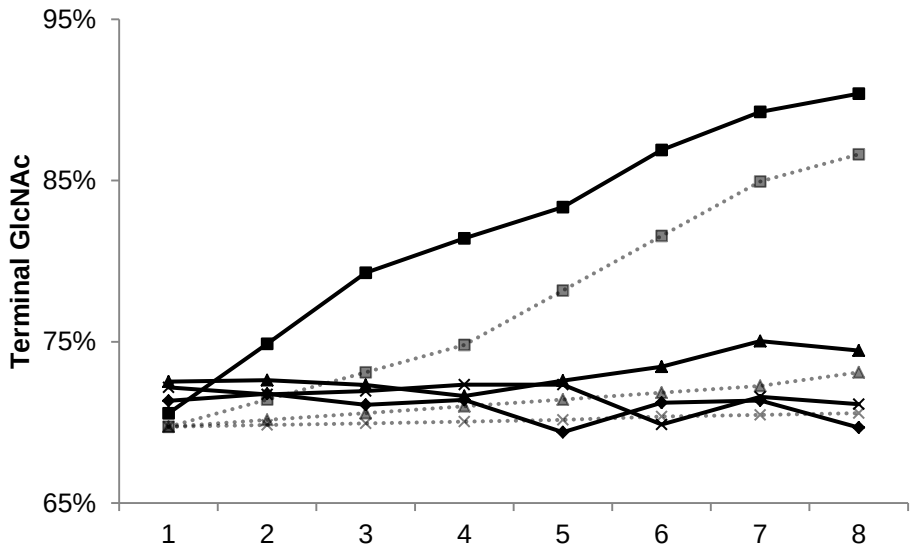


**Figure 10: Terminal GlcNAc levels after enzymatic degalactosylation. Experiment 1 (diamond), experiment 2 (square), experiment 3 (triangle) and experiment 4 (cross). Dashed lines in the same color indicate the theoretical values.**

### 4.3.8. Robustness of the N-glycan PK profiling method

The final experiment to qualify the N-glycan PK profiling method was a robustness experiment. Two different operators performed the complete work-flow including affinity purification, nanoLC-MS and data interpretation without sharing any reagents. Resulting glycan maps are shown in Figure 11A and B. Error bars show the standard deviation determined from full replicates. The results of the two operators were in very good agreement. For example most abundant G0F was 75.9+/-0.3% for operator A and 74.9%+/-0.8% for operator B and for the low abundant core structure M3 percentages were 0.54+/-0.06% and 0.63+/-0.07% for operator A and B respectively. The standard deviation was smaller than 1% for all glycans with overlapping error bars. These results demonstrated the robustness of the developed approach.

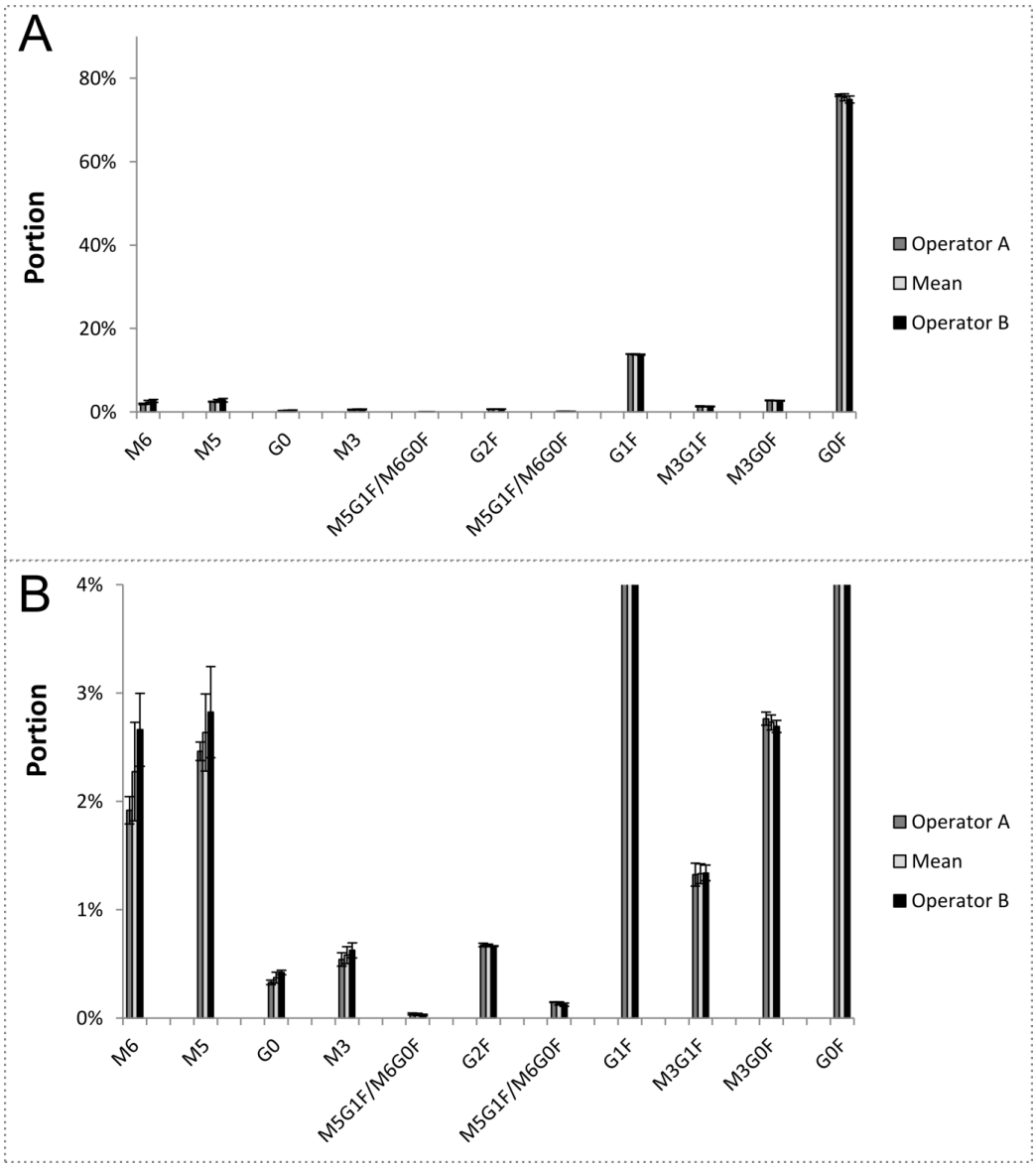


**Figure 11: Robustness of the N-glycan PK profiling method. Results of glycan PK profiling of spiked samples performed by two different operators (A). Magnified view to show minor abundant N-glycans (B)**

## 4.4. Conclusion

In this chapter the development of a glycan PK profiling approach with high-throughput 96-well plate based sample preparation is described in detail. Different development steps from the preparation of affinity columns and optimization of antigen coupling to the NHS resin to the implementation of stable heavy isotope 2-AA glycan standards are pictured. Furthermore the qualification of the method is shown which encompasses a proof of concept study demonstrating the general suitability to analyze N-glycans from serum samples, the determination of linearity, robustness experiments and a second study simulating a decrease of terminal galactose residues.

The results demonstrate that N-glycan PK profiling can be performed using only 50 µl of serum samples with linearity between 3 µg/ml and 100 µg/ml for N-glycans with a portion of 0.5%. With the developed method it is possible to detect relative changes of approx. 10 – 15 % of individual N-glycans which was demonstrated with the spiking of degalactosylated mAb and the method can be performed by different operators with minimal variation of the results which allows routine use. Analysis of major N-glycans is possible from 50 µl serum samples at concentrations below 1 µg/ml.

Summarizing, the development was successful resulting in a method a sensitivity which has not been previously described in the literature. The minimal sample consumption allows implementation into the existing (pre)clinical development work-flow and no additional studies have to be performed.

## 4.5. References

1. E. D. Lobo, R. J. Hansen, J. P. Balthasar, Antibody pharmacokinetics and pharmacodynamics., *J. Pharm. Sci.* **93**, 2645–68 (2004).

2. N. L. Anderson, The Human Plasma Proteome: History, Character, and Diagnostic Prospects, *Mol. Cell. Proteomics* **1**, 845–867 (2002).

3. D. C. Roopenian, S. Akilesh, FcRn: the neonatal Fc receptor comes of age., *Nat. Rev. Immunol.* **7**, 715–25 (2007).

4. L. Tang, A. M. Persky, G. Hochhaus, B. Meibohm, Pharmacokinetic aspects of biotechnology products., *J. Pharm. Sci.* **93**, 2184–204 (2004).

5. L. Alessandri, D. Ouellette, A. Acquah, Increased serum clearance of oligomannose species present on a human IgG1 molecule, *MAbs* **4**, 1–12 (2012).

6. X. Chen, Y. D. Liu, G. C. Flynn, The effect of Fc glycan forms on human IgG2 antibody clearance in humans., *Glycobiology* **19**, 240–9 (2009).

7. A. M. Goetze *et al.*, High-mannose glycans on the Fc region of therapeutic IgG antibodies increase serum clearance in humans., *Glycobiology* **21**, 949–59 (2011).

8. A. J. S. Jones *et al.*, Selective clearance of glycoforms of a complex glycoprotein pharmaceutical caused by terminal N-acetylglucosamine is similar in humans and cynomolgus monkeys., *Glycobiology* **17**, 529–40 (2007).

9. H. Kogelberg *et al.*, Clearance mechanism of a mannosylated antibody-enzyme fusion protein used in experimental cancer therapy., *Glycobiology* **17**, 36–45 (2007).

10. M. M. Newkirk, J. Novick, M. M. Stevenson, M. J. Fournier, P. Apostolakos, Differential clearance of glycoforms of IgG in normal and autoimmune-prone mice., *Clin. Exp. Immunol.* **106**, 259–64 (1996).

11. L. Huang, S. Biolsi, K. R. Bales, U. Kuchibhotla, Impact of variable domain glycosylation on antibody clearance: an LC/MS characterization., *Anal. Biochem.* **349**, 197–207 (2006).

12. T. a Millward *et al.*, Effect of constant and variable domain glycosylation on pharmacokinetics of therapeutic antibodies in mice., *Biologicals* **36**, 41–7 (2008).

13. W. C. Cheung *et al.*, A proteomics approach for the identification and cloning of monoclonal antibodies from serum., *Nat. Biotechnol.* **30**, 447–452 (2012).

14. V. Brun *et al.*, Isotope-labeled protein standards: toward absolute quantitative proteomics., *Mol. Cell. Proteomics* **6**, 2139–49 (2007).

15. E. Ezan, M. Dubois, F. Becher, Bioanalysis of recombinant proteins and antibodies by mass spectrometry., *Analyst* **134**, 825–34 (2009).

16. O. Heudi *et al.*, Towards absolute quantification of therapeutic monoclonal antibody in serum by LC-MS/MS using isotope-labeled antibody standard and protein cleavage isotope dilution mass spectrometry., *Anal. Chem.* **80**, 4200–7 (2008).

17. H. Liu, A. V Manuilov, C. Chumsae, M. L. Babineau, E. Tarcsa, Quantitation of a recombinant monoclonal antibody in monkey serum by liquid chromatography-mass spectrometry., *Anal. Biochem.* **414**, 147–53 (2011).

18. J. M. Prien, B. D. Prater, Q. Qin, S. L. Cockrill, Mass spectrometric-based stable isotopic 2-aminobenzoic acid glycan mapping for rapid glycan screening of biotherapeutics., *Anal. Chem.* **82**, 1498–508 (2010).

19. C. Hagman *et al.*, Absolute quantification of monoclonal antibodies in biofluids by liquid chromatography-tandem mass spectrometry., *Anal. Chem.* **80**, 1290–6 (2008).

# Chapter 5

## *Influence of glyco-variants on the pharmacokinetics of an IgG1 biopharmaceutical*

This chapter is intended for publication.


### Abstract

N-glycosylation as the most complex post translational modification can impact safety and efficacy of biopharmaceuticals. Possible effects on the pharmacokinetics caused by glyco-variants have been subject of several studies with in part contradictory results which can be related to differences in the set-up. In this study a work-flow is presented that allows the analysis of a possible influence of individual glyco-variants on the PK. Prerequisite of individual glycan PK analysis was a reference standard based on stable heavy isotope labeled glycans. The high sensitivity and low sample consumption enabled the integration into the preclinical and clinical development program of a biopharmaceutical. Analysis of samples from a preclinical rabbit study demonstrated the feasibility of the approach. The data of an IgG1 biopharmaceutical showed that some N-glycans have a different PK profile compared with the average molecule as determined by ELISA. IgG1 high mannose glycans M5 and M6 were removed from circulation at a higher rate by two different mechanisms. First M6 was converted to M5 in circulation by glycosidases and thereby completely removed. Second M5 glycosylated IgG1 was selectively removed by the mannose receptor. It was concluded with data from intact antibody resolving the major glycoforms that the observed incomplete removal of M5 was because of the favored M5:M5 pairing on the IgG1 and the resulting structural changes of the Fc part caused by the size of the glycoforms. This change made the N-glycans accessible for the mannose receptor to bind and selectively removed the glycoform containing IgG.



**Keywords**: monoclonal antibody, N-glycosylation, pharmacokinetics, mass spectrometry, heavy isotope standard

## 5.1 Introduction

N-glycosylation, one of the most complex post-translational modifications is under suspicion to influence the pharmacokinetics of therapeutic proteins. One class of therapeutic proteins, mAbs that carry one N-glycan per heavy chain at their Fc part were subject of several studies (*1*–*3*). Newkirk et al generated degalactosylated IgG1 and IgG2 and showed that the degalactosylated mAb was cleared at a slower rate in mice (*4*). In another study an IgG enriched in high mannose glycostructures was compared to complex glycosylated IgG. No difference in PK was found by ELISA. Fab glycosylation was investigated too via enrichment of an IgG to contain one N-glycosylation in its variable domain. However no influence on PK was observed (*5*).

The major drawback of enrichment experiments is the generation of an artificial new IgG N-glycoform pattern that does not necessarily give the same results as the individual glycoforms in the original IgG. LC-MS based approaches allow the direct analysis of the N-glycosylation from the heterogenic mAb N-glycoform mixture. Using a LC-MS method an increasing clearance of high mannose N-glycans was reported by several groups (*6*–*10*). With a single subject case study *Chen et al.* were the first to describe a conversion of high mannose glycans M6-M9 to M5 on an IgG2 which occurred in the blood stream due to circulating glycosidases (*6*). The same group demonstrated for an IgG1 an increased clearance of M5 glycoforms in addition to this conversion (*7*). *Alessandri et al*. reported a conversion of M6 and M7 to M5 in circulation *in vitro* and increased *in vivo* clearance of the high mannose glycans compared to complex structures, however the significance of the *in vivo* data of M6 and M7 is questionable (*9*). Using mAbs exclusively glycosylated with M9 and M8 or M5, studies were performed in mice showing that M8/9 and M5 IgGs were cleared much faster compared to complex glycosylated IgGs and that M8/9 glycans were *in vivo* converted to M6 (*8*). It was concluded that these faster cleared N-glycans bound to N-glycan specific receptors and were subsequently removed via endocytosis (*11*–*13*). Correspondingly, the mannose specific receptor was thought to bind terminal mannose residues resulting in fast clearance of high mannose structures (*14*–*17*). In contrast to the immunoassay and studies with enriched IgG fractions the results obtained with LC-MS methods from the human case studies are in good agreement. However, the studies have some drawbacks as e.g. the number of subjects is small and does not allow for statistically significant conclusions, the *in vitro* data are significant but the *in vivo* results or the serum sample volumes do prevent the use of the study setup N-glycan PK profiling as an accompanying analysis to clinical studies. The most important drawback is that clinical studies are performed late from a development perspective and an adjustment of the mAb N-glycosylation based on the findings from the N-glycan PK profiling is hardly possible at this development stage. Therefore it would be

advantageous if the influence of N-glycans could be studied earlier, e.g. already during the preclinical phase to be able to optimize the biopharmaceutical, for example by glyco-engineering. This requires that effects observed in human studies like the increased clearance of high mannose glycans must be identical in animals used in preclinical development (e.g. rabbits or monkeys). Furthermore, serum sample consumption must be minimal and the sensitivity of the LC-MS methods must be increased drastically as serum volume is more limited in animal studies. Finally, the throughput of the methods must be increased to analyze a statistically powerful number of animals.

In this study a possible approach circumventing the mentioned limitations is presented. The method comprises a high-throughput sample preparation procedure encompassing affinity purification using immobilized antigen and glycan processing. The work-flow was completely based on 96-well plate format. Analysis of 2-AA labeled N-glycans was performed with a highly sensitive nanoLCMS using reversed phase chromatography which was previously shown to be robust and sensitive (*18*). Quantification by MS was achieved using a stable heavy isotope 2-AA label that contains six $^{13}C$ atoms (*22*). The use of this internal standard compensated for variations in the sample preparation and resulted in a higher precision of the nanoLCMS analysis. Together with the small scale sample preparation N-glycan PK data were obtained from 50 µl serum samples from an IgG1 s.c. PK study performed in rabbits.

## 5.2 Materials and Methods

### 5.2.1 Materials

2-Aminobenzoic acid, ethanolamine, formic acid, picoline borane, DMSO, $^{13}C$ aminobenzoic acid were from Sigma (Munich, Germany). PNGaseF was from Roche (Penzberg, Germany). Acetic acid, acetonitrile and hydrochloric acid were from Merck (Darmstadt, Germany). NHS activated sepharose, Sephadex® G-10 96-well plates and 96-well deep well plates were from GE Healthcare (Munich, Germany). Antigen was from Peprotech (Hamburg, Germany). Phosphate buffered saline was from Gibco/Life technologies (Darmstadt, Germany).

Multicreen THS HV filter plates were from Milipore. Fabricator was Genovis (Lund, Sweden). 96-well plates were from Nunc/Thermo Scientific (Munich, Germany). AcroPrep™ Advance Omega™ 10K 96-well filter plates were from Pall (Dreieich, Germany). Pre-clinical rabbit serum samples were obtained from clinical bioanalytics at Sandoz.

### 5.2.2 Methods

#### 5.2.2.1 Preclinical rabbit study

The preclinical study was performed in New Zealand White rabbits. Following single subcutaneous administration of 10 mg $kg^{-1}$ b.w. of an IgG1 blood samples were drawn over 29 days including one pre-dose blood sample. Detailed sampling is listed in Table 1. Concentration of mAb2 in serum was determined by ELISA. From remaining serum 2 x 50 µl aliquots were used for glycan PK profiling. The first aliquot was analyzed and the second aliquot served as back-up aliquot. mAb concentration in pre-clinical serum samples was determined using a sandwich ELISA. Free mAb2 was quantitatively analyzed using immobilized antigen and a horse radish peroxidase conjugated probe specifically binding mAb2 for detection.

#### 5.2.2.2 Reconstitution of the antigen

Recombinant human antigen was reconstituted according to the manufacturer instructions. Antigen was dissolved in $H_2O$ (1 mg/mL) and reconstituted for 2 hours at room temperature. Reconstituted antigen was diluted (0.5 mg/ml) with $H_2O$ and stored at -20°C until use. Prior to immobilization the antigen was diluted with PBS (0.05 mg/ml).

#### 5.2.2.3 Preparation of $^{13}C$ 2-AA labeled glycan standard

N-glycans of desalted mAb (1 mg) were released using PNGaseF overnight (17 h) at 37°C. The N-glycans were separated from the proteins by use of Amicon 30K filter devices and

were brought to dryness (Speedvac). Picoline borane and [$^{13}$C] 2-AA were dissolved in 70:30 (% *v/v)* DMSO-acetic acid to furnish labeling solutions of 63 and 50 mg mL$^{-1}$, respectively. Labeling solution (15 µL) and deionized water (10 µL) were added to 15 nmol glycans. The labeling reaction was performed at 37°C for 17 h. Excess label was removed by gel filtration on G-10 columns. Columns were conditioned with 10ml $H_2O$. Samples were diluted to 100 µl with deionized $H_2O$ before application to the column. After rinsing the column with 700 µl $H_2O$ the purified fluorescence labeled N-glycans were eluted with 600 µl $H_2O$. Purified [13C] 2-AA labeled N-glycans (25 pmol/µl) were aliquoted and stored at -20°C until use.

#### 5.2.2.4 Preparation of 96-well plate affinity columns with immobilized antigen

The membranes of a 96 well filter plate were wetted with 1 mM HCl (100 µL) before addition of 200 µL NHS activated sepharose-isopropanol slurry per well. Isopropanol was removed by centrifugation and the columns were washed with 1 mM HCl (150 µL) for four times. Antigen solution (100 µL) was centrifuged into the columns and coupling reaction was allowed to take place for 2 hours at ambient temperature. Affinity columns were washed and remaining NHS groups were inactivated using of ethanolamine buffer (150 µL). Finally columns were equilibrated with PBS.

#### 5.2.2.5 Affinity purification of an IgG1 biopharmaceutical and glycan release

Serum samples (50 µL) were diluted to 100 µL with PBS and applied to the affinity purification column by centrifugation. Bound mAb was washed several times with PBS to remove serum and unspecific bound proteins. Fabricator® solution was centrifuged into the columns to release the glycosylated Fc part of the mAb. Reaction was performed at 37°C for 30 minutes. Released Fc parts were eluted with PBS and PNGaseF with $^{13}$C-2-AA labeled N-glycan standards was added. This mixture was incubated for 17 hours at 37°C. Remaining proteins were removed by ultrafiltration using 96-well plates with 10K cut-off membranes. Released N-glycans with glycan standard were dried by vacuum centrifugation.

#### 5.2.2.6 N-glycan labeling

Dried samples containing free reducing end N-glycans and 13C 2-AA labeled glycan standard were dissolved in $H_2O$ (10 µL) and 2-AA labeling solution (15 µL; 100 mg/mL picoline borane, 50 mg/mL 2-AA in a 7:3 mixture of DMSO and acetic acid) was added. Labeling reaction took place for 17 hours at 37°C.

#### 5.2.2.7 Gel filtration

Custom made 96-well plate Sephadex G-10 columns were equilibrated with 800 µL $H_2O$. Labeled samples were filled up to 100 µL with $H_2O$ and applied to the gel filtration columns. 2-AA and 13C 2-AA labeled N-glycans were eluted with 150 µl $H_2O$. Finally samples were brought to dryness by vacuum centrifugation and were redissolved in 20 µL $H_2O$ for nanoLC-MS analysis.

#### 5.2.2.8 NanoLC of labeled N-glycans

NanoLC (Thermo/Dionex Ultimate 3000) was set-up in “preconcentration” mode according to the manufacturer manual with a pre-concentration column (3 µm particles, 75 µm x 2 cm) and an analytical column (2 µm particles, 75 µm x 25 cm). The column compartment was held at 40°C. The mobile phase of the nano pump consisted of 0.5% formic acid in $H_2O$ (component A) and 0.5% formic acid in 50% ACN (component B). Mobile phase of the capillary pump consisted of 0.5% formic acid and 1% ACN in $H_2O$ (component C). The analytical column was equilibrated with 2% component B at a flow rate of 300 nl/min. The preconcentration column was equilibrated with 100% component C. With a user defined injection routine 8 µl sample were stacked between loading solution (0.1% formic acid, 1% ACN in ultrapure water) in a 20 µl sample loop. Sample loop was switched for 2 minutes in-line of the capillary pump flow to allow optimal trapping. Prior to the next injection sample the loop was washed with loading solution. After trapping the pre-concentration column was switched into the nano pump flow and component B was raised to 30% over 60 minutes, then to 95% over 5 minutes. After holding at 95% component B for 5 minutes the column was finally re-equilibrated at 2% component B for 15 minutes. Column outlet was connected to a UV detector with a 3 nl flow-cell.

#### 5.2.2.9 Mass Spectrometry

The outlet of the nanoLC was directly coupled to an ion trap ESI-MS (Bruker AmaZon) equipped with an on-line nano source (Bruker CaptiveSpray®). The ion trap was operated in Enhanced Resolution Mode with a capillary voltage of 1.7 kV. Source temperature was set to 200°C and a dry gas flow of 3 l/min was used to heat the source.

## 5.3 Results and discussion

### 5.3.1 Preclinical study and ELISA

The preclinical study was performed in New Zealand White Rabbits. 15 animals were included in this study. A single subcutaneous dose of an IgG1 biopharmaceutical (mAb2) with 10 mg per kg body weight was administered. Serum samples were taken at 12 time points after administration. Details to the sampling are listed in Table 1. Concentration levels of mAb2 were determined by ELISA. The mean PK profile of all variants and glycoform as determined by ELISA is shown in Figure 1. Remaining serum samples were used for N-glycan PK profiling.

**Table 1: Sampling schedule of the pre-clinical study of an IgG1. At each sampling time point ~500 µl of serum were drawn.**

| Day | 1 | 1 | 1 | 2 | 2 | 3 | 3 | 4 | 5 | 8 | 15 | 22 | 29 |
|---|---|---|---|---|---|---|---|---|---|---|---|---|---|
| Hours [post-dose] | 0 (pre-dose) | 2 | 8 | 24 | 40 | 48 | 60 | 72 | 96 | 168 | 336 | 504 | 672 |

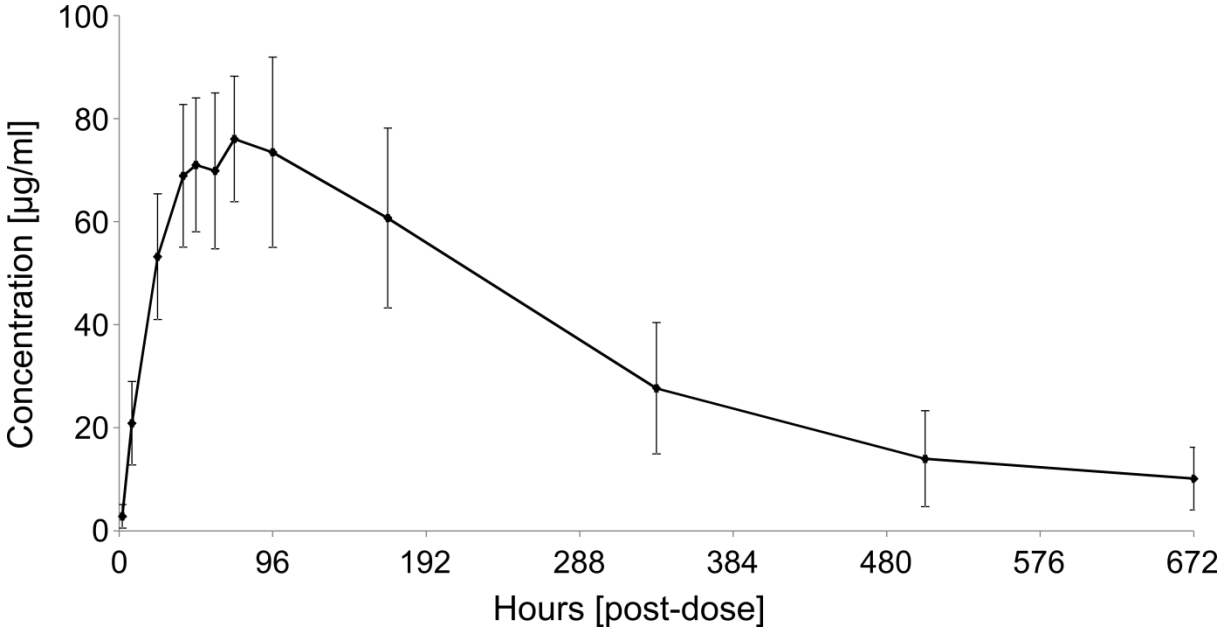


**Figure 1: ELISA results with standard deviation from 15 rabbits that were included in the preclinical study of an IgG1 biopharmaceutical.**

### 5.3.2 Affinity purification and N-glycan processing

Glycoforms can only be studied on the intact protein level usually limited to the major glycoforms due to the relative distribution of N-glycans. For glycan PK profiling N-glycans are studied instead which can be performed with more sensitivity. A high throughput affinity purification method based on 96 well plates was previously developed. Detailed development and qualification of the method were described in Chapter 4.

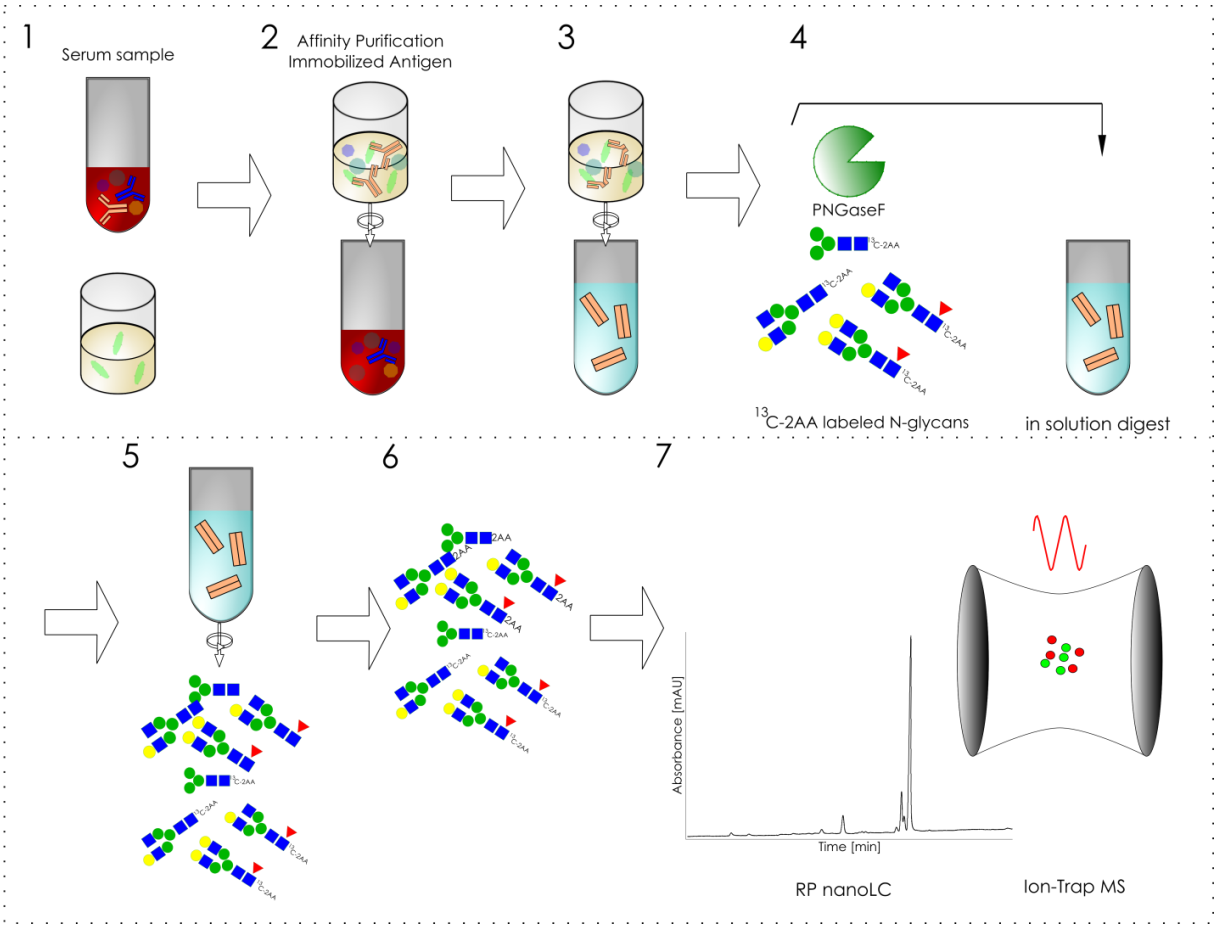


**Figure 2: Glycan PK work-flow. 1. Serum samples are applied to 96-well based affinity purification columns with immobilized antigen (light green). 2. The column is extensively washed. 3. The N-glycan containing Fc part is released by centrifugation of Fabricator enzyme into the column and incubation at 37°C for 30 minutes. Fab and unspecific bound proteins remain on the column. 4. PNGaseF and heavy isotope standard ($^{13}$C 2-AA N-glycans) are added to the Fc part. Incubation for 17 h at 37°C. 5. Released sample N-glycans and heavy isotope standard are purified from proteins by ultrafiltration. 6. 2-AA labeling of sample glycans and subsequent gelfiltration to remove excess label. 7. NanoLC-MS analysis.**

In brief the workflow was as followed: Affinity columns were prepared as described in the methods section. Sepharose columns with NHS groups were prepared in 96 well filter plates. 5 µg antigen of mAb2 per well were immobilized by coupling to the NHS groups. Remaining free NHS groups were deactivated by washing of affinity columns with ethanolamine buffer. Columns were finally equilibrated with PBS. Recovery of mAb2 from rabbit serum is

schematically shown in Figure 2. mAb containing serum samples were applied to the sepharose columns with the immobilized antigen. The samples were centrifuged through the column and the column was washed several times to remove unspecific bound proteins.

Affinity purification with the respective antigen has the advantage of very high affinity and specificity due to the strong interaction of mAbs with their antigen. However, one major drawback is the limited recovery of mAbs after acidic elution. With the limited sample volume available an alternative to the acidic elution with higher yield had to be established which is described in the following paragraph:

On-column deglycosylation as described in chapter 3 could not be used because of endogenous serum glycoproteins that were bound unspecific to the sepharose resin and could not be removed by additional washing steps. With only one N-glycosylation site at the Fc part mAbs are suitable for an enzymatically elution step. The enzyme IdeS selectively cleaves IgG heavy chains C-terminal of the disulfide connection thereby releasing the two glycosylated heavy chain fragments that can subsequently be deglycosylated with high efficiency. Deglycosylation was performed by use of PNGaseF. Together with PNGaseF a stable heavy isotope standard was added to the samples. $^{13}C$ 2-AA labeled N-glycans obtained from mAb2 was used as the internal standard. Released N-glycans were labeled with 2-AA. Excess label was subsequently removed by gelfiltration. Labeled sample N-glycans and the heavy isotope standard were analyzed by RP nanoLC-MS.

Data interpretation was done by determining the peak area of the respective light sample glycan and its appropriate heavy isotope standard from their EICs. This light to heavy ratio (L/H) was determined for each N-glycan at each time point and animal. By plotting the L/H ratio against time PK profiles for each N-glycan are obtained. The N-glycan percentages were calculated with the known relative distribution of heavy isotope standard glycans for each sampling time point.

### 5.3.3 mAb2 N-glycosylation and qualification of the study

To qualify and control the affinity purification quality check samples were prepared by spiking known amounts of mAb2 into NZW rabbit serum. The quality check samples covered the concentration range of the study which was previously determined by ELISA. Figure 3 shows the mean percentages of the 1, 10 and 100 µg/ml mAb2 quality check samples. The mean percentages of the glycans obtained from the quality check samples represented the mAb2 N-glycan composition. With the developed enzymatic elution of the glycosylated antibody fragments very high selectivity and purity was achieved. No interfering N-glycans of mAb2

were co-purified with the exception of two minor abundant bisecting variants that were excluded from analysis. No additional serum related N-glycans were detected. Sensitivity was sufficient to analyze all N-glycans with a percentage of at least 0.1 % at a concentration of 10 µg/ml.

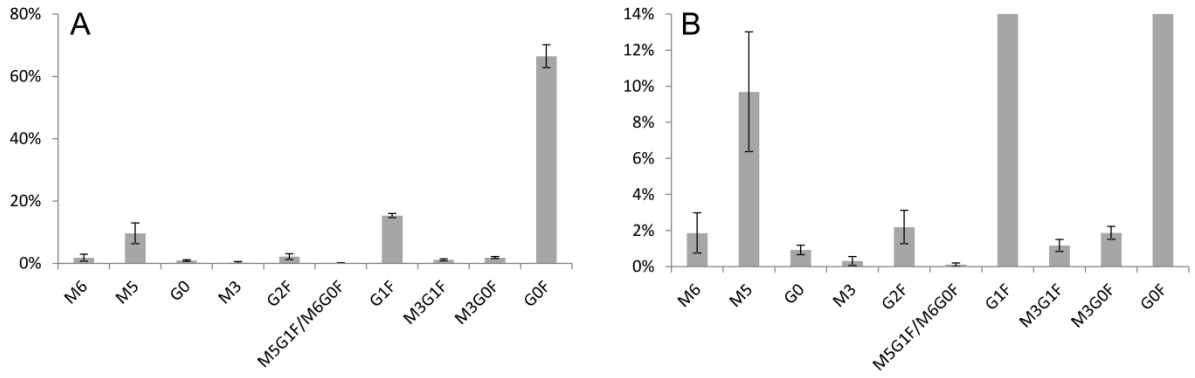


**Figure 3: (A) Average glycan map obtained from 10 and 100 µg/ml quality check samples shows the relative N-glycan composition. (B) Magnified view shows the minor abundant N-glycans. Error bars show the standard deviation of the method.**

The N-glycans were mainly complex biantennary with core fucose. The most abundant N-glycan was G0F (65 %) with terminal N-acetylglucosamine residues followed by G1F (16 %) with one additional terminal galactose. High mannose glycan M5 (9.5 %) was the third most abundant N-glycan. All other N-glycans had a portion of less than 3%. mAb2 contained no N-glycans with terminal sialic acids. Glycan structures are shown in Figure 4.

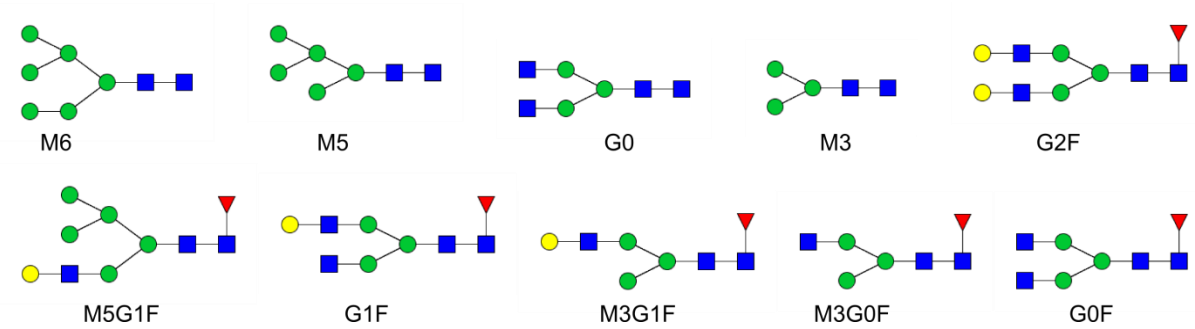


**Figure 4: N-glycan structures of mAb2. Blue square stands for N-Acetylglucosamine, green circle for mannose, yellow circle for galactose and red triangle for fucose.**

### 5.3.4 Glycan PK profiles of mAb2

The determined glycan L/H ratios were plotted against the sampling time to obtain PK profiles for each N-glycan. Mean L/H ratios for each N-glycan were normalized to the maximum of each N-glycan L/H curve (Figure 5). ELISA data were normalized in the same

way. The PK profile of the most abundant complex type G0F was very similar to the ELISA profile (Figure 5A). The maximum concentration ($t_{max}$) was reached after 72 h with congruency of the ELISA and the L/H graph. Elimination occured at identical rates and the PK profiles were regarded as comparable. This finding was expected for the major N-glycan contributing 70 % of the total mAb2 as the ELISA represents the average profile of all glycoforms which is dominated by G0F. The second most abundant complex type N-glycan G1F that accounted for approximately 16 % also showed a PK profile which was very similar compared to the ELISA profile (Figure 5B). Again $t_{max}$ was reached at 72 h. Complex type G2F with a portion of 2 % had the best match with the ELISA profile showing almost perfect congruency (Figure 5C). The $t_{max}$ was reached one sampling time point earlier after 60, but the two profiles could still be regarded identical. The profile of the M6G0F/M5G1F hybrid type glycan represented two isomers that could not be differentiated with the nanoLC-MS approach and which had a relative content of only 0.1 %. The profile and $t_{max}$ were similar to the ELISA profile as well (Figure 5D). The low abundance brought the analysis close to the LLOQ which resulted in lower precision and higher variation. The glycan PK profiles of M3, M3G0F and M3G1F were also highly similar to the ELISA profile (Figure 5E, F, G). These results demonstrated that PK profiles could be obtained for each N-glycan individually. The glycan PK profiles were highly similar to the ELISA for the most abundant glycans. For N-glycans with a portion smaller than 0.5 % the graphs showed higher variation.

Considering all the glycan forms analyzed, only the high mannose type N-glycans M5 and M6 with 9.5 % and 2 % relative abundance respectively showed a clear discrepancy from the ELISA profile (Figure 6) The maximum concentration of M6 was reached after 24 h followed by either a conversion to M5 or an increased elimination rate that led to a faster clearance to a level below the LLOD or a complete removal from circulation at the 168 h time point. The high mannose glycan M5 profile also differed from the overall mAb ELISA PK profile (Figure 6B). The $t_{max}$ was reached 24 h earlier already after 48 h and these molecules were cleared faster between 48 h and 168 h.

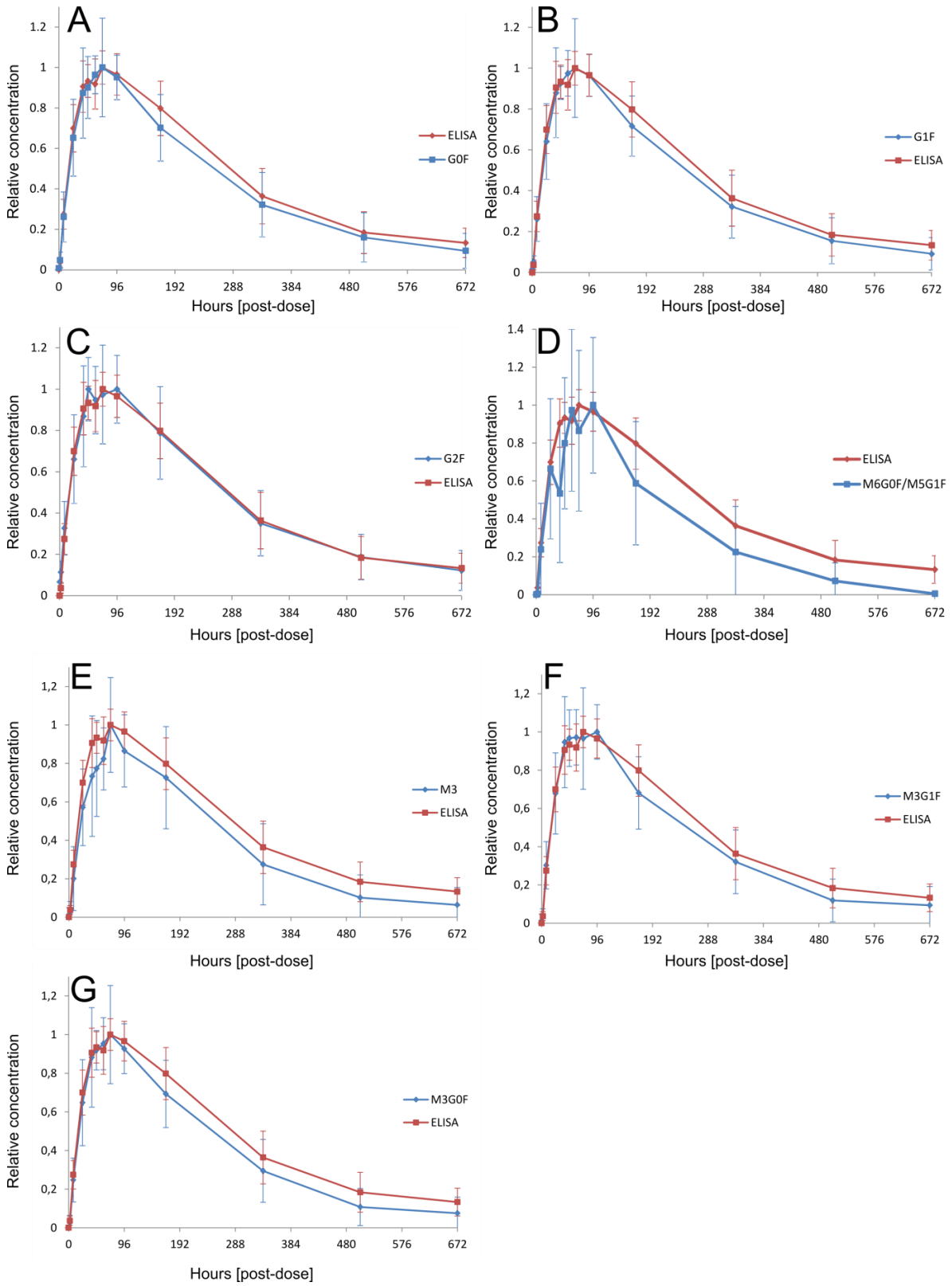


**Figure 5: Comparison of nanoLC-MS based glycan PK data and ELISA data for G0F (A), G1F (B), G2F (C), M5G1F/M6G0F (D), M3 (E), M3G1F (F), M3G0F (G). Concentration is relative to the maximum of each curve to enable comparison. Mean profiles from 15 animals are shown.**

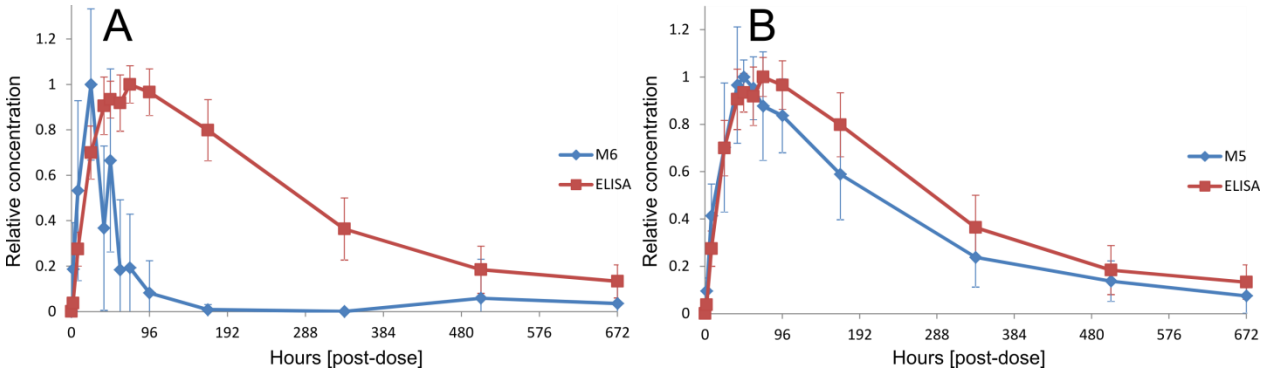


**Figure 6: Comparison of high mannose glycan M6 (A) and M5 (B) PK profiles obtained by nanoLC-MS (diamond) and ELISA (squares) profiles.**

### 5.3.5 Selective clearance of M5 and M6

As shown above high mannose glycan PK profiles differed from the ELISA profile of mAb2 which represented the average concentration of all protein variants. The findings should be reflected in the glycan maps at each time point (Figure 7). PK profiles for G0 could not be obtained due to co-elution of a contaminant with the same m/z value. Glycan maps could be calculated for time points between 8 h and 336 h. At 2 h, 504 h and 672 h the mAb2 serum concentration was below the LLOQ of 10 µg/ml for many rabbits.

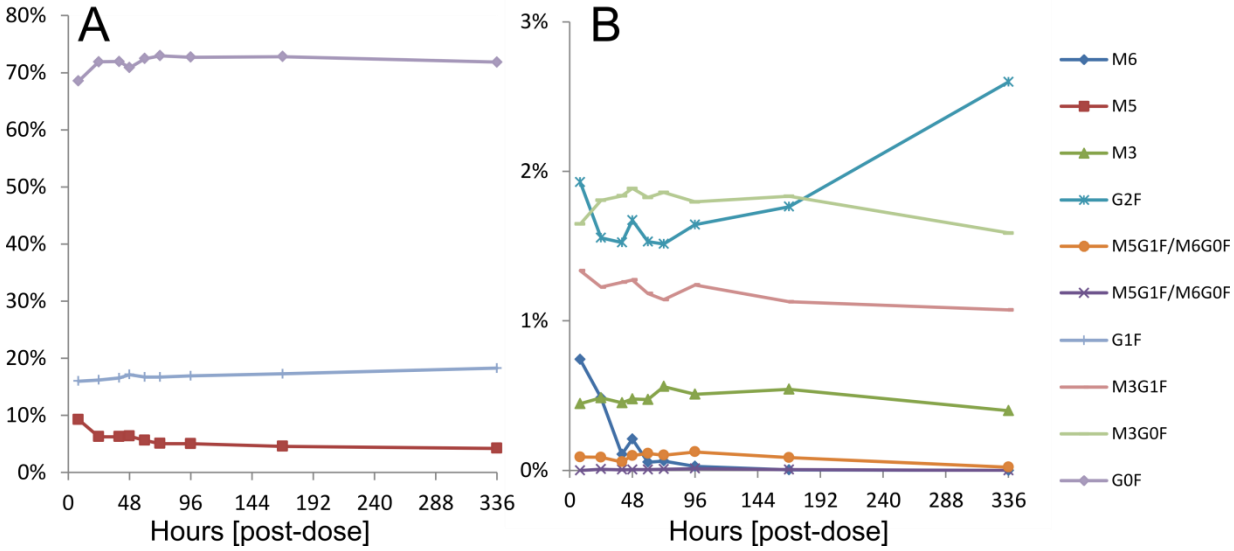


**Figure 7: Glycan Maps of mAb2 for each time point. Mean percentage of recovered mAb2 N-glycans after single subcutaneous administration in rabbits. Full view (A) and magnified view (B) are shown.**

Mean percentages of the most abundant N-glycans G0F and G1F stayed constant which confirmed the previously made observations based on the glycan PK profiles (Figure 7). The magnified view demonstrates that the contribution of all N-glycans was constant except for the high mannose glycans M5 and M6 portions which decreased over time. M6 was removed

from circulation below the LLOQ or completely within 168h whereas the M5 portion decreased from the initial percentage of 9 % to approximately 4 % after 336 h.

High mannose species M6-M9 were converted by glycosidases in circulation to the smaller high mannose glycans M5 in humans (*6*, *9*). In mice a similar observation was made as high mannose species M7-M9 were converted to M6 (*8*). Both observations were made with *in vitro* incubation of antibody in serum. In the present rabbit study M5 was removed selectively from circulation. An increase of smaller glycans like M4 (not present in mAb2) or M3 (core structure) was not observed. A further conversion of M5 would require additional enzymes with other specificities in serum because the linkage of the terminal mannose residues of M5 is different to that of M6-M9. Removal of mannose residues from M6-M9 requires cleavage of α 1,2 glycosidic bonds whereas M5 terminal mannose residues are connected via α 1,3 and α 1,6 glycosidic bonds. It is very likely that M5 and in conclusion M5 containing glycoforms are removed by a specific clearance mechanism from circulation involving the mannose receptor.

**Table 2: Portions of glycoforms containing M5. Theoretical values were calculated based on the assumption of random pairing.**

| | M5:M5 | M5:G1F | M5:M3G1F | M5:G0F | M5:M3G0F | G0F:G0F |
|---|---|---|---|---|---|---|
| **Calculated relative** | 0.62% | 1.12% | 0.11% | 5.29% | 0.18% | 45.43% |
| **Calculated relative to the most abundant G0F:G0F** | 1.36% | 2.46% | 0.24% | 11.64% | 0.40% | 100% |
| **Observed relative to the most abundant G0F:G0F** | 5.13% | - | - | 12.73% | - | 100% |

The incomplete removal of M5 from circulation observed in this study could be explained by the structural conformation of the Fc part. Several investigations showed that IgGs exhibiting N-glycans with terminal galactosylation on both heavy chains change the conformation of the Fc part to a horseshoe conformation which makes the N-glycans accessible for receptors (*23*). Compared to M5 these galactosylated N-glycans (e.g. G1F or G2F) have a similar size. This implies that glycoforms containing M5 and a second N-glycan of similar size (e.g. M5, G1F or G2F) could be large enough to force the Fc part into an open conformation. The mannose receptor is then able to bind M5 and remove the IgG from circulation.

It was shown that the assembly of the glycosylated heavy chains during protein biosynthesis in the ER is not random (*24*). For an IgG2 biopharmaceutical it was demonstrated that the glycoform M5:M5 is favored (*7*). For mAb2 in the present study similar observations were made (Table 2). Assuming random pairing all theoretical glycoforms percentages can be

calculated which is shown in Table 2 for M5 containing glycoforms. MS data from intact mAb2 showed that the M5:M5 glycoform content was four times higher than the theoretically value assuming random heavy chain assembly. M5:M5 was strongly favored during protein biosynthesis and as mentioned above it is likely that mAb2 Fc part with this glycoform has a horseshoe conformation which in turn results in an increased clearance from circulation by binding to the Mannose receptor. The remaining 4 % M5 observed in the preclinical study were M5:G0F and other glycoforms that are small enough for a closed Fc conformation. Other glycoforms with an open Fc part would be M5:G1F or M5:G2F, however analysis of these glycoforms was not possible for mAb2 because of the major glycoforms overlaying the M5:G1F and M5:G2F glycoforms in the intact mass spectrum. Thus, the incomplete clearance of M5 glycoforms from circulation could be explained by the glycan pairing and the corresponding effect on Fc structure.

## 5.4 Conclusion

An innovative approach for the investigation of individual N-glycan pharmacokinetics was utilized to analyze a preclinical rabbit study of an IgG1 biopharmaceutical. Using 96 well plate based high throughput affinity purification with immobilized antigen and stable heavy isotope standard nanoLC-MS quantification glycan PK data from only 50 µl serum samples was obtained for mAb concentrations between 10 and 90 µg/ml. A rabbit study including 15 animals was successfully analyzed and demonstrated the feasibility of the developed approach as an accompanying method in preclinical development. PK profiles for individual N-glycans were obtained which was so far not described in literature. These glycan PK profiles were compared to ELISA data demonstrating that high mannose glycans M5 and M6 had a different PK profile. Glycan maps showed that M6 was either removed below the LLOQ or was completely removed during the first 48 h and M5 levels decreased from 9.5 % to approximately 4 %.

The results are similar to data from human case studies. This demonstrates the value of glycan PK profiling with preclinical samples. The observed decrease of glycoforms containing high mannose glycans M5 and M6 can be explained by two mechanisms. The decrease of M6 is due to conversion to M5 by specific glycosidases present in serum and has been reported for several species (*6*, *8*, *9*). However, this conversion mechanism is not applicable for the M5 decrease because of the enzyme specificity. This is in agreement with the observation of constant M3 and no detection of M4 glycoforms in the study. M5 decrease can be explained by a second mechanism. Glycoforms containing M5 are selectively cleared from circulation through receptor mediated endocytosis. The responsible mannose receptor binds among others specific to mannose containing glycoproteins and removes them from circulation (*11*, *12*, *14*, *16*, *17*). The M5 glycoforms do not disappear completely but instead decrease to a level of approximately 4 %. This incomplete clearance can be explained with the structural conformation of the Fc part associated with glycan pairing favoring M5:M5 glycoforms. The mannose receptor can only bind to M5 glycoforms that are large enough to open the Fc part like the M5:M5 glycoform and provide access for the mannose receptor to the attached N-glycans. Smaller glycan structures like the M5:G0F glycoform result in a closed Fc part structure that prevents the mannose receptor from binding. Thus, a certain fraction of M5 containing protein molecules show a similar, slower clearance as the non M5 or M6 containing glycoforms. The observed disappearing of M6 is contradictory to literature. It was reported that after an initial decrease of M6 of about 50 % the levels remain fairly constant over time (*6*, *9*). In the present case it is either due to a different M6 removal or conversion mechanism in rabbits or simply due to a drop of more than 50 % of initial M6

levels below the detection limit of the method. The latter is rather likely due to the low abundance of M6 especially after initial decrease.

Summarizing the innovative approach for glycan PK profiling with its high sensitivity works with preclinical samples. The preclinical study results confirm previous findings from individual human case studies. Thus effect of N-glycosylation can be detected earlier in biopharmaceutical development which allows optimizing N-glycosylation via glyco-engineering before entering clinical phases.

## 5.5 References

1. H. Li, M. d'Anjou, Pharmacological significance of glycosylation in therapeutic proteins., *Curr. Opin. Biotechnol.* **20**, 678–84 (2009).

2. W. S. Putnam, S. Prabhu, Y. Zheng, M. Subramanyam, Y.-M. C. Wang, Pharmacokinetic, pharmacodynamic and immunogenicity comparability assessment strategies for monoclonal antibodies., *Trends Biotechnol.* **28**, 509–16 (2010).

3. I. R. Correia, Stability of IgG isotypes in serum., *MAbs* **2**, 221–32 (2010).

4. M. M. Newkirk, J. Novick, M. M. Stevenson, M. J. Fournier, P. Apostolakos, Differential clearance of glycoforms of IgG in normal and autoimmune-prone mice., *Clin. Exp. Immunol.* **106**, 259–64 (1996).

5. T. a Millward *et al.*, Effect of constant and variable domain glycosylation on pharmacokinetics of therapeutic antibodies in mice., *Biologicals* **36**, 41–7 (2008).

6. X. Chen, Y. D. Liu, G. C. Flynn, The effect of Fc glycan forms on human IgG2 antibody clearance in humans., *Glycobiology* **19**, 240–9 (2009).

7. A. M. Goetze *et al.*, High-mannose glycans on the Fc region of therapeutic IgG antibodies increase serum clearance in humans., *Glycobiology* **21**, 949–59 (2011).

8. M. Yu, D. Brown, C. Reed, S. Chung, J. Lutman, Production, characterization, and pharmacokinetic properties of antibodies with N-linked Mannose-5 glycans, *MAbs* , 1–13 (2012).

9. L. Alessandri, D. Ouellette, A. Acquah, Increased serum clearance of oligomannose species present on a human IgG1 molecule, *MAbs* , 1–12 (2012).

10. L. Liu *et al.*, Pharmacokinetics of IgG1 monoclonal antibodies produced in humanized Pichia pastoris with specific glycoforms: a comparative study with CHO produced materials., *Biologicals* **39**, 205–10 (2011).

11. G. Ashwell, J. Harford, Carbohydrate-specific receptors of the liver., *Annu. Rev. Biochem.* **51**, 531–54 (1982).

12. R. J. Stockert, The asialoglycoprotein receptor: relationships between structure, function, and expression., *Physiol. Rev.* **75**, 591–609 (1995).

13. Y. Kaneko, F. Nimmerjahn, J. V Ravetch, Anti-inflammatory activity of immunoglobulin G resulting from Fc sialylation., *Science* **313**, 670–3 (2006).

14. H. Kogelberg *et al.*, Clearance mechanism of a mannosylated antibody-enzyme fusion protein used in experimental cancer therapy., *Glycobiology* **17**, 36–45 (2007).

15. P. Allavena, M. Chieppa, P. Monti, L. Piemonti, From Pattern Recognition Receptor to Regulator of Homeostasis: The Double-Faced Macrophage Mannose Receptor, *Crit. Rev. Immunol.* **24**, 179–192 (2004).

16. S. J. Lee *et al.*, Mannose receptor-mediated regulation of serum glycoprotein homeostasis., *Science* **295**, 1898–901 (2002).

17. P. R. Taylor, S. Gordon, L. Martinez-Pomares, The mannose receptor: linking homeostasis and immunity through sugar recognition., *Trends Immunol.* **26**, 104–10 (2005).

18. F. Higel, U. Demelbauer, A. Seidl, W. Friess, F. Sörgel, Reversed-phase liquid-chromatographic mass spectrometric N-glycan analysis of biopharmaceuticals., *Anal. Bioanal. Chem.* **405**, 2481–93 (2013).

19. O. Heudi *et al.*, Towards absolute quantification of therapeutic monoclonal antibody in serum by LC-MS/MS using isotope-labeled antibody standard and protein cleavage isotope dilution mass spectrometry., *Anal. Chem.* **80**, 4200–7 (2008).

20. C. Hagman *et al.*, Absolute quantification of monoclonal antibodies in biofluids by liquid chromatography-tandem mass spectrometry., *Anal. Chem.* **80**, 1290–6 (2008).

21. E. Ezan, F. Bitsch, Critical comparison of MS and immunoassays for the bioanalysis of therapeutic antibodies., *Bioanalysis* **1**, 1375–88 (2009).

22. J. M. Prien, B. D. Prater, S. L. Cockrill, A multi-method approach toward de novo glycan characterization: a Man-5 case study., *Glycobiology* **20**, 629–47 (2010).

23. S. Krapp, Y. Mimura, R. Jefferis, R. Huber, P. Sondermann, Structural Analysis of Human IgG-Fc Glycoforms Reveals a Correlation Between Glycosylation and Structural Integrity, *J. Mol. Biol.* **325**, 979–989 (2003).

24. K. Masuda *et al.*, Pairing of oligosaccharides in the Fc region of immunoglobulin G., *FEBS Lett.* **473**, 349–57 (2000).

# Chapter 6

## *The influence of glyco-variants on the pharmacokinetics of a multiply glycosylated therapeutic Fc fusion protein*

This chapter is intended for publication


### Abstract

Fc fusion proteins are closely related to monoclonal antibodies and can carry several N-glycans which possibly influence the pharmacokinetics. The effect of N-glycans on the pharmacokinetics of two batches of a Fc fusion protein was investigated in a rabbit study. The proteins were recovered from serum using a two-step 96-well format based affinity purification. Subsequently the N-glycans were released and analyzed after 2-AA labeling by nanoLCMS with site specificity. Individual glycan PK analysis was achieved using stable heavy isotope labeled N-glycans as internal standards. High sensitivity and low sample consumption enabled the integration of the technology into the preclinical and clinical biopharmaceutical development. It could be demonstrated that terminally galactosylated glycoforms located at the fusion protein receptor part were cleared faster from circulation than the average of all protein variants as determined by conventional ELISA technologies. Terminal sialic acids in contrast increased the serum half-life. Fc glycans were constant and showed no influence on the pharmacokinetics. These site specific investigations of individual N-glycan influence on the PK performed during preclinical development are useful to guide biopharmaceutical development with respect to N-glycosylation



Keywords: Fusion protein, N-glycosylation, pharmacokinetics, nanoLCMS, stable heavy isotope standard

## 6.1 Introduction

Fc fusion proteins are closely related to mAbs, both having an IgG related Fc part resulting in similar effector functions. The target binding part of Fc fusion proteins is usually a receptor or receptor domain that binds with high specificity and selectivity to their ligand. In contrast to IgG glycosylation fusion proteins often carry several N-glycosylation sites in the non-IgG receptor part (*1*–*4*). N-glycosylation has been demonstrated to influence structure and function of IgGs and distinct N-glycans were connected with increased clearance of mAbs in several studies (*5*–*10*). Carbohydrate-specific receptors were thought to selectively bind N-glycans of glycoproteins which resulted in a faster removal of these glycovariants from circulation by endocytosis (*11*, *12*). An influence from N-glycosylation on fusion protein PK has been reported in a few studies. Comparing the PK parameters of different batches of lenercept, an Fc fusion protein with two extracellular domains of a TNF-α receptor, showed that proteins carrying terminal N-acetylglucosamine residues were cleared at an increased rate. It was hypothesized that the mannose receptor is responsible for the observed clearance which was earlier described to bind N-acetylglucosamine residues (*3*, *13*). *Jones et al.* came to a similar conclusion, again using lenercept and also stated that terminal GlcNAc residues may have a higher clearance rate. In contrast terminal sialic acids and terminal galactosylation had no impact on the PK (*2*). *Kogelberg et al.* studied an antibody-enzyme fusion protein produced in *P. Pastoris* with a high portion of high mannose N-glycans, mainly M8 and M9. This fusion protein was substantially cleared via the mannose receptor as well (*14*). A glyco-engineered version of the same expression system *P. Pastoris* was used to produce fusion proteins and mAbs which were compared to the same biopharmaceuticals produced in CHO cells in transgenic mice studies. It was found that sialic acid content of the fusion proteins modulated the pharmacokinetics (*15*, *16*). All published studies analyzed the N-glycans as a mixture of Fc and receptor N-glycans although there might be substantial structural variations at the N-glycosylation sites resulting in different accessibility of the glycans to receptors. It has been reported several times that Fc N-glycans of a certain size, e.g. bi-antennary complex type with terminal galactosylation are buried and protected from receptor binding (*17*, *18*). In comparison N-glycans located at the non IgG domain might be more exposed on the protein surface and accessible for receptors. It is therefore of great interest to analyze the influence of Fc fusion protein N-glycans on the PK with site specificity. This will lead to a more comprehensive structure-function relationship of N-glycans and the fate of therapeutic fusion proteins in circulation.

To enable analysis of the PK of differently glycosylated protein species including differentiation of the glyco-structures attached to the Fc and the receptor part, a previously developed affinity purification approach (Chapter 4) was optimized. In this study a high-

throughput sample preparation procedure encompassing two affinity purification steps using Protein G columns and immobilized antigen columns with subsequent N-glycan processing and nanoLCMS analysis is presented. This procedure enables investigation of the Fc part and the non IgG receptor part located N-glycans individually. The work-flow is completely based on a 96-well format. Analysis of 2-AA labeled N-glycans is performed with a highly sensitive nanoLCMS approach using reversed phase chromatography which was previously shown to be robust and sensitive (*19*) (and Chapter 3). Quantification is achieved using heavy isotopes 2-AA glycan label (*20*). (*20*). The use of an internal stable heavy isotope standard compensates variations in the sample preparation and nanoLCMS analysis resulting in more precise results. Together with the small scale sample preparation N-glycan PK data is obtained from 50µl serum samples from a study comparing two different batches of the Fc fusion protein performed s.c. in rabbits.

## 6.2 Materials and Methods

### 6.2.1 Materials

2-Aminobenzoic acid, ethanolamine, formic acid, picoline borane, DMSO and $^{13}C$ aminobenzoic acid were from Sigma (Munich, Germany). PNGaseF was from Roche (Penzberg, Germany). Acetic acid and acetonitrile were from Merck (Darmstadt, Germany). Protein G sepharose, NHS activated sepharose, Sephadex® G-10 96-well plates and 96-well deep well plates were from GE Healthcare (Munich, Germany). Multicreen THS HV filter plates were from Milipore. Fabricator® (IdeS) was Genovis (Lund, Sweden). 96-well plates were from Nunc/Thermo Scientific (Munich, Germany). AcroPrep™ Advance Omega™ 10K 96-well filter plates were from Pall (Dreieich, Germany). Pre-clinical rabbit serum samples were obtained from pre-clinical development/bioanalytics at Sandoz.

### 6.2.2 Methods

#### 6.2.2.1 Fc containing fusion protein

The Fc fusion protein consisted of two chains linked together by disulfide bonds in the Fc region. Each chain was composed of a ligand binding receptor domain fused to the Fc part containing a CH2 and a CH3 domain. Each chain carried three N-glycosylation sites, two at the receptor part and one at the CH2 domain of the Fc part making a total of six N-glycans per molecule.

#### 6.2.2.2 Preclinical rabbit study

The preclinical study was performed in Himalayan rabbits. Following single subcutaneous administration of 8 mg $kg^{-1}$ b.w. of two different batches of a fusion protein (FP1 or FP2) blood samples (~600 µl) were drawn over a period of time including one pre-dose blood sample. Detailed sampling is listed in Table 1. Concentration of FP1 and FP2 in serum was determined by ELISA. From remaining serum 2 x 50 µl aliquots were used for glycan PK profiling. The first aliquot was analyzed and the second aliquot served as back-up.

**Table 1: Sampling schedule of the pre-clinical study of FP1 and FP2. Prior to the administration a pre-dose sample was taken from each rabbit.**

| Day | 1 | 1 | 1 | 1 | 2 | 2 | 2 | 3 | 4 | 6 | 8 |
|---|---|---|---|---|---|---|---|---|---|---|---|
| Hours [post-dose] | 0 (pre-dose) | 2 | 6 | 12 | 18 | 24 | 32 | 48 | 72 | 120 | 168 |

#### 6.2.2.3 Preparation of $^{13}C$ 2-AA labeled glycan standard

N-glycans of desalted fusion protein (1 mg of a 50/50 mixture of FP1 and FP2) were released with use of PNGaseF overnight (17 h) at 37°C. The N-glycans were separated from the proteins by use Amicon 30K filter devices and were brought to dryness by use of a speedvac. Picoline borane and [$^{13}C$] 2-AA were dissolved in 70:30 (% *v/v)* DMSO-acetic acid to furnish concentrations of 63 and 50 mg $mL^{-1}$, respectively. Labeling solution (15 µL) and deionized $H_2O$ (10 µL) were added to 59 nmol enzymatically released and dried glycans. The Labeling reaction was performed at 37°C for 17 h.

Excess label was removed by gel filtration on G-10 columns. Columns were conditioned with 10 ml $H_2O$. Samples were diluted to 100 µl with deionized $H_2O$ then applied to the column. After rinsing the column with 700 µl $H_2O$ the purified fluorescence labeled N-glycans were eluted with 600 µl $H_2O$. Purified [13C] 2-AA labeled N-glycans were aliquoted and stored at -20°C until use.

#### 6.2.2.4 Preparation of 96-well plate affinity columns with immobilized Protein G

Protein G sepharose slurry (200 µL) was added to each well of the 96-well filter plate. Protein G sepharose was stored in 20% ethanol which had to be removed before affinity purification. Columns were therefore equilibrated with PBS (150 µL) for four times. Liquid was removed by centrifugation.

#### 6.2.2.5 Preparation of 96-well plate affinity columns with immobilized antigen

Recombinant human produced antigen was reconstituted according to the manufacturer instructions. Antigen was dissolved in $H_2O$ (1 mg/mL) and reconstituted for 2 hours at room temperature. The membranes of a 96 well filter plate were wetted with 1mM HCl (100 µL) before addition of 200 µL NHS activated sepharose-isopropanol slurry per well. Isopropanol was removed by centrifugation and the columns were washed with 1 mM HCl (150 µL) for four times. Antigen solution (100 µL) was centrifuged into the columns and coupling reaction took place for 2 hours at ambient temperature. Affinity columns were washed and remaining NHS groups were inactivated with use of ethanolamine buffer (4x 150 µL). Finally columns were equilibrated with PBS.

#### 6.2.2.6 Affinity purification of a fusion protein and glycan release

Serum samples (50 µL) were added onto the equilibrated Protein G column and centrifuged through the column. The column was subsequently washed with PBS (150 µL) for six times by centrifugation. Bound IgGs were eluted with three times 100 µL elution buffer (0.1 M

glycine pH 2.7). Eluat was immediately neutralized with 1 M Tris HCl pH 8.0. The eluat contained the target protein as well as other IgGs from serum.

The eluat containing the target protein as well as other IgGs from serum is immediately neutralized with 1 M Tris HCl pH 8.0. Eluat was centrifuged through the affinity columns with immobilized antigen and the columns were washed six times with PBS (150 µL). Fabricator solution (100 µl; 1U/µl) was centrifuged into the columns to release the glycosylated Fc part of the fusion protein. Reaction was performed at 37°C for 30 minutes. Released Fc parts were eluted with PBS. PNGaseF with $^{13}$C-2-AA labeled N-glycan standards was added to the eluted Fc parts as well as onto the column with the antigen bound part. Digests were incubated for 17 hours at 37°C. The N-glycans released from the antigen bound protein part were eluted with PBS (2x 150 µl). Remaining proteins were removed by ultrafiltration using 96-well plates with 10K cut-off membranes. Released N-glycans with glycan standard were dried by vacuum centrifugation

#### 6.2.2.7 N-glycan labeling

Dried sample N-glycans and 13C 2-AA labeled glycan standard were dissolved in $H_2O$ (10 µL) and 2-AA labeling solution (15 µL; 100mg/mL picoline borane, 50 mg/mL 2-AA in a 7:3 mixture of DMSO and acetic acid) was added. Labeling reaction took place for 17 hours at 37°C.

#### 6.2.2.8 Gel filtration

96-well plate Sephadex G-10 columns were equilibrated with 800µL $H_2O$. Labeled samples were filled up to 100 µL with $H_2O$ and applied to the gel filtration columns. 2-AA and 13C 2-AA labeled N-glycans were eluted with $H_2O$ (150 µL). Finally samples were brought to dryness by vacuum centrifugation and dissolved in 20 µL $H_2O$ for nanoLC-MS analysis.

#### 6.2.2.9 NanoLC of labeled N-glycans

NanoLC (Thermo/Dionex Ultimate 3000) was set-up in “preconcentration” mode according to the manufacturer manual with a preconcentration column (3µm particles, 75µm x 2cm) and an analytical column (2µm particles, 75µm x 25cm). The column compartment was held at 40°C. The mobile phase of the nano pump consisted of 0.5% formic acid in $H_2O$ (component A) and 0.5% formic acid in 50% ACN (component B). Mobile phase of the capillary pump consisted of 0.5% formic acid and 1% ACN in $H_2O$ (component C). The analytical column was equilibrated with 2% component B at a flow rate of 300 nl/min. The preconcentration column was equilibrated with 100% component C. With a user defined injection routine 8 µl sample were stacked between loading solution (0.1% formic acid, 1% ACN in ultrapure $H_2O$) in a 20µl sample loop. The sample loop was switched for 2 minutes in-line of the capillary

pump flow to allow optimal trapping. Prior to the next injection sample the loop was washed with loading solution. After trapping the pre-concentration column was switched into the nano pump flow and component B was raised to 30% over 60 minutes, then to 95% over 5 minutes. After holding at 95% component B for 5 minutes the column was finally re-equilibrated at 2% component B for 15 minutes. The column outlet was connected to a UV detector with a 3 nl flow-cell.

#### 6.2.2.10 Mass Spectrometry

The outlet of the nanoLC was directly coupled to an ion trap ESI-MS (Bruker AmaZon) equipped with an on-line nano source (Bruker CaptiveSpray®). The ion trap was operated in Enhanced Resolution Mode with a capillary voltage of 1.7 kV. Source temperature was set to 200°C and a dry gas flow of 3 l/min was used to heat the source.

## 6.3 Results and Discussion

### 6.3.1 Glycan maps of the two batches tested in the PK study

N-glycan PK profiling of mAbs is in general less sophisticated than PK profiling of other biopharmaceuticals, because mAbs typically carry only one conserved N-glycosylation site on each heavy chain at the Fc part. In this case it is not necessary to analyze the N-glycans with site specificity. For more complex glycosylated biopharmaceuticals site specificity provides additional information that could help understanding the mechanism of clearance. In the present case the Fc part carries one N-glycan per chain and the receptor receptor part two additional N-glycosylation sites making a total of six N-glycans per molecule.

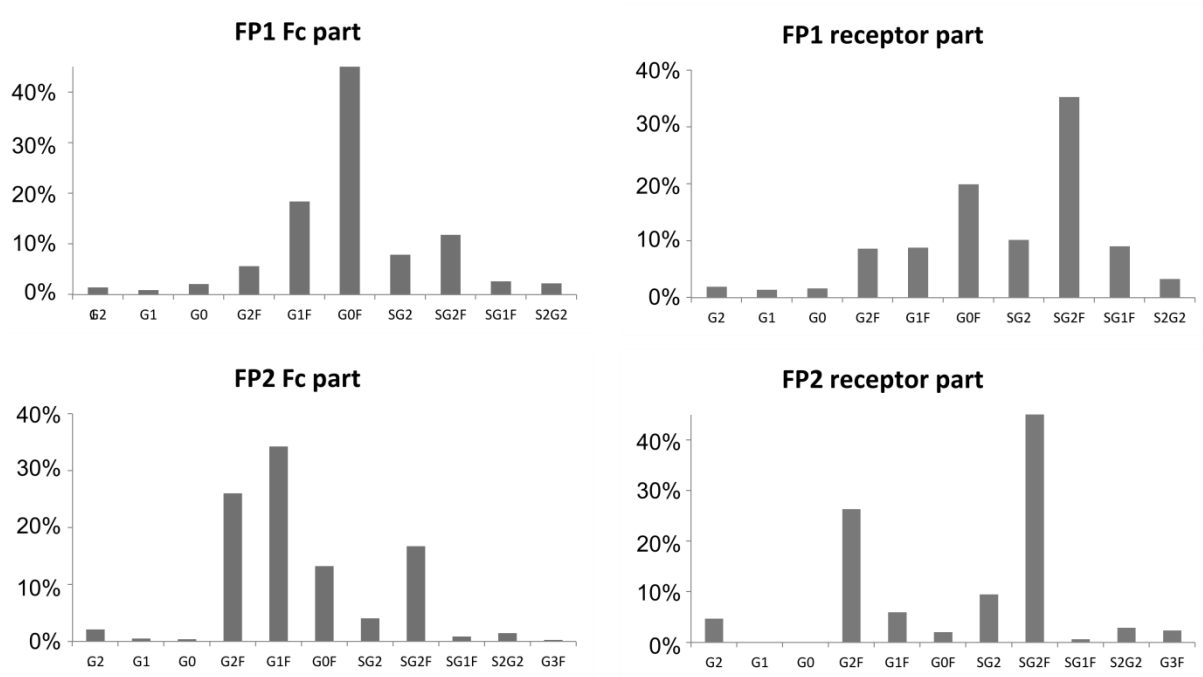


**Figure 1: Fc fusion protein N-glycans of the two different batches (FP1 and FP2) separated into Fc part and receptor part.**

For individual analysis of the Fc part and the receptor part N-glycans the two parts had to be separated. The Fc fusion protein was therefore immobilized via its interaction partner or antigen on a sepharose resin and the Fc part was released enzymatically using the IdeS enzyme (Fabricator®). IdeS is an endopeptidase which selectively cleaves IgGs and related molecules with high specificity below the hinge region producing a Fab2 and Fc/2 fragments. IdeS cleaved the IgG Fc part containing fusion protein into a receptor part which is connected by disulfide bridges and able to bind the interaction partner or antigen and two Fc/2 fragments. After separation and deglycosylation the generated fragments were analyzed individually. The resulting glycan maps of FP1 and FP2 are shown in Figure 1.

The two batches had a different N-glycosylation pattern. FP1 showed a more heterogenic glycosylation pattern whereas FP2 had higher portions of a lower number of different N-glycans. Both batches contained high percentages of glycan structures with terminal sialic acid at their receptor part. Fc glycosylation was typical for antibodies with a high portion of complex bi-antennary N-glycans with core fucosylation; some carried an additional sialic acid. The main difference between FP1 and FP2 was based on the terminal groups. FP1 had a high percentage of terminal GlcNAc residues. In contrast FP2 had a high degree of terminal galactose. The level of sialylation was comparable. The glycan structures are depicted in Figure 2.

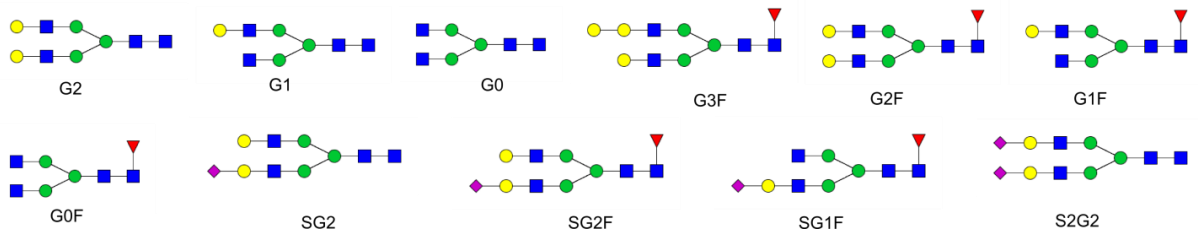


**Figure 2: N-glycan structures found in FP1 and FP2. Blue square stands for N-Acetylglucosamine, green circle for mannose, yellow circle for galactose, red triangle for fucose.**

### 6.3.2 ELISA analysis of samples from a preclinical PK study of FP1 and FP2 in rabbits

The preclinical rabbit samples were analyzed via ELISA for overall concentration of FP1 and FP2. The ELISA results of the five animals of both arms demonstrated a trend to higher concentrations of FP1 as compared to FP2 (Figure 3), but significance could not be demonstrated. Both profiles reached their $t_{max}$ after 18 h. Clearance of FP1 appeared to be slightly faster which resulted in congruency at 72 h. This discrepancy of the ELISA profiles and the differences in N-glycosylation between the two batches stressed the importance of a detailed investigation of a potential relationship between these two aspects. Overall the serum half-life was shorter compared to mAbs. This indicated different clearance mechanisms and probably a reduced affinity towards the FcRn which is involved in recycling of antibodies and the resulting long half-life (*21*, *22*).

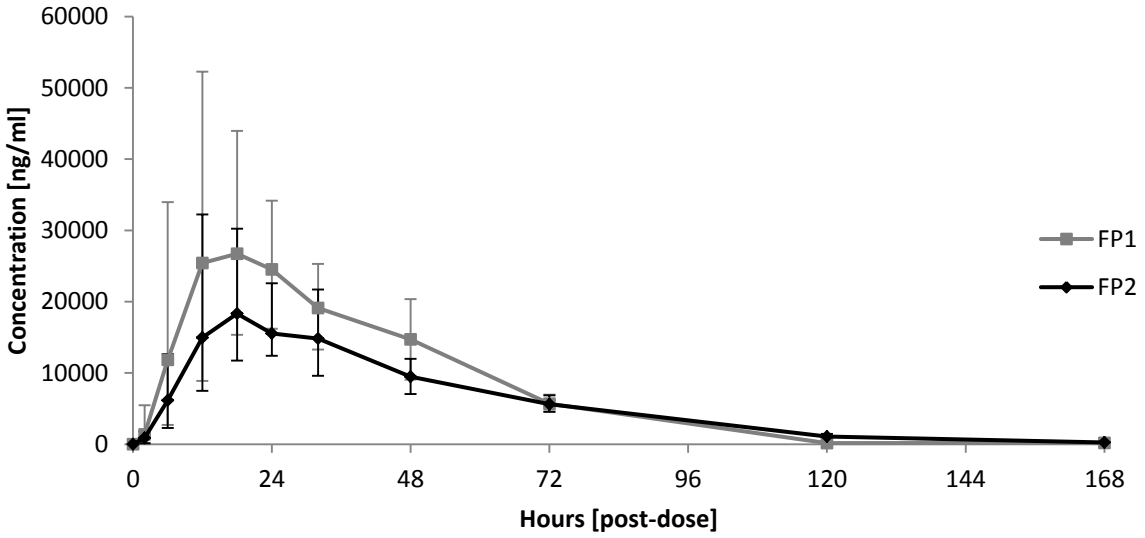


**Figure 3: PK profiles (mean, SD) of FP1 (square) and FP2 (diamond) determined by ELISA; average of five animals respectively.**

### 6.3.3 Optimization of affinity purification and N-glycan processing

Before analyzing Fc fusion protein samples from the preclinical study the glycan PK method developed previously for mAbs had to be adapted and optimized (Chapter 5). For individual analysis of N-glycans attached to the Fc part and attached to the fusion part a new work-flow, depicted in Figure 4, was developed. Affinity purification from serum samples (Figure 4A) included a pre-clearing step. Protein G sepharose was used to purify IgGs including fusion proteins from serum. After protein G binding and intensive washing, IgGs and fusion proteins were eluted using acidic conditions. Unspecifically bound glycoproteins that could falsify the analysis remain bound to the protein G column. The precleared serum was neutralized and added to an affinity column with immobilized antigen. Serum related IgGs were washed from the column and the immobilized fusion protein was digested with IdeS (Fabricator®). The Fc part was eluted from the column and the receptor part stayed bound to the antigen.

In the next step N-glycans were released (Figure 4B). The receptor part N-glycans on column and the Fc N-glycans in solution. In this step the stable heavy isotope 2-AA N-glycans were added. The released N-glycans were labeled with 2-AA separately and analyzed by nanoLCMS (Figure 4C). L/H ratios of the sample N-glycan MS intensities (light signal; L) to the constant heavy isotope standard N-glycan MS intensities (heavy signal; H) plotted against time resulted in glycan PK profiles for individual N-glycans.

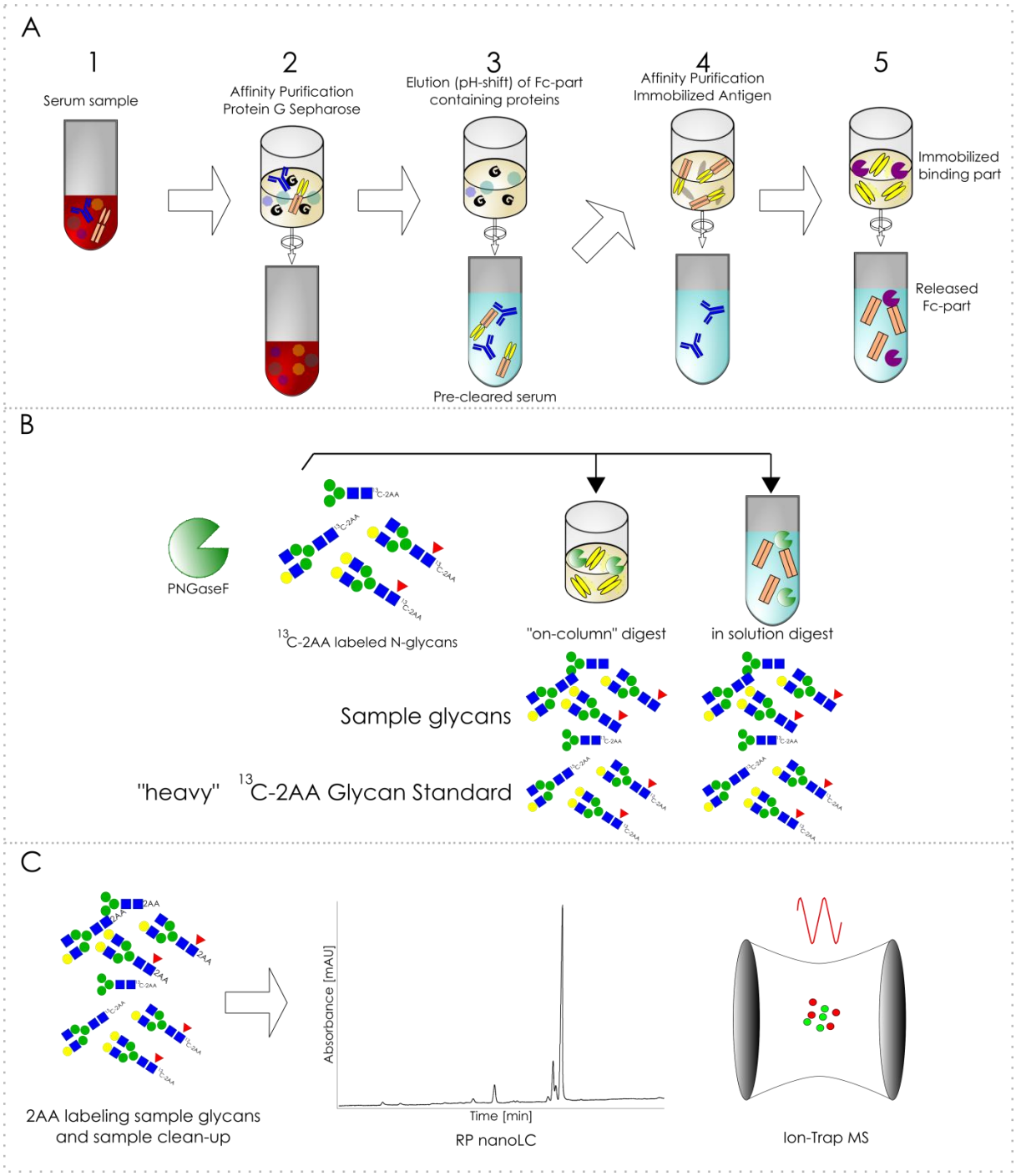


**Figure 4: Work-flow of the glycan PK profiling method for fusion proteins (yellow/orange). A) Fusion proteins are recovered from serum. A protein G preclearing step captures IgGs and the fusion protein (2). After intense washing IgG and fusion proteins are eluted. Unspecific bound proteins (colored dots) remain on the column (3). The fusion protein is captured with its immobilized antigen (4) and the Fc part (orange) is eluted (5). B) PNGaseF and glycan standard is added to eluted Fc parts (orange) and immobilized receptor parts (yellow). C) Released N-glycans are labeled and analyzed by nanoLCMS.**

### 6.3.4 Comparison of N-glycan with ELISA PK profiles

To enable the comparison between the ELISA PK profiles and the N-glycan analysis data, relative ELISA concentration were determined by normalizing average profiles to the maximal concentration ($c_{max}$). Furthermore, the relative concentrations of the individual N-glycan profiles were determined by normalizing the average profiles, based on the determined L/H ratios, to the maximal L/H ratio. Figure 5 shows the average PK profiles of the most abundant N-glycan of the Fc part and the receptor part of both fusion protein lots determined by nanoLCMS compared to the appropriate average ELISA profiles. N-glycan profiles of FP1 G0F, FP1 SG2F, FP2 G1F and FP2 SG2F showed a similar profile compared to the ELISA which was somehow expected as the ELISA represented the average profile of all protein variants. The $t_{max}$ of the ELISA and FP2 SG2F curve was reached 18 h after administration. The $t_{max}$ of FP1 G0F, FP1 SG2F and FP2 G1F was reached one sampling time point later after 24 h. Elimination rates were similar, too. These findings confirmed that the developed and optimized method worked.

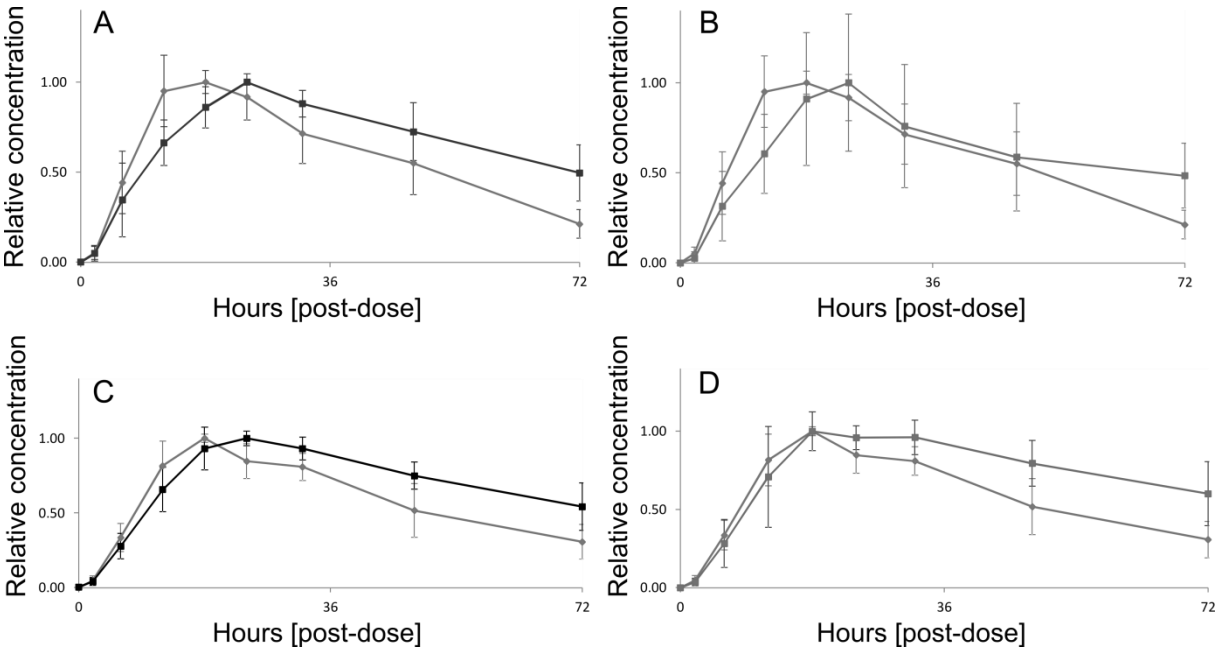


**Figure 5: Average glycan PK profiles of the most abundant N-glycans compared to the ELISA profile (diamond). A) FP1 Fc part G0F (square). B) FP1 receptor part SG2F (square). C) FP2 Fc part G1F (square). D) FP2 receptor part SG2F (square). Average of five animals for each fusion protein.**

Detailed glycan maps of the Fc and receptor protein part from FP1 and FP2 are shown in Figure 6. The N-glycans of the Fc parts were mostly complex biantennary type N-glycans, whereas receptor glycans were acidic N-glycans at high percentage. The glycan maps were in good agreement with the glycan maps obtained from the drug product (Figure 1). For the FP1 Fc part G0F was the most abundant N-glycan (60%) and G1F the second most

abundant N-glycan (30%). All other N-glycans were below 10%. The Fc part of FP2 was more heterogeneous glycosylated with G1F (50%) as the most abundant N-glycan followed by G2F (25%), G0F (15%) and SG2F (10%). The percentages of all glycans were constant over time indicating identical PK profiles of the individual glycans for both Fc fusion protein lots. The deviation at 32 h (Figure 6A) was most likely due to variations during the affinity purification or nanoLCMS analysis and not a short change of the N-glycosylation pattern. Also the variation observed between 6 h and 12 h in the Fc part of FP2 (Figure 6C) was due to variation of the method and not a significant change of the N-glycan percentages.

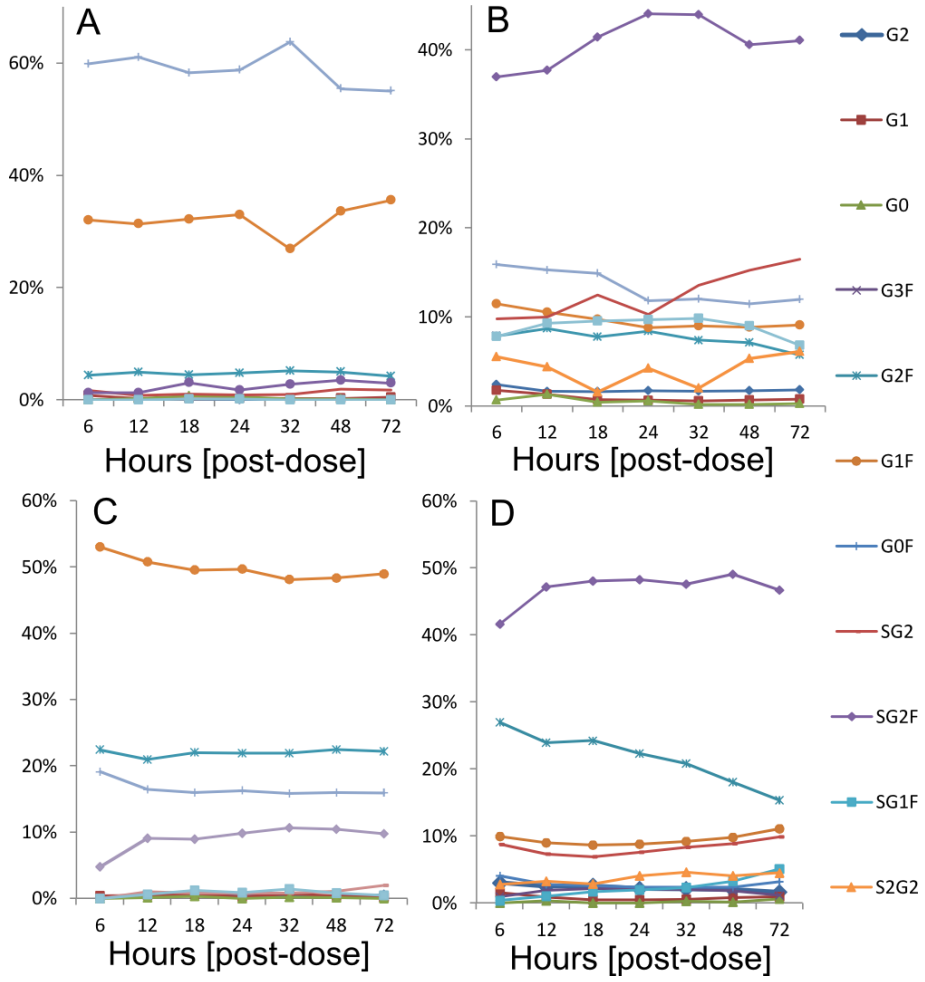


**Figure 6: Glycan Maps (mean) of FP1 Fc part (A) and receptor part (B) and glycan maps of FP2 Fc part (C) and receptor part (D).**

SG2F was the most abundant N-glycan at both receptor parts with approximately 40%. At the FP1 receptor part G0F (15%) was the second most abundant N-glycan followed by G1F (12%), SG2 (10%), G2F (8%), SG1F (8%) and S2G2 (5%). The FP2 receptor part N-glycosylation was different with G2F (28%) as the second most abundant N-glycan. G1F and SG2 were present with approximately 10%. Both receptor parts contained several minor abundant N-glycans with percentages below 5%. In contrast to the Fc parts the percentages

of some receptor part N-glycans changed over time in both lots. For FP1 the portion of G0F and G2F decreased whereas the portions of SG2F and SG2 showed a trend towards higher portions. For FP2 the major N-glycan SG2F increased slightly whereas N-glycan G2F decreased drastically over time.

Figure 7 shows the N-glycans with terminal galactosylation (G1F and G2F) and the N-glycan G0F with a terminal N-acetylglucosamine for Fc and receptor parts. Minor abundant glycans G2, G1 and G0 lacking the core fucose had constant portions and are not shown. G2F contribution decreased over time for both FP1 and FP2. G1F and G0F decreased slightly in case of FP1 but remained constant for FP2. These results indicate that FP1 and FP2 carrying terminal galactosylated G2F were more rapidly removed from circulation. The mechanism behind this clearance could be asialoglycoprotein receptor mediated which is a C-type lectin expressed in parenchymal cells of the liver (*11*, *12*). This receptor binds selectively to exposed galactose residues and sialic acid α2,6Gal/GlcNAc motifs of glycoproteins. Binding initiates endocytosis and degradation of these proteins thereby regulating the glycoprotein serum concentration (*23*). The receptor furthermore exhibits decreasing affinity from high to small number of terminal galactosylated antennae. This would explain the observations for the slight decrease or constant portion of G1F respectively. A similar decrease of G0F as observed for FP1 was reported by *Jones et al* for the Fc fusion protein lenercept which was composed of a IgG1 Fc part fused to the soluble TNF-α receptor p55 (*2*). The selective clearance was explained by binding of the mannose receptor to the terminal GlcNAc. The mannose receptor has high affinity to terminal mannose residues but is also able to bind terminal GlcNAc of smaller N-glycans (*14*, *24*). The difference between FP1 and FP2 for the G1F and G0F N-glycan might be due to different N-glycosylation pairing on the protein and a different accessibility for receptors to bind. The receptor part had two N-glycosylation sites in close proximity that could influence the surrounding protein structure depending on the combination of N-glycans. The receptor part of FP1 was more heterogeneously glycosylated with a higher portion of bigger acidic N-glycans (Figure 6B) This might facilitated the decrease of G1F and G0F, when paired with a bigger glycan, by the asialoglycoprotein or mannose receptor. In contrast FP2 carried mostly SG2F and G2F, the latter with decreasing percentages over time and had different N-glycosylation pairing. In addition the portion of G0F was significantly lower at the FP2 receptor part (Figure 7C) compared to FP1 (Figure 7A). Therefore a G1F and G0F decrease was not detectable.

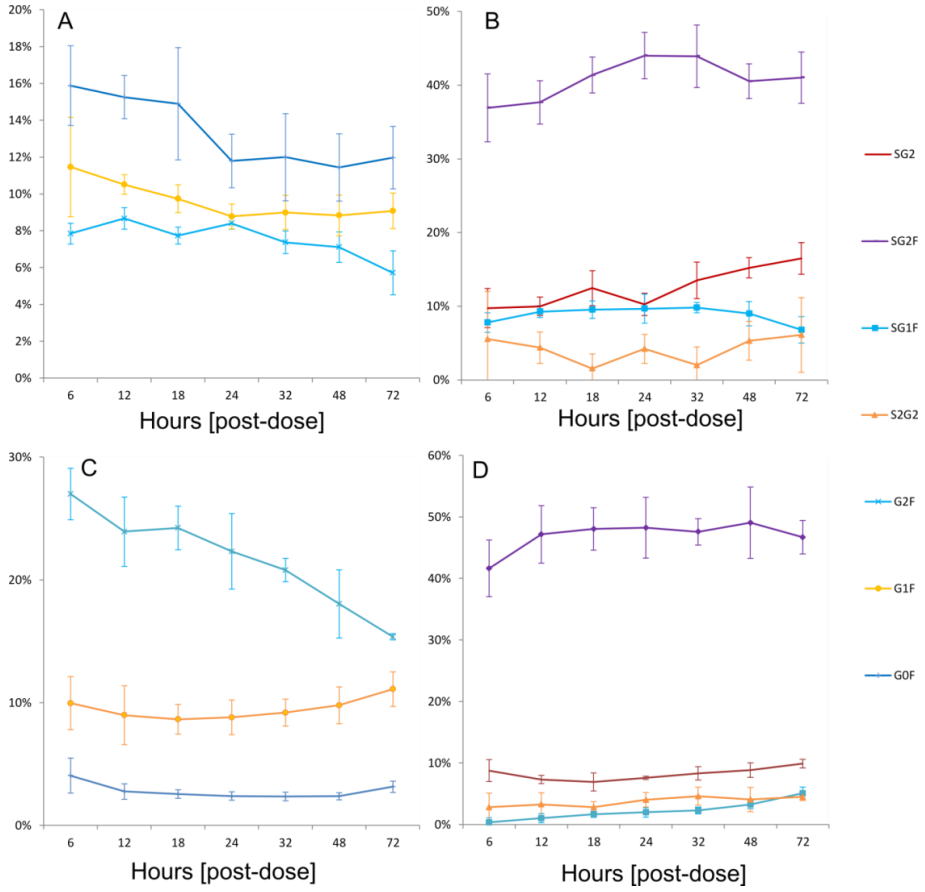


**Figure 7: N-glycans with terminal galactose residues and terminal N-actetylglucosamine residues located at the receptor parts of FP1 (A) and FP2 (C) (mean, SD). Terminal sialylated N-glycans present on FP1 (B) and FP2 (D) receptor parts are depicted as well.**

Plots for terminal sialic acid containing N-glycans of FP1 and FP2 are shown in Figure 7B and C. As described earlier the major N-glycan SG2F had a slight trend to increase over time, indicating slower plasma clearance. For FP1 also the SG2 contribution and for FP2 that of SG1F increased over time. The other acidic N-glycans had constant percentages. Thus the addition of at least one terminal sialic acid to the galactosylated N-glycan structure seemed to prevent the protein from selective clearance. The discrepancy between FP1 and FP2 that increased over time was again maybe related to the glycosylation site. The observation that sialylated glycans increase the serum half-life was already discovered in the 1970s by *Morell et al.* (*25*). The investigators compared sialylated and de-sialylated thus terminal galactosylated glycoproteins. They observed fast clearance of the latter in the liver. However in the present study an increased half-life of sialylated N-glycans was not only observed compared to terminally galactosylated N-glycans, but also compared to all other N-glycans. Consequently there must be another underlying clearance mechanism which discriminates between sialic and neutral N-glycans of glycoproteins independent of the asialoglycoprotein or mannose receptor.

An overview of the contributions of all attached glycans with different terminal groups is given in Figure 8. The N-glycans were divided into three different groups: i) sialylated containing one or two terminal sialic acids; ii) galactosylated summing up all N-glycans with at least one terminal galactose moiety and iii) terminal GlcNAc combining all N-glycans with a terminal N-acetylglucosamine. N-glycans with two characteristics like SG1F which exhibits a terminal sialic acid on one arm and a terminal GlcNAc on the other arm was counted to the sialylation group. This is justified by the observations that this N-glycan behaved more like a sialic glycan than like a terminal GlcNAc glycan as an increase over time was observed at the FP2 receptor part (Figure 7D) like for other sialic N-glycans. This was most likely due to shielding of the charged terminal sialic acid group. The same rule was applied for other N-glycans, e.g. G1F had properties of a terminally galactosylated N-glycan.

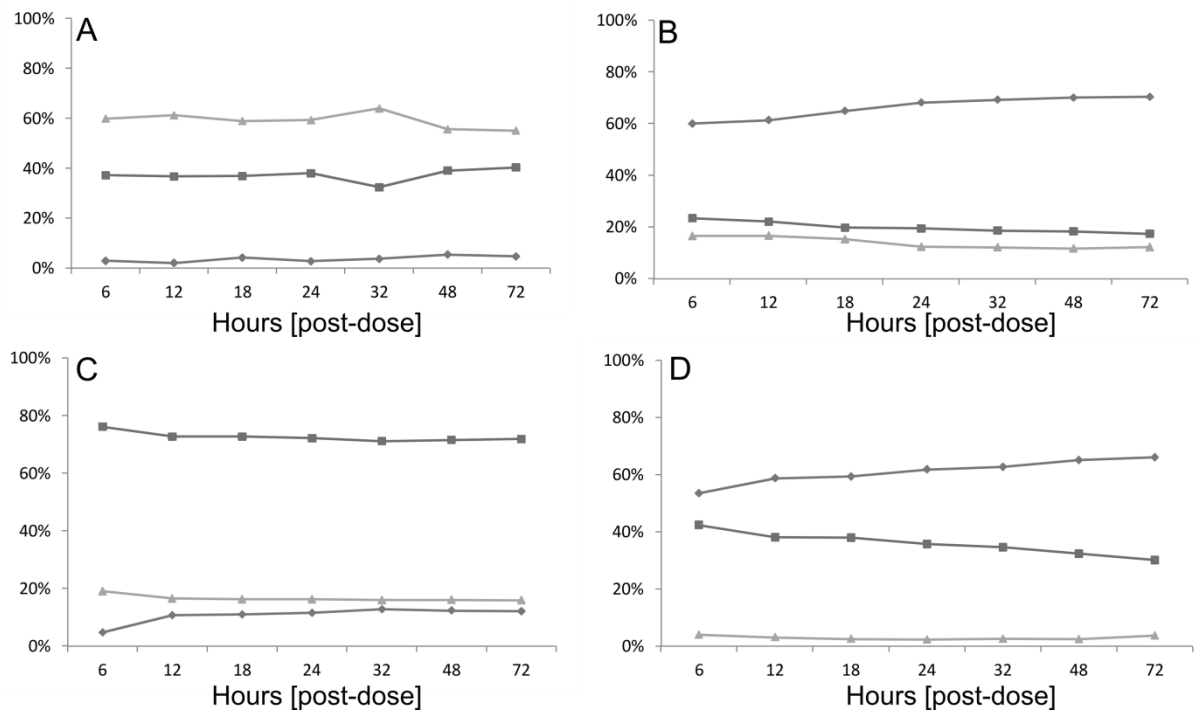


**Figure 8: Influence of terminal sugar moieties. Percentages of terminal sialylation (diamond), terminal galactosylation (square) and terminal N-acetylglucosamine (triangle) are pictured for Fc parts (A: FP1; C:FP2) and receptor parts (B: FP1; D: FP2).**

The composition of the terminal groups at the Fc parts did not change for FP1 (Figure 8A) and FP2 (Figure 8C). The two deviations at 6 h (FP2; Figure 8C) or at 32 h (FP1; Figure 8A) were most likely related to the analytical method. In contrast the composition of the terminal groups at the receptor part (Figure 8B/D) showed a decreasing contribution of protein carrying terminal galactose. This decrease corresponded to an increasing fraction of glycosylated protein with terminal sialylation. This indicated that the change in receptor part glycan levels and the constant glycan levels at the Fc parts were independent.

## 6.4 Conclusion

N-glycan PK profiling of Fc fusion proteins without domain specificity has been reported several times (*2*, *3*). Since Fc fusion proteins usually carry several N-glycans distributed over the molecule the value of these studies is limited. The influence of Fc N-glycans might be completely different compared to non-Fc glycans because of the protein structure surrounding the glycosylation sites. Therefore a new N-glycan PK profiling approach was established that allows the specific and separate analysis of Fc and receptor part N-glycans of multiply glycosylated Fc fusion proteins. The work-flow included the recovery of the Fc fusion protein from serum samples. In a first affinity step using Protein G chromatography the complexity of the serum was drastically reduced. The pre-cleared serum was then applied to antigen columns. After washing of the immobilized target protein, enzymatic elution of the Fc part and N-glycan processing, the labeled N-glycans of the two protein parts were analyzed individually. By incorporation of stable heavy isotope 2-AA labeled glycan standards variations during N-glycan processing and nanoLCMS analysis were compensated.

Two different batches of a Fc fusion protein (FP1 and FP2) were compared in a rabbit study. The PK profiles of each N-glycan and the relative distribution of the N-glycans over time were determined. The two batches were different glycosylated at the Fc and at the receptor part. The Fc parts were IgG typically glycosylated with mostly neutral bi-antennary N-glycans and 10% acidic N-glycans at FP2. FP1 Fc part contained mostly terminal GlcNAc G0F whereas FP2 contained mostly terminal galactosylated G1F and G2F. The receptor part of FP1 was heterogeneously glycosylated with acidic N-glycans, terminal GlcNAc and terminal galactosylated N-glycans. FP2 showed a high level of acidic N-glycans and a higher level of terminal galactosylated N-glycans than FP1. The N-glycan PK profiling results demonstrated that fusion protein molecules with terminal galactosylated N-glycans that were located at the receptor part were cleared at a faster rate than the average molecule. This clearance was most likely a receptor mediated process of the asialoglycprotein receptor. This receptor is located in the liver, involved in the uptake and clearance of glycoproteins and known for its affinity to terminal galactosylated N-glycans (*11*, *12*). This indicated that the N-glycans located at the receptor part located were more exposed at the surface than Fc glycans. This better access to galactosylated N-glycans at the receptor part for the asialoglycoprotein receptor resulted in selective clearance from circulation. The faster clearance of molecules carrying a G0F glyan at the receptor part, clearly observed for FP1, might be mediated by the mannose receptor as proposed by *Jones et al.* (*2*). However, this was not observed for the receptor part of FP2 which contained 3% G0F. Additionally, a prolonged half-life of protein molecules carrying sialylated N-glycans was observed but could not be explained with the two mentioned clearance routes.

Thus N-glycosylation of fusion proteins influences the PK. Fc part N-glycosylation (complex bi-antennary) had no influence on PK which is in agreement with previous studies (see Chapter 5). Protein molecules carrying terminal galactosylated N-glycans and to some extend terminal GlcNac N-glycans at the receptor part were cleared faster. If these glycan structures are attached to the Fc part the clearance was not accelerated which points to a limited accessibility of N-glycans in the Fc structure. The clearance of galactosylated structures was due to asiaglycoprotein receptor mediated binding. The clearance of terminal GlcNAc was most likely mediated by the mannose receptor. Terminal sialylation led to an increase in serum half-life. The mechanism of increased half-life of sialylated receptor parts cannot be explained with known clearance pathways. This study was the first reporting detailed site specific N-glycan PK profiling of biopharmaceuticals. It was clearly demonstrated that domain specific N-glycan profiling provides very important and detailed insights.

## 6.5 References

1. J. Bongers *et al.*, Characterization of glycosylation sites for a recombinant IgG1 monoclonal antibody and a CTLA4-Ig fusion protein by liquid chromatography-mass spectrometry peptide mapping., *J. Chromatogr. A* **1218**, 8140–9 (2011).

2. A. J. S. Jones *et al.*, Selective clearance of glycoforms of a complex glycoprotein pharmaceutical caused by terminal N-acetylglucosamine is similar in humans and cynomolgus monkeys., *Glycobiology* **17**, 529–40 (2007).

3. R. Keck *et al.*, Characterization of a complex glycoprotein whose variable metabolic clearance in humans is dependent on terminal N-acetylglucosamine content., *Biologicals* **36**, 49–60 (2008).

4. A. Beck *et al.*, Trends in glycosylation, glycoanalysis and glycoengineering of therapeutic antibodies and Fc-fusion proteins., *Curr. Pharm. Biotechnol.* **9**, 482–501 (2008).

5. H. Li, M. d'Anjou, Pharmacological significance of glycosylation in therapeutic proteins., *Curr. Opin. Biotechnol.* **20**, 678–84 (2009).

6. L. Alessandri, D. Ouellette, A. Acquah, Increased serum clearance of oligomannose species present on a human IgG1 molecule, *MAbs* **4**, 1–12 (2012).

7. A. M. Goetze *et al.*, High-mannose glycans on the Fc region of therapeutic IgG antibodies increase serum clearance in humans., *Glycobiology* **21**, 949–59 (2011).

8. X. Chen, Y. D. Liu, G. C. Flynn, The effect of Fc glycan forms on human IgG2 antibody clearance in humans., *Glycobiology* **19**, 240–9 (2009).

9. M. Yu, D. Brown, C. Reed, S. Chung, J. Lutman, Production, characterization, and pharmacokinetic properties of antibodies with N-linked Mannose-5 glycans, *MAbs* , 1–13 (2012).

10. Y. Kaneko, F. Nimmerjahn, J. V Ravetch, Anti-inflammatory activity of immunoglobulin G resulting from Fc sialylation., *Science* **313**, 670–3 (2006).

11. G. Ashwell, J. Harford, Carbohydrate-specific receptors of the liver., *Annu. Rev. Biochem.* **51**, 531–54 (1982).

12. R. J. Stockert, The asialoglycoprotein receptor: relationships between structure, function, and expression., *Physiol. Rev.* **75**, 591–609 (1995).

13. D. T. Achord, F. E. Brot, W. S. Sly, Inhibition of the rat clearance system for agalacto-orosomucoid by yeast mannans and by mannose, *Biochem. Biophys. Res. Commun.* **77**, 409–415 (1977).

14. H. Kogelberg *et al.*, Clearance mechanism of a mannosylated antibody-enzyme fusion protein used in experimental cancer therapy., *Glycobiology* **17**, 36–45 (2007).

15. L. Liu *et al.*, Pharmacokinetics of IgG1 monoclonal antibodies produced in humanized Pichia pastoris with specific glycoforms: a comparative study with CHO produced materials., *Biologicals* **39**, 205–10 (2011).

16. L. Liu *et al.*, The Impact of Glycosylation on the Pharmacokinetics of a TNFR2:Fc Fusion Protein Expressed in Glycoengineered Pichia Pastoris., *Pharm. Res.* (2012), doi:10.1007/s11095-012-0921-3.

17. S. Krapp, Y. Mimura, R. Jefferis, R. Huber, P. Sondermann, Structural Analysis of Human IgG-Fc Glycoforms Reveals a Correlation Between Glycosylation and Structural Integrity, *J. Mol. Biol.* **325**, 979–989 (2003).

18. D. Houde, Y. Peng, S. a Berkowitz, J. R. Engen, Post-translational modifications differentially affect IgG1 conformation and receptor binding., *Mol. Cell. Proteomics* **9**, 1716–28 (2010).

19. F. Higel, U. Demelbauer, A. Seidl, W. Friess, F. Sörgel, Reversed-phase liquid-chromatographic mass spectrometric N-glycan analysis of biopharmaceuticals., *Anal. Bioanal. Chem.* **405**, 2481–93 (2013).

20. J. M. Prien, B. D. Prater, S. L. Cockrill, A multi-method approach toward de novo glycan characterization: a Man-5 case study., *Glycobiology* **20**, 629–47 (2010).

21. E. D. Lobo, R. J. Hansen, J. P. Balthasar, Antibody pharmacokinetics and pharmacodynamics., *J. Pharm. Sci.* **93**, 2645–68 (2004).

22. D. C. Roopenian, S. Akilesh, FcRn: the neonatal Fc receptor comes of age., *Nat. Rev. Immunol.* **7**, 715–25 (2007).

23. E. I. Park, Y. Mi, C. Unverzagt, H.-J. Gabius, J. U. Baenziger, The asialoglycoprotein receptor clears glycoconjugates terminating with sialic acid alpha 2,6GalNAc., *Proc. Natl. Acad. Sci. U. S. A.* **102**, 17125–9 (2005).

24. P. R. Taylor, S. Gordon, L. Martinez-Pomares, The mannose receptor: linking homeostasis and immunity through sugar recognition., *Trends Immunol.* **26**, 104–10 (2005).

25. A. G. Morell, G. Gregoriadis, I. H. Scheinberg, J. Hickman, G. Ashwell, The role of sialic acid in determining the survival of glycoproteins in the circulation., *J. Biol. Chem.* **246**, 1461–7 (1971).

26. L. Tang, A. M. Persky, G. Hochhaus, B. Meibohm, Pharmacokinetic aspects of biotechnology products., *J. Pharm. Sci.* **93**, 2184–204 (2004).

27. M. a Tabrizi, C.-M. L. Tseng, L. K. Roskos, Elimination mechanisms of therapeutic monoclonal antibodies., *Drug Discov. Today* **11**, 81–8 (2006).

# Chapter 7

## *Final summary*

The overall aim of this PhD-Thesis was to investigate the influence of N-glycosylation of biopharmaceuticals (monoclonal antibodies and fusion proteins) on the pharmacokinetics and to establish a structure-function relationship. N-glycosylation is one of the most complex post-translational modifications with a possible impact on the structure, function, efficacy and safety of therapeutic proteins. The analysis of N-glycosylation is difficult especially if the protein of interest must be purified from a complex matrix like serum. The heterogeneity of N-glycosylation and the numerous possible isoforms further complicate analysis and require sensitive and robust methods. The analysis of preclinical or clinical samples poses additional challenges with high numbers of sample at varying protein concentrations.

To overcome these challenges several methods had to be developed. First, analytical methods for high sensitivity N-glycan analysis with high resolving power had to be established. Furthermore, a high-sensitivity sample preparation approach had to be developed to enable analysis of preclinical and clinical samples. The methods were finally combined and used to characterize samples obtained from two preclinical studies.

The first step was to develop a LC-MS method for comprehensive N-glycan characterization which is described in chapter 2. Therefore, two fluorescence labels 2-AA and 2-AB are evaluated in combination with reversed phase chromatography which is a proven chromatography system with a highly MS compatible mobile phase for protein analysis. The labeled N-glycans are separated according to their glycan type and fucosylation. The method enables the reproducible analysis of sialic and neutral N-glycans. 2-AA as reducing end label was demonstrated to be advantageous in comparison with the frequently used 2-AB since the retention of 2-AA labeled glycans on the reversed phase is stronger resulting in a higher resolving power of the method. In addition MS ionization efficiency in positive ionization mode is increased in combination with the acidic mobile phase. Quantitative data of neutral 2-AA N-glycans obtained by LC-MS were highly comparable to results of RP-HPLC analysis of the 2-AA labeled glycans using fluorescence detection.

The developed on-line LC-MS approach was further improved to achieve a higher sensitivity necessary for (pre)clinical samples by decreasing dimensions to nanoLC with on-line nanoESI-MS which is described in chapter 3. In comparison with the previously developed

LC-MS approach the nanoLC-MS method has an increased resolving power and higher sensitivity. Injection of 400 amol of G0F standard N-glycan can still be analyzed with good signal to noise ratio and with method linearity over more than three orders of magnitude. Like for the LC-MS method neutral and acidic N-glycans can be analyzed by nanoLC-MS in a single run. Furthermore it was demonstrated that quantitative MS data of neutral and acidic 2-AA glycans is highly comparable to UV data. Three possible applications were shown exemplarily: First, highly sensitive glycan mapping of recombinant IgGs drug substance, second, nanoLC-MS glycan mapping of recombinant Fc fusion protein after protein A affinity purification in 96 well plates from cell culture supernatant or harvest broth to support pool and clone selection and third, for N-glycan biomarker discovery in serum.

In chapter 4 the development and qualification of a sample preparation and N-glycan processing approach for preclinical and clinical samples is described in detail. The method was a 96 well format based affinity purification. This antigen based approach was shown to be suitable to recover monoclonal antibodies from preclinical and clinical serum samples and can easily be implemented in existing development work-flows. The purification was efficient and highly reproducible and enabled the analysis of mAb N-glycans from 50 µl serum. The nanoLC-MS analysis in combination with stable heavy isotope internal standards was advantageous compared to nanoLC-MS alone (chapter 3) or when using the developed LC-MS method as described in chapter 2. The method was further qualified with respect to linearity, reproducibility and robustness. A study simulating decrease of terminal galactosylation of an IgG1 biopharmaceutical proofed the viability of the N-glycan PK profiling methodology.

The developed N-glycan PK profiling method was subsequently used to analyze the glycan PK profiles of an IgG1 biopharmaceutical in a preclinical rabbit study (chapter 5). Ten N-glycans of the mAb with a portion of at least 0.1% and at a minimal concentration of 10 µg/ml were successfully analyzed. The glycan composition contained high mannose type, bi-antennary complex type and hybrid type. Relative ELISA concentration which represents the average PK profile of variants/glycoforms present was compared to the relative concentration of individual N-glycans obtained from ratios of sample N-glycan to stable heavy isotope internal standard N-glycan. It was shown that the PK profiles are highly similar with total congruency for most N-glycans with except of high mannose type. High mannose glycans M6 and M5 showed different PK profiles compared to ELISA, differences that were also observed in glycan maps showing the relative N-glycan composition over time. The relative amounts of M6 and M5 decreased over time. M6 totally disappeared and M5 levels dropped from initially 10% to approximately 6%. M6 decrease could be explained by mannosidase activity in the blood stream. Accordingly M6 is rather converted to M5 than selectively

cleared. M5 decrease in contrast can be explained with selective clearance of M5 glycoforms through the mannose receptor. The incomplete clearance of M5 in turn might be due to favored M5:M5 glycoforms of the investigated IgG1 that are thought to open the Fc part making the N-glycans accessible for receptor binding. The results confirmed previously published N-glycan PK data in a single human subject by another group and demonstrated the usefulness of the developed approach in preclinical development. On the basis of the presented data structure-function relationships can be established and the uncertainty of individual N-glycan contribution to the PK can be reduced.

The developed N-glycan PK profiling method was finally adapted to investigate a preclinical rabbit study of a fusion protein which is described in chapter 6. The fusion protein consists of a receptor part connected to an IgG Fc part. Both domains are glycosylated. Therefore affinity purification was extended with an additional purification step using protein G columns in 96 well format. The additional step reduced the serum complexity drastically and allowed on-column deglycosylation of the immobilized receptor part after enzymatic release and elution of the Fc part in the antigen affinity purification step. With this procedure the N-glycans can be analyzed domain specifically (receptor part and Fc part). In the rabbit study two differently glycosylated batches of the fusion protein were compared. Comparison of N-glycan PK profiles with the respective ELISA profile revealed differences indicating an influence of the N-glycans. Glycan maps showed that percentages of terminal galactosylated N-glycans decreased over time whereas percentages of terminal sialylated N-glycans increased relatively over time. This observation only applied for N-glycans located on the receptor part, whereas Fc part N-glycan portions were constant. The decrease of terminal galactosylated N-glycans could again be explained with a receptor mediated clearance. The asialoglycoprotein receptor expressed in the liver binds selective terminal galactose moieties and removes the glycoprotein from circulation by endocytosis. Capping of the terminal galactose residues with sialic acids might prevent this clearance. In contrast to Fc part N-glycans the receptor N-glycans are thought to be exposed and more accessible to receptor binding. The two investigated batches of the fusion protein exhibited different galactosylation and sialylation levels which might explain the slightly different PK profiles. These findings are the first to demonstrate site specific influence on the PK through N-glycans. The results clearly show that complex type Fc glycans do not influence PK, but receptor N-glycans of the same molecule do. These findings were so far not described in literature.

In summary, a novel N-glycan PK profiling technology applying MS methods was successfully developed. To achieve this a sample preparation workflow had to be optimized including isolation of the target protein from the complex matrix, selective release of the N-glycans and labeling with 2-AA. In addition a (nano)LC-MS based method had to be

developed as well. Quantification was achieved using isotopically labeled 2-AA as reference standard. The applicability of the developed technology was demonstrated analyzing samples of two pre-clinical studies. The results obtained from these studies contribute to the understanding of N-glycosylation related influence on the pharmacokinetics of biopharmaceuticals.

## List of abbreviations:

| | |
|---|---|
| 2-AA | Anthranilic acid or 2-Aminobenzoic acid |
| 2-AB | 2-Aminobenzamide |
| ACN | Acetonitrile |
| ADCC | Antibody dependent cell-mediated cytotoxicity |
| ANTS | 8-Aminonaphththalene-1,3,6-trisulfonic acid |
| b.w. | body weight |
| CE | Capillary electrophoresis |
| CDC | Complement-dependent cytotoxicity |
| CHO | Chinese hamster ovary |
| CID | Collision induced dissociation |
| DMSO | Dimethyl sulfoxide |
| EIC | Extracted ion chromatogram |
| ELISA | Enzyme linked immunosorbent assay |
| ER | Endoplasmatic reticulum |
| ESI | Electrospray ionization |
| Fc | Fragment crystalizable |
| FcRn | neonatal Fc receptor |
| FLD | Fluorescence detector |
| FP | Fusion protein |
| GlcNAc | N-actetyl-D-glucosamine |
| HILIC | Hydrophilic interaction liquid chromatography |
| HPAEC-PAD | High-Performance Anion-Exchange Chromatography with Pulsed Amperometric Detection |
| HPLC | High-performance liquid chromatography |
| IgG | Immunoglobulin G |
| LC | Liquid chromatography |
| LLOQ | Lower Limit of Quantification |
| mAb | Monoclonal antibody |
| MALDI | Matrix assisted laser desorption ionization |
| MS | Mass spectrometry |
| NMR | Nuclear magnetic resonance spectroscopy |
| PK | Pharmacokinetics |
| PNGaseF | Peptide N-Glycosidase F |
| PGC | Porous graphitized carbon |
| RNase B | Ribonuclease B |
| RP | Reversed phase |
| RPC | Reversed phase chromatography |

## Publications and presentations associated with this thesis:

### Research articles:

Fabian Higel, Uwe Demelbauer, Andreas Seidl, Wolfgang Friess & Fritz Sörgel
***Reversed-phase liquid-chromatographic mass spectrometric N-glycan analysis of biopharmaceuticals***
*Analytical and Bioanalytical Chemistry,* 2013, 405:2481-2493, doi: 10.1007/s00216-012-6690-3

Fabian Higel, Andreas Seidl, Uwe Demelbauer, Fritz Sörgel, Wolfgang Frieß
**Small scale affinity purification and high sensitivity reversed phase nanoLC-MS N glycan characterization of mAbs and fusion proteins**
*mAbs* 2014 May 21; 6(4), doi: 10.4161/mabs.29263

### Poster presentation:

Fabian Higel, Andreas Seidl, Uwe Demelbauer, Fritz Sörgel, Wolfgang Frieß
**Acetonitrile boosted nanoLCMS of N-glycans and its applications in biopharmaceutical development**
*47. Jahrestagung der Deutschen Gesellschaft für Massenspektrometrie*; Frankfurt; Germany; March 2014

### Oral presentation:

**Characterization of N-glycans using ion-trap Mass Spectrometry**
Bruker Daltonik User Meeting 2012; Kassel; Germany; March 2012

# Curriculum vitea

## Fabian Benjamin Higel

Nationality: German

Date of birth: 1st November 1985

Place of birth: Villingen Schwenningen

## Education and professional experience

| | |
|---|---|
| Since 01/2014 | Scientist<br>HEXAL AG/ Sandoz Biopharmaceuticals |
| 01/2011 – 12/2013 | PhD studies<br>HEXAL AG/ Sandoz Bioparmaceuticals in collaboration with Institute for Biomedical and Pharmaceutical Research (IBMP) in Nürnberg-Heroldsberg<br>Supervisor: Prof. Dr. Fritz Sörgel<br>and<br>Pharmaceutical Technology and Biopharmaceutics<br>LMU München; Fakultät für Chemie und Pharmazie<br>Supervisor: Prof. Dr. Wolfgang Frieß |
| 10/2008 – 09/2010 | Studies of „Molekulare Biotechnologie“ (Master of Science)<br>Technische Universität München |
| 10/2005 – 09/2008 | Studies of „Molekulare Biotechnologie“ (Bachelor of Science)<br>Technische Universität München |
| 09/1996 – 07/2005 | Allgemeine Hochschulreife<br>Fürstenberg-Gymnasium Donaueschingen |